



**Calhoun: The NPS Institutional Archive**  
**DSpace Repository**

---

Theses and Dissertations

1. Thesis and Dissertation Collection, all items

---

1978-05

# A comparison of fillet weld strength and U.S. Navy design specifications for non-combatant ships and the economic implications

McCabe, William Carl

Cambridge, Massachusetts; Massachusetts Institute of Technology

---

<http://hdl.handle.net/10945/28044>

---

This publication is a work of the U.S. Government as defined in Title 17, United States Code, Section 101. Copyright protection is not available for this work in the United States.

*Downloaded from NPS Archive: Calhoun*



Calhoun is the Naval Postgraduate School's public access digital repository for research materials and institutional publications created by the NPS community.

Calhoun is named for Professor of Mathematics Guy K. Calhoun, NPS's first appointed -- and published -- scholarly author.

**Dudley Knox Library / Naval Postgraduate School**  
**411 Dyer Road / 1 University Circle**  
**Monterey, California USA 93943**

<http://www.nps.edu/library>

A COMPARISON OF FILLET WELD STRENGTH AND U.S.  
NAVY DESIGN SPECIFICATIONS FOR NON-COMBATANT  
SHIPS AND THE ECONOMIC IMPLICATIONS

William C. McCabe

7 MAR 1979

WILLIAM LEWIS  
WILLIAM LEWIS HIGH SCHOOL  
MURFREESBORO, TENNESSEE

## REPORT DOCUMENTATION PAGE

READ INSTRUCTIONS  
BEFORE COMPLETING FORM

1. REPORT NUMBER	2. GOVT ACCESSION NO.	3. RECIPIENT'S CATALOG NUMBER
4. TITLE (and Subtitle)  A COMPARISON OF FILLET WELD STRENGTH AND U.S. NAVY DESIGN SPECIFICATIONS FOR NON-COMBATANT SHIPS AND THE ECONOMIC IMPLICATIONS		5. TYPE OF REPORT & PERIOD COVERED  THESIS
6. AUTHOR(s)  McCABE, WILLIAM C.		7. CONTRACT OR GRANT NUMBER(s)
8. PERFORMING ORGANIZATION NAME AND ADDRESS  MASS. INST. OF TECHNOLOGY		10. PROGRAM ELEMENT, PROJECT, TASK AREA & WORK UNIT NUMBERS
11. CONTROLLING OFFICE NAME AND ADDRESS  CODE 031 NAVAL POSTGRADUATE SCHOOL MONTEREY, CALIFORNIA, 93940		12. REPORT DATE  MAY 78
14. MONITORING AGENCY NAME & ADDRESS (if different from Controlling Office)		13. NUMBER OF PAGES  204
		15. SECURITY CLASS. (of this report)  UNCLASS
		16a. DECLASSIFICATION/DOWNGRADING SCHEDULE
16. DISTRIBUTION STATEMENT (of this Report)  APPROVED FOR PUBLIC RELEASE; DISTRIBUTION UNLIMITED		
17. DISTRIBUTION STATEMENT (of the abstract entered in Block 20, if different from Report)		
18. SUPPLEMENTARY NOTES		
19. KEY WORDS (Continue on reverse side if necessary and identify by block number)  FILLET WELD STRENGTH; FILLET WELD; WELD STRENGTH; NAVY DESIGN SPECIFICATIONS; NON-COMBATANT SHIPS		
20. ABSTRACT (Continue on reverse side if necessary and identify by block number)  SEE REVERSE.		

T 195468



Approved for public release;  
distribution unlimited.

A COMPARISON OF FILLET WELD STRENGTH AND U.S. NAVY DESIGN  
SPECIFICATIONS FOR NON-COMBATANT SHIPS AND THE ECONOMIC IMPLICATIONS

by

WILLIAM CARL MCCABE

B.S., Cleveland State University  
(1968)

SUBMITTED IN PARTIAL FULFILLMENT  
OF THE REQUIREMENTS FOR THE  
DEGREE OF

OCEAN ENGINEER

AND THE DEGREE OF

MASTER OF SCIENCE IN SHIPPING  
AND SHIPBUILDING MANAGEMENT

at the

MASSACHUSETTS INSTITUTE OF TECHNOLOGY

MAY, 1978

(C) WILLIAM CARL MCCABE 1978

Thesis  
M1633  
2.1

A COMPARISON OF FILLET WELD STRENGTH AND U.S. NAVY DESIGN  
SPECIFICATIONS FOR NON-COMBATANT SHIPS AND THE ECONOMIC IMPLICATIONS

by

WILLIAM CARL MCCABE

DUDLEY KNOX LIBRARY  
NAVAL POSTGRADUATE SCHOOL  
MONTEREY, CA 93940

Submitted to the Department of Ocean Engineering  
on May 5, 1978, in partial fulfillment of the requirements  
for the Degree of Ocean Engineer  
and the Degree of Master of Science in Shipping  
and Shipbuilding Management

ABSTRACT

There is a great interest in the strength of fillet welds because the welding operation accounts for about 30% of the labor cost in planning and constructing ship hulls. One way to reduce welding cost is to reduce the required weld size. Background information is obtained by reviewing the major experimental and theoretical work in the areas of static strength, fatigue strength, and shear strength of fillet welds.

In order to appreciate the conditions in the real world, design considerations, fabrication considerations, and corrosion considerations are discussed. Typical joints from existing U.S. Navy ships are employed to obtain detailed geometry and local loading information to be used as input for a computer model which was developed at Massachusetts Institute of Technology which uses the finite element method for determining the static strength for fillet welds. In one particular joint a reduction of 30% in the required weld size is justified.



A future system for analyzing fillet weld strength is proposed and explained by the use of an example.

The economics of intermittent and continuous welds are examined, and the economic impact that a reduction in the required fillet weld size would have on ship construction cost is estimated.



## ACKNOWLEDGEMENTS

I would like to express my deep gratitude to Professor Koichi Masubuchi and to Research Associates Kouyu Itoga and Chon-Liang Tsai who were the motivating force behind this work. Their interest in and support of this study aided in its successful completion. Their suggestions and recommendations were a tremendous help in the development, organization, and presentation of the thesis.

A portion of this work was supported by the Ship Structure Committee under project SR-1248, "Updating of Fillet Weld Strength Parameters for Shipbuilding," (DOT-CG-71455-A).

My deepest appreciation goes to my wife, Dorothy Louise, who completed the monumental task of typing from my handwritten draft.

And, I dedicate this work to my wife, my daughter, Jo Ann Lynne, and my son, William Carl, Jr., whose patience and understanding during these three years have been responsible for making this period a pleasurable experience.



## TABLE OF CONTENTS

	Page
TITLE PAGE. . . . .	1
ABSTRACT. . . . .	2
ACKNOWLEDGEMENTS. . . . .	4
TABLE OF CONTENTS . . . . .	5
LIST OF FIGURES . . . . .	7
LIST OF TABLES. . . . .	12

## SECTIONS

I. INTRODUCTION . . . . .	13
II. EXPERIMENTAL AND THEORETICAL WORK CONCERNING STATIC STRENGTH . . . . .	18
III. EXPERIMENTAL AND THEORETICAL WORK CONCERNING FATIGUE STRENGTH . . . . .	43
IV. EXPERIMENTAL AND THEORETICAL WORK CONCERNING SHEAR STRENGTH . . . . .	57
V. DESIGN CONSIDERATIONS. . . . .	64
VI. FABRICATION CONSIDERATIONS . . . . .	79
VII. A PROPOSED SYSTEM FOR ANALYZING FILLET WELD STRENGTH .	88
VIII. CURRENT WELDING SPECIFICATIONS FOR SHIP CONSTRUCTION .	92
IX. TYPICAL FILLET WELDED JOINTS . . . . .	105
X. STRUCTURAL ANALYSIS OF LOADING IN SELECTED MEMBERS .	114
XI. COMPUTER ANALYSIS OF STRENGTH OF SELECTED FILLET WELDED JOINTS. . . . .	126
XII. CORROSION CONSIDERATIONS . . . . .	133
XIII. ECONOMIC ANALYSIS OF INTERMITTENT VERSUS CONTINUOUS WELDING. . . . .	142
XIV. THE ECONOMIC IMPACT OF THE REDUCTION OF WELD SIZE REQUIREMENTS IN SHIP CONSTRUCTION. . . . .	166



## TABLE OF CONTENTS CONTINUED

SECTIONS	Page
XV. RECOMMENDATIONS AND CONCLUSIONS. . . . .	171
APPENDIX. . . . .	175
REFERENCES. . . . .	200



## LIST OF FIGURES

Figure	Title	Page
1.1	Inter-relationships Between Various Aspects of the Study of the Strength of Fillet Welds	15
2.1	Schematic Representation of the Test Coupons	19
2.2	Ultimate Load VS Weld Angle	22
2.3	Maximum Deformation VS Weld Angle	23
2.4	Load VS Deformation $\theta = 0$ to $90^\circ$ $\frac{1}{4}$ Inch Fillet Welds	25
2.5	Transverse Fillet Weld	27
2.6	Forms of V-Shape Steels	30
2.7	Shear Test Piece of Side Fillet Weld	31
2.8	Tensile Test Piece of Front Fillet Weld	31
2.9	Shape of E-Type Test Pieces	33
2.10	Relation Between Intersecting Angle and the Unit Breaking Stress (Theoretical Throat Depth)	35
2.11	Relation Between Intersecting Angle and the Unit Breaking Stress (Actual Throat Depth)	36
2.12	Shape of F-Type Test Pieces	37
2.13	Shape of Deformed Weld	38
2.14	Theoretical Throat Depth Necessary to Have the Same Strength as a 5 mm $90^\circ$ Manual Arc Weld	42
3.1	Diagram of Test Specimens	44
3.2	Test Piece of a Non-Load Carrying Double Fillet	46
3.3	Details for Test Specimens	48



## LIST OF FIGURES CONTINUED

Figure	Title	Page
3.4	Fatigue Test Results for Mild Steel Specimens with Longitudinal Gussets Showing the Effects of Grinding and Peening	50
3.5	Fatigue Test Results for Mild Steel Specimens with Transverse Gussets Showing the Effects of Grinding and Peening	51
3.6	Semi-Elliptical Surface Crack in a Plate in Tension	53
3.7	Variation of $(M_s M_t / \Phi_o)$ with Crack Depth for Various Shapes $(a/2_c)$	55
4.1	Details of Test Pieces	58
4.2	Relationship Between Apparent Surface Strain and Shearing Intensity	60
5.1	The Geometry of a Typical Joint	65
5.2	Stress Concentration Factor at the Fillet Weld Toe Adjacent to the Tube	66
5.3	Force System of a Fillet Weld Load at Right Angles to Its Longitudinal Axis	68
5.4	Stress in a Fillet Weld	71
5.5	A Continuous Double Fillet Welded T Joint	74
5.6	A Simplified Riveted Joint	77
6.1	A Typical Model of a Continuous Double Fillet Weld	80
6.2	Average Double Fillet Joint as Welded	81
6.3	A Typical Convex Double Fillet Weld	82
6.4	A Fillet Weld with an Unacceptable Re-entrant Angle	83
6.5	A Skewed Fillet Welded Tee Joint	84



## LIST OF FIGURES CONTINUED

Figure	Title	Page
6.6	Another Skewed Fillet Welded Tee Joint	85
6.7	A Double Fillet Welded Joint with a Gap (Y)	86
8.1	Current Welding Specifications for Joints Between Double Bottom Floors and Shell Plating	93
8.2	Current Welding Specifications for Joints Between Web Frames and Shell Plate	94
8.3	Current Welding Specifications for Joints Between Decks and Shell Plating	95
8.4	Efficiency Chart for Continuous Double-Fillet Welded Tee Joints Made Between Medium Steel Made with MIL-6011 Electrodes	97
8.5	Weld Size of a Concave Fillet Weld	100
8.6	Weld Size of a Convex Fillet Weld	101
8.7	Maximum Allowable Convexity for Fillet Weld Sizes	102
8.8	A Double Fillet Weld with a Gap (Y)	103
9.1	Typical Joint Between a Transverse Bulkhead and the Shell Plating of the AD-37 Class Ship	107
9.2	Typical Joint Between a Transverse Bulkhead and the Inner Bottom Floor of the AD-37 Class Ship	108
9.3	Typical Joint Between a Longitudinal and the Shell Plating of the AD-37 Class Ship	109
9.4	Typical Joint Between a Stringer and the Shell Plating of the AD-37 Class Ship	111
9.5	Typical Joint Between a Longitudinal and the Shell Plating of the AO-143 Class Ship	112



## LIST OF FIGURES CONTINUED

Figure	Title	Page
9.6	Typical Joint Between Transverse Bulkhead and the Shell Plating of the AO-143 Class Ship	113
10.1	Bending Stresses in Ships	115
10.2	The Variation of $K_L$ with Aspect Ratio, $a/b$	117
10.3	Typical Bottom Structure of an AD-37 Class Ship	119
10.4	The Variation of $\sigma_1$ with Distance from the Keel of the AD-37 Class Ship in the Sagging Condition	121
10.5	The Variation of $\sigma_1$ with Distance from the Keel of the AO-143 Class Ship in the Sagging Condition	122
11.1	The Boundary Conditions and the Applied Loads of the Fillet Weld Model	127
11.2	Finite Element Model Mesh	128
11.3	Loading Function of the Finite Element Model	129
11.4	Resulting Displacement of the Toe Element	130
11.5	Reduction in Fillet Weld Size Versus Quantity X, for the Transverse Bulkhead Joint	132
12.1	A Comparison of the Amount of Metal Loss Before Failure for: <ul style="list-style-type: none"> <li>a. General Corrosion</li> <li>b. Localized Corrosion</li> </ul>	134
12.2	Design of Tank Supports	137
12.3	A Schematic Diagram of the Use of a Corrosion Margin for a Fillet Weld	138
12.4	A Fillet Weld with a Crevice at the Toe Results in a Poor Quality Weld	140



## LIST OF FIGURES CONTINUED

Figure	Title	Page
13.1	Test Piece for Continuous Welding	146
13.2	Test Piece for Intermittent Welding	147
13.3	Weld Metal Requirements for 45 Degree Fillet Welds	164
14.1	A Diagram of the Ship Model Used for the Economic Impact Study	167
14.3	The Variation of Arc Time with Fillet Weld Size for CO <sub>2</sub> Solid Wire Welding	169



## LIST OF TABLES

Table	Title	Page
2-1	Test Results and Predicted Values	24
4-1	Details of Tests	61
7-1	$d_i$ Values for Different Joint Classifications	90
7-2	Fillet Weld Analysis System Elements	91
8-1	Required Joint Efficiencies for Various Fillet Welded Joints	99
10-1	A Summary of Stresses in Structural Members of Joints	125
13-1	Estimating Welding Cost	143
13-2	Continuous Manual Welding (Experimental Approach)	148
13-3	Intermittent Manual Welding (Experimental Approach)	150
13-4	Continuous Automatic Welding (Experimental Approach)	152
13-5	Continuous Manual Welding (Industrial Data Approach)	156
13-6	Intermittent Manual Welding (Industrial Data Approach)	158
13-7	Continuous Automatic Welding (Industrial Data Approach)	160
13-8	A Comparison of Welding Costs	162



## I INTRODUCTION

Presently there is great interest in the strength of fillet welds. Most of this interest stems from the fact that welding cost is a very important variable in the total construction cost of a ship's hull. The welding and assembly of ship hulls require approximately the same number of manhours, and these two functions combined amount to about 60% of the total manhours for the completion of the hull structure.<sup>1</sup> This indicates that the welding operation accounts for about 30% of the labor cost in planning and constructing ship hulls. If we look at the total linear measure of the welded joints employed in ship construction, we find that approximately 75% of these welds are fillet welds.<sup>2</sup>

Since one way to reduce welding cost is to reduce the required weld size, the big question becomes "Are current welding specifications too conservative?" In order to answer this question, we must explore the strength of fillet welds. Many of the welding specifications were developed many years ago, and the history of their development is not clear. Some resemble the specifications that were used when rivets were used to join structural members in ships.

To provide background information, this work will attempt to present the major experimental and theoretical work in the field of fillet weld strength. The main areas that will be discussed are static strength, fatigue strength, and shear strength of fillet welds.

Then we will move from the theoretical environment to the real



world and discuss the design considerations and fabrication considerations that will help to bridge the gap between the ideal theoretical model and the joint, as welded, that can be found in every location on a ship.

Before discussing the current welding specifications for the construction, we will look into the future and develop a system for analyzing fillet weld strength that is capable of taking into account all of the factors which affect the strength of fillet welds.

At this point, it might be beneficial to look at Figure 1.1, which shows how all of the different aspects concerning the strength of fillet welds are related to one another.

We will take a brief look at the current welding specifications for the construction of ships as used by the United States Navy for non-combatant type ships and compare these specifications to the requirements of other organizations that are interested in the construction and safety of ships. The U.S. Navy specifications are neither the most conservative nor the most liberal requirements.

In order to evaluate these specifications, we will examine some typical fillet welded joints that are found on non-combatants. Two ship types were chosen to study. These were a destroyer tender (AD-37 class) and an oiler (AO-143 class).

The typical joints were taken from the midship section of these ships because the principle bending stress reaches a maximum in this area. Once the joints are selected, the loading of the structural members of the joint will be determined by



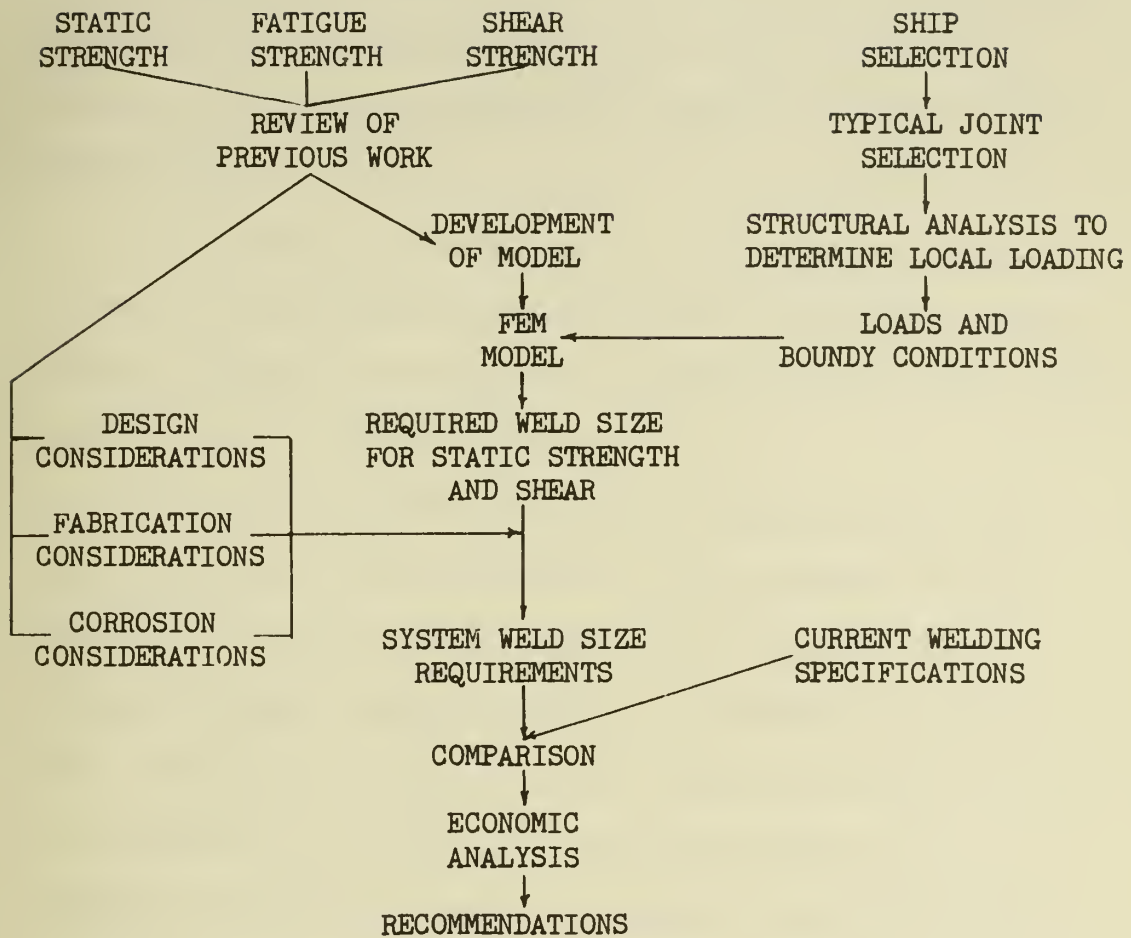


FIGURE 1.1.  
INTER-RELATIONSHIPS BETWEEN VARIOUS ASPECTS  
OF THE STUDY OF THE STRENGTH  
OF FILLET WELDS



structural analysis. Having obtained the loading of these members, we can then analyze the strength of the fillet welded joints by employing a computer program based on the finite element approach. From this we can determine the size of weld that is required for static strength considerations. Another aspect that we will examine is the corrosion margin that should be included in the requirements.

By following the diagram shown in Figure 1.1, we can then compare the resulting required weld size to the current specifications, and then we can answer the question, "Are current welding specifications too conservative?"

One of the reasons that people are concerned whether the specifications are too conservative is the economics of ship building. In order to determine the most economic method of joining low shear carrying stiffeners to bulkheads or decks, we will examine the cases where current welding rules permit the use of intermittent fillet welds. The welding methods that will be compared are continuous manual arc welding, manual intermittent welding, and automatic continuous welding. The two approaches that will be used in this study are an experimental approach and an industrial data approach.

To probe the economics of welding in the construction of ships further, we will look at a rough first cut answer to the question, "How much can we save if the welding requirements can be reduced?"

It is much too early in the study to give a precise answer,



but the indication is there that potential savings are waiting to be discovered.

And finally, we will review the conclusions of this work and look at possible areas of future work in the study of strength of fillet welds.



## II EXPERIMENTAL AND THEORETICAL WORK CONCERNING STATIC STRENGTH

In this section, we will review some of the experimental and theoretical work that has been done in the area of static strength of fillet welds. In order to study the effect of the direction of applied load on the strength of fillet welds, Butler and Kulak<sup>3</sup> ran some experimental tests and analyzed their data theoretically.

Their tests were conducted using 23 coupons with 1/4 inch fillet welds. They divided these coupons into four groups. The first group consisted of five coupons with the weld axis being parallel to the direction of the applied load. Groups two, three, and four were made up of six coupons each with the weld axis being inclined at angles of 30, 60, and 90 degrees respectively to the direction of the applied load. The material used in the fabrication of coupons was CSA G40.12 which has a specified yield stress of 44 ksi and a minimum tensile strength of 62 ksi.

AWS E 60XX electrodes were used for welding the coupons. In order to assure weld failure before rupture of the plate portions of the coupons, the cross sectional area of the connected parts was designed sufficiently large. Since uniform quality was desired throughout the various coupons, all welding was accomplished by the same operator using electrodes from the same lot. In addition, the start and finish of all welds were sawed free.

A schematic representation of the test coupons is presented in Figure 2.1.

During the tests, weld deformation was measured using two



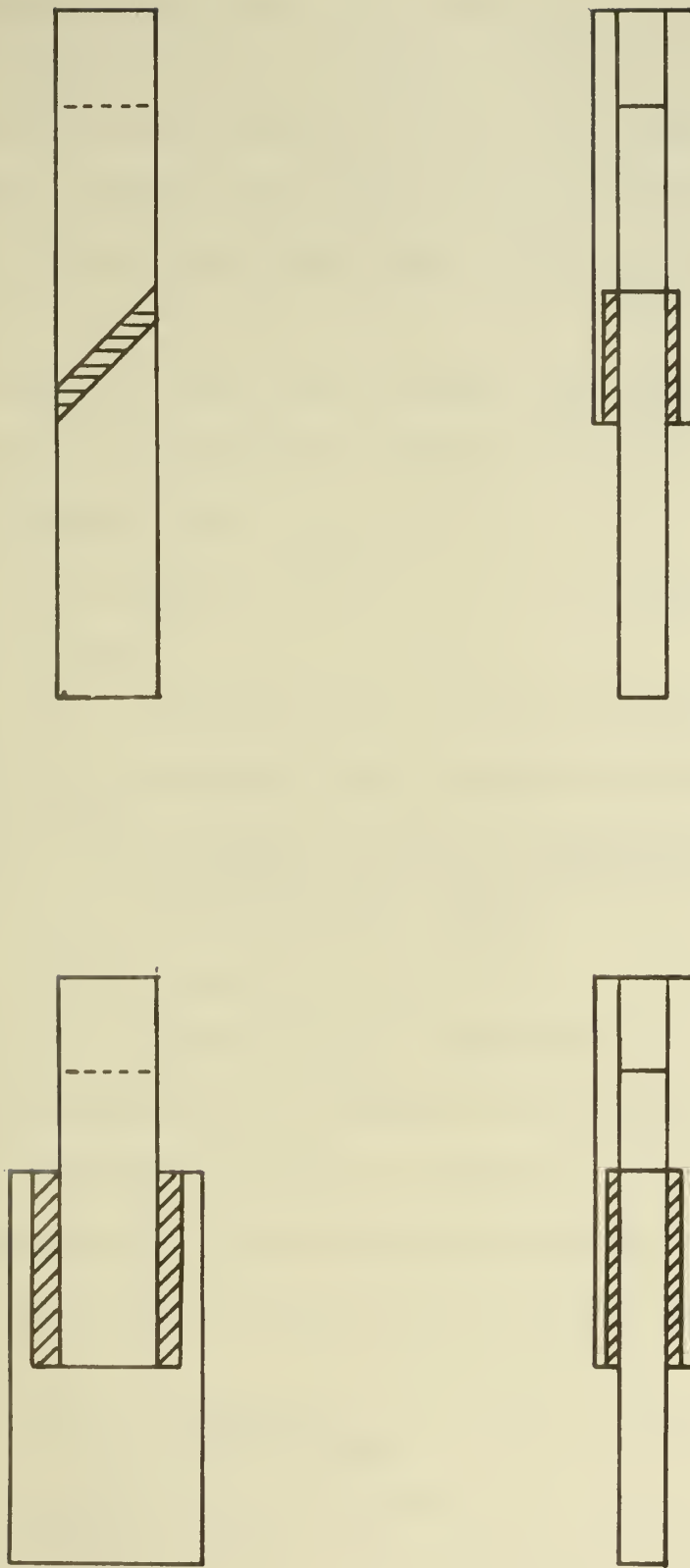


FIGURE 2.1. SCHEMATIC REPRESENTATION OF THE TEST COUPONS<sup>3</sup>



0.001 inch dial gauges fastened to each specimen. An electro-mechanical testing machine with a capacity of 440,000 lb. was used to load the coupons in tension. Reading increments were 5 kip in the lower ranges and 2.5 kip as the response became inelastic. Readings were taken until the ultimate load was reached. Gauges were removed before loading was continued until failure.

Butler and Kulak<sup>3</sup> chose to analyze their experimental data employing a load-deformation response for mechanical fasteners of the following form:

$$R = R_{ult} (1 - e^{-\mu \Delta})^\lambda \quad (2.1)$$

Where:

$R$  = fastener load at any given deformation

$R_{ult}$  = ultimate load attainable by fastener

$\Delta$  = shearing, bending, and bearing deformation of fastener and local bearing deformation of the connected plates

$\mu, \lambda$  = regression coefficients

$e$  = base of natural logarithms

For welded joints, in contrast to a mechanical joint such as a high strength bolt, one has to take into account the direction of the applied load. Trial-and-error curve-fitting was used to obtain the following expressions for the variables in equation (2.1).

$$R_{ult} = \frac{10 + \theta}{0.92 + 0.0603\theta} \quad (2.2)$$

$$\Delta_{max} = 0.225 (\theta + 5)^{-0.47} \quad (2.3)$$



$$u = 75 e^{0.0114\theta} \quad (2.4)$$

$$\lambda = 0.4 e^{0.0146\theta} \quad (2.5)$$

Where:

$\theta$  = the angle between the direction of the applied load and the longitudinal axis of the weld.

A word of caution is justified. These expressions were developed specifically for 1/4 inch fillet welds made using E 60XX electrodes; and, therefore, care should be used before applying these to other size welds or welds using different electrodes.

Equation (2.2) is plotted in Figure 2.2, and equation (2.3) is plotted in Figure 2.3. Table 2-1 compares test results and predicted values for the ultimate load and the maximum deformation. The calculated ultimate loads are within 2% of the mean test data for all groups except the 60 degree group which is within about 9%.

Substituting equations (2.2) - (2.5) into equation (2.1) yields results which are plotted in Figure 2.4. Butler and Kulak stated that agreement between the theoretical and actual load deformation responses is excellent for the two extreme cases ( $\theta$  = zero and 90 degrees) and adequate for the two intermediate angles of 30 and 60 degrees.

The strength of the fillet welds tested increased approximately 44% as the angle of the load changed from zero degrees (longitudinal weld) to 90 degrees (transverse weld); however, there was a substantial decrease in deformation capacity as the strength increased.

This study produced the following conclusions:<sup>3</sup>



FIGURE 2.2.  
ULTIMATE LOAD VS WELD ANGLE<sup>3</sup>

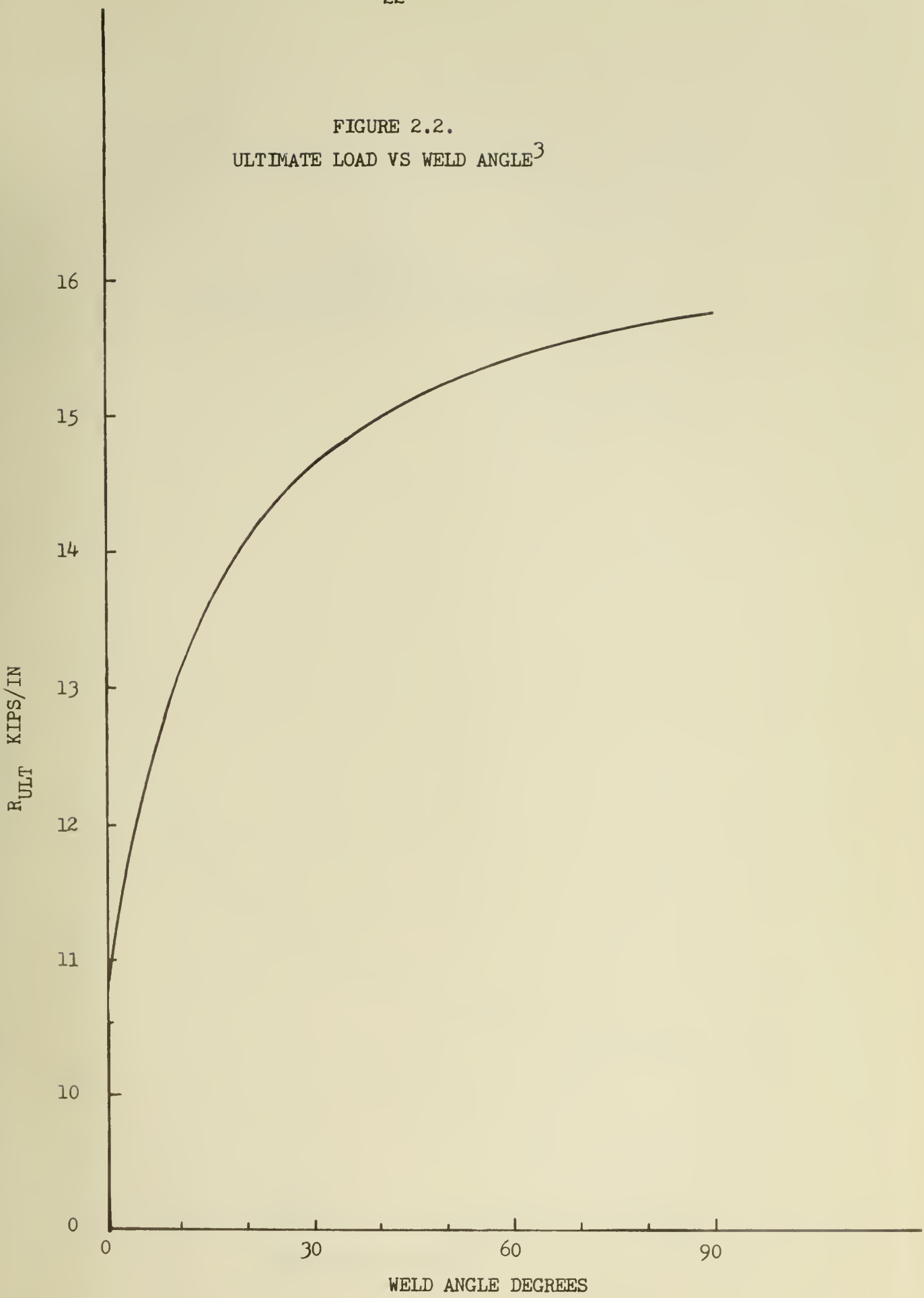




FIGURE 2.3.  
MAXIMUM DEFORMATION VS WELD ANGLE<sup>3</sup>

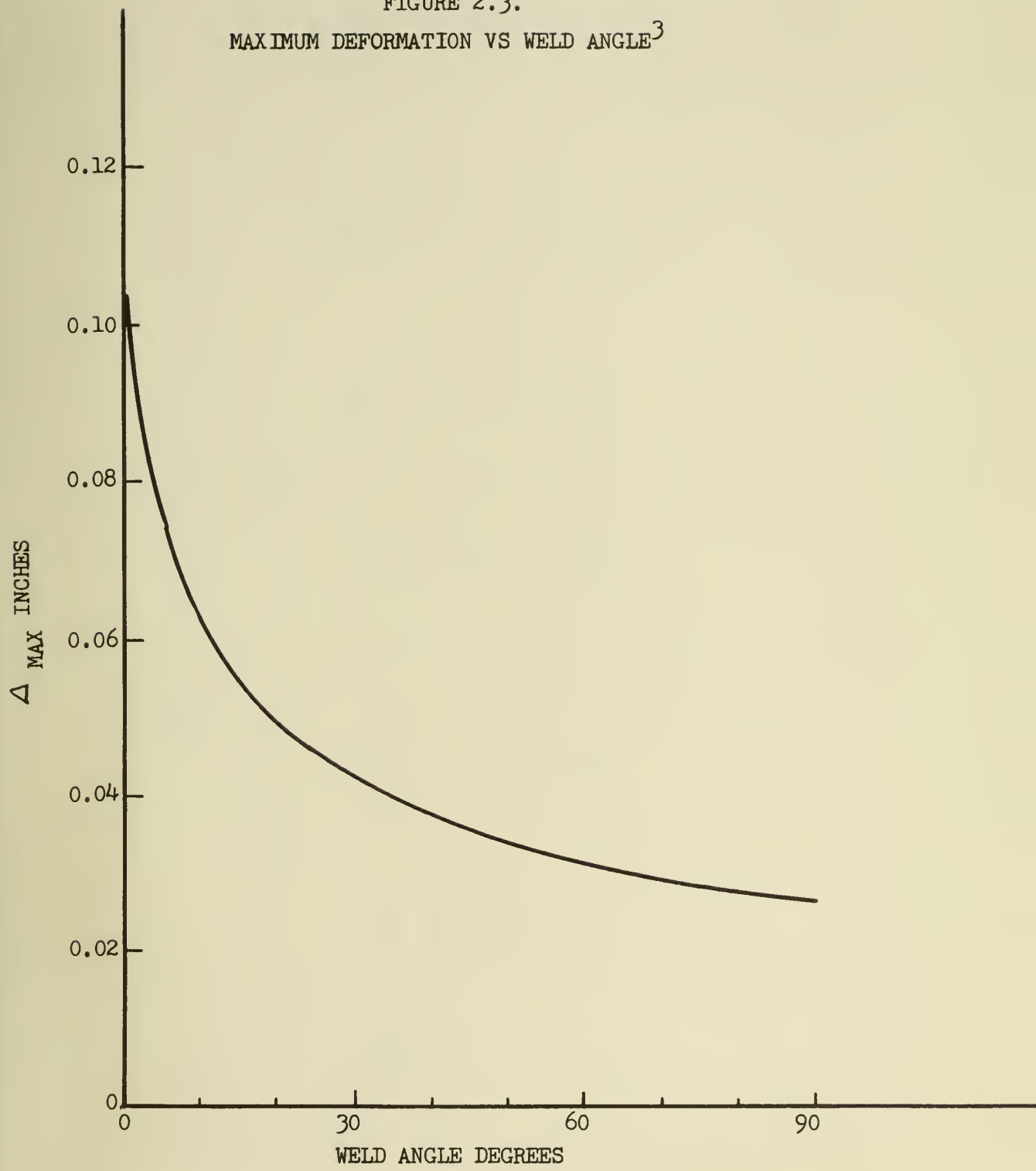
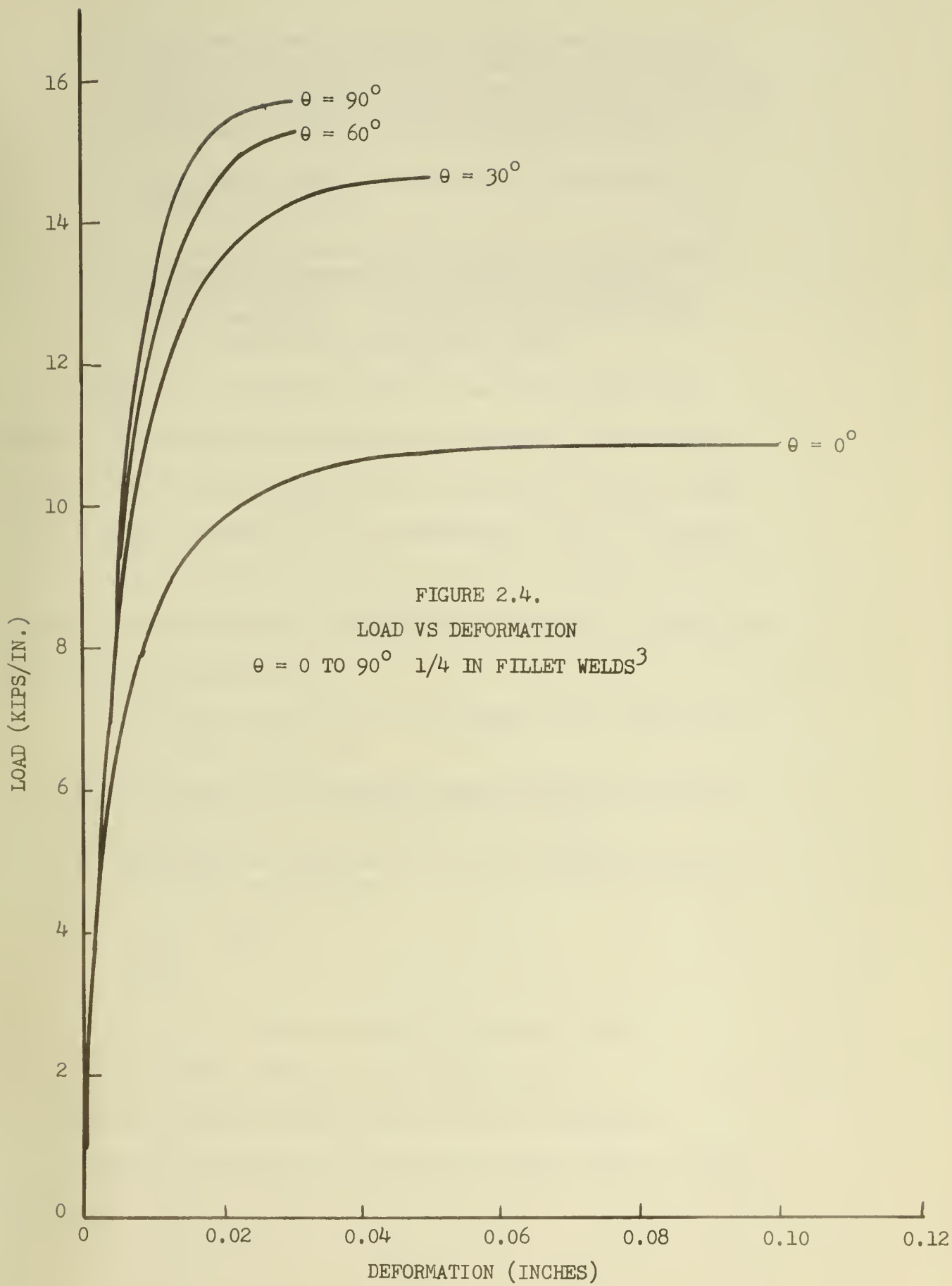




TABLE 2-1. Test Results and Predicted Values<sup>3</sup>

Group $\theta$ , deg	Ultimate load kips/in.	Maximum deformation, in.		Predicted values	
		Mean	Std. deviation	Mean	Std. deviation
0	10.9	0.67	0.101	0.008	10.9
30	14.6	0.03	0.049	0.011	14.6
60	14.1	0.51	0.031	0.004	15.4
90	15.5	0.95	0.026	0.002	15.7







- "1. The strength and ductility of fillet welds loaded in shear are markedly dependent upon the orientation of the weld with respect to the line of action of the load. Welds placed parallel to the direction of the load have the lowest strength and the highest ductility.
- "2. Fillet welds loaded in shear do not exhibit any well-defined yield point.
- "3. The load-deformation response of fillet welds cannot be generally represented as elastic or elastic-perfectly plastic. Mathematical expressions have been presented for all values of weld inclination to the direction of the applied load."

Another study related to this one was done by Kato and Morita,<sup>4</sup> who studied the strength of transverse fillet welded joints theoretically by employing an approximate solution based on the theory of elasticity and supplemented this by an elastic-plastic strain hardening analysis performed numerically using the finite element technique. The approximate solution is based upon the following assumptions:<sup>4</sup>

1. The direct stress ( $\sigma$ ) on the tensile face of the weld is uniformly distributed.
2. The pattern of the elastic stress distribution remains unchanged until the breaking of the weld.
3. Breaking will occur when the shear stress at a point of the fillet weld reaches

$$\tau_{\max} = \sigma_t / \sqrt{3}$$

Where:

$\sigma_t$  = the tensile strength of the weld metal

4. The fillet weld has legs of equal size.

The model used for this study is shown in Figure 2.5.

The maximum strength of a transverse fillet weld was found to be:



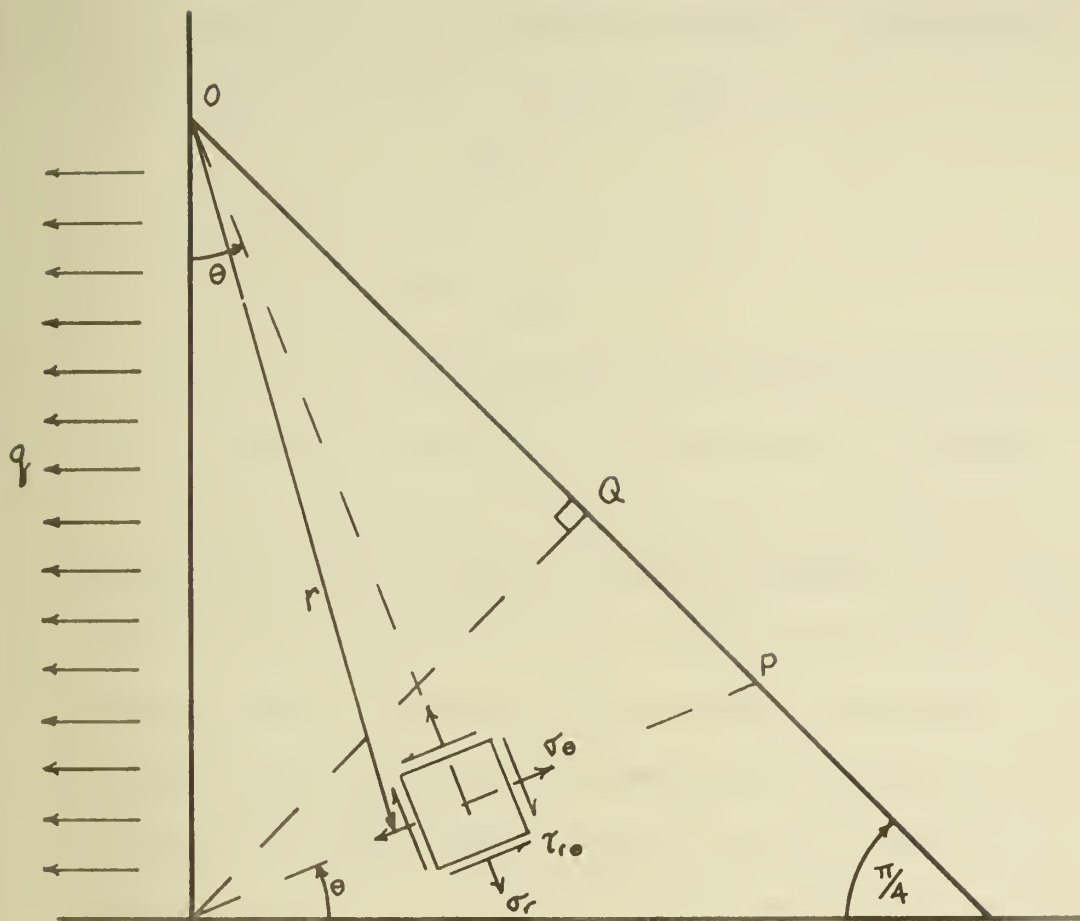


FIGURE 2.5. TRANSVERSE FILLET WELD<sup>4</sup>



$$T_{t \max} = (1 - \pi/4) (\sin^{-2} \pi/8) A_w \sigma_t / \sqrt{3}$$

The oblique plane RP in the above figure which is normal to the coordinate line  $\theta = \pi/8$  is considered to be the fracture plane.

For the longitudinal fillet weld, the critical section would be the throat RQ. And the maximum strength of a longitudinal fillet weld with the same size and length is:

$$T_{l \max} = A_w \sigma_t / \sqrt{3}$$

Therefore we obtain

$$T_{t \max} = 1.46 T_{l \max}$$

This indicates that transverse fillet welds are 46% stronger than longitudinal fillet welds of the same size and length.

Since assumptions as stated above are not precise, the researchers applied a numerical analysis employing the finite element method to extend the study to the elastic-plastic strain hardening range. Incremental strain theory is the basis of this analysis, and the material is assumed to be isotropic and ductile and obey the von Mises yield condition with the Prandtl-Reuss loading function. The results from this analysis and experimental test results agree with the result from the elastic approximate solution in spite of its theoretical shortcomings.

Another study concerning the strength of fillet welds was done by Nishida, Tanaka, and Tanaka.<sup>5</sup> These investigators ran tests on what is called a "SUMI FRAME V." When a V shape is used as a flange in a modified I beam, the resulting angle between the two members becomes  $135^\circ$ . This result exceeds the value prescribed



in the design standards for steel structures by the Architectural Institute of Japan. However, the V-shape steel has advantages in dynamics because of its excellent sectional abilities for Y axis. In using these members to build up columns or beams, one can minimize the welding strain because of the provision of a V-shaped projection. The general form of these V-shaped steel members is shown in Figure 2.6.

Experiments were performed to determine whether the fillet weld used in the build-up members of V-shape steel causes any degradation of the joint. Examples of the test specimens are shown in Figures 2.7 and 2.8.

The researchers pointed out that the test involving the front fillet welded with strap plates results in various influences due to friction between the base metal and the strap plates; thus, the test results were inconclusive. Tests for the front fillet welded joint was performed by the cross type joint, which is considered by some to be inferior to strapped joints in strength.

The weld sizes were chosen in such a way to equalize the sum of the theoretical throat depth to a nominal thickness of base plate. The welding procedures that were employed included manual arc welding, automatic submerged arc welding, and one-side and both-sides fillet welding.

Nishida, et al, reached the following conclusions:<sup>5</sup>

1. The shear test for side fillet weld and the tensile test for front fillet weld showed that the strength of the welded part was always above the allowable shear stress of the base metal. (This value was obtained by multiplying the allowable tensile unit stress of the base metal by  $1/\sqrt{3}$ )



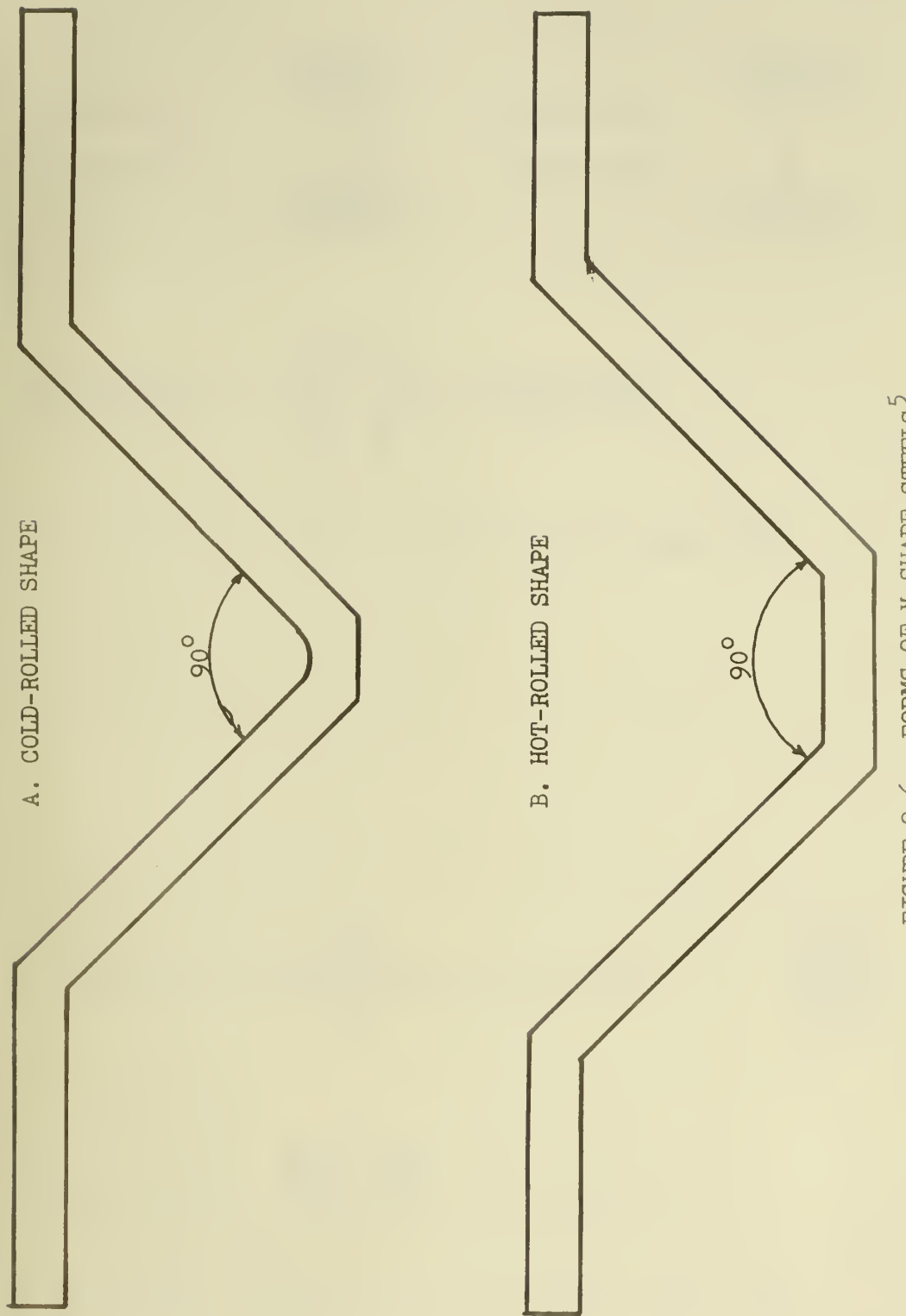


FIGURE 2.6. FORMS OF V-SHAPE STEELS<sup>5</sup>



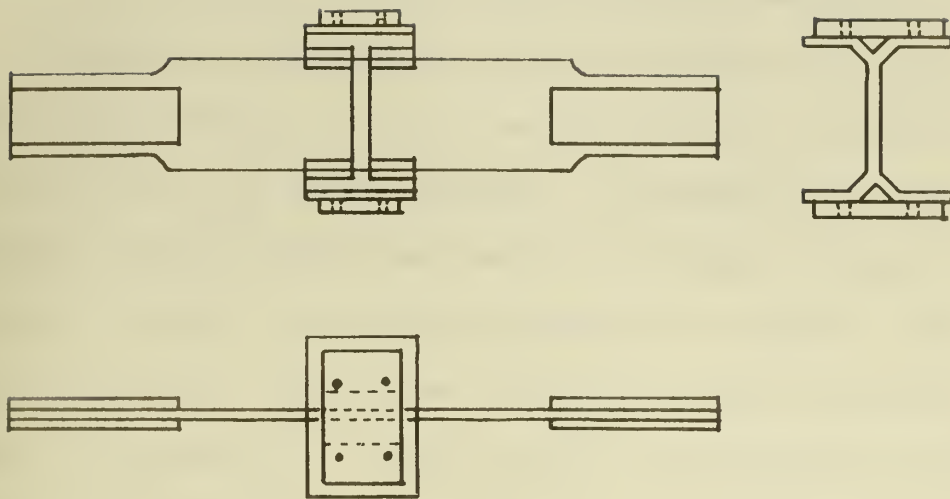


FIGURE 2.7. SHEAR TEST PIECE OF SIDE FILLET WELD

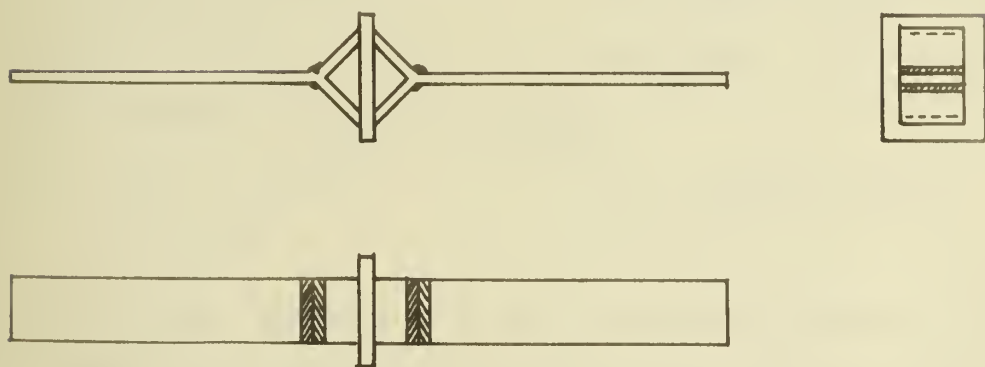


FIGURE 2.8. TENSILE TEST PIECE OF FRONT FILLET WELD



2. The experiments proved that, when the V-shape steels (produced by their factory) are connected by fillet welds, the resulting members are completely satisfactory for the welding methods investigated.

These same investigators continued experiments for cases where angles between the welded materials are wider in order to collect data on the overall strength of deformed fillet welds. The three welding methods were manual arc welding,  $\text{CO}_2$  semi-automatic welding, and automatic submerged arc welding. Weld penetration depth  $P$  (in mm) was correlated to the intersecting angle  $\theta$  (in degrees). It was found that weld penetration depth increased proportionally to an increase in the intersection angle until a constant value was reached. The following relations were obtained for different welding conditions.<sup>5</sup>

1. Manual Arc Welding

$$\text{at } 45^\circ \leq \theta < 120^\circ \quad P = 0.0423 \theta - 3.67$$

$$\text{at } \theta \geq 120^\circ \quad P = 1.40$$

2.  $\text{CO}_2$  Semi-automatic Arc Welding

$$\text{at } 45^\circ \leq \theta < 90^\circ \quad P = 0.0849 \theta - 5.43$$

$$\text{at } \theta \geq 90^\circ \quad P = 1.97$$

3. Automatic Submerged Arc Welding

$$\text{at } 45^\circ \leq \theta < 90^\circ \quad P = 0.0577 \theta - 2.36$$

$$\text{at } \theta \geq 90^\circ \quad P = 2.6$$

It was found, however, that at an intersecting angle of  $30^\circ$  an extremely large reduction of weld penetration occurs in all of the above methods.

The test pieces used to determine weld strength at various intersecting angles can be viewed in Figure 2.9.



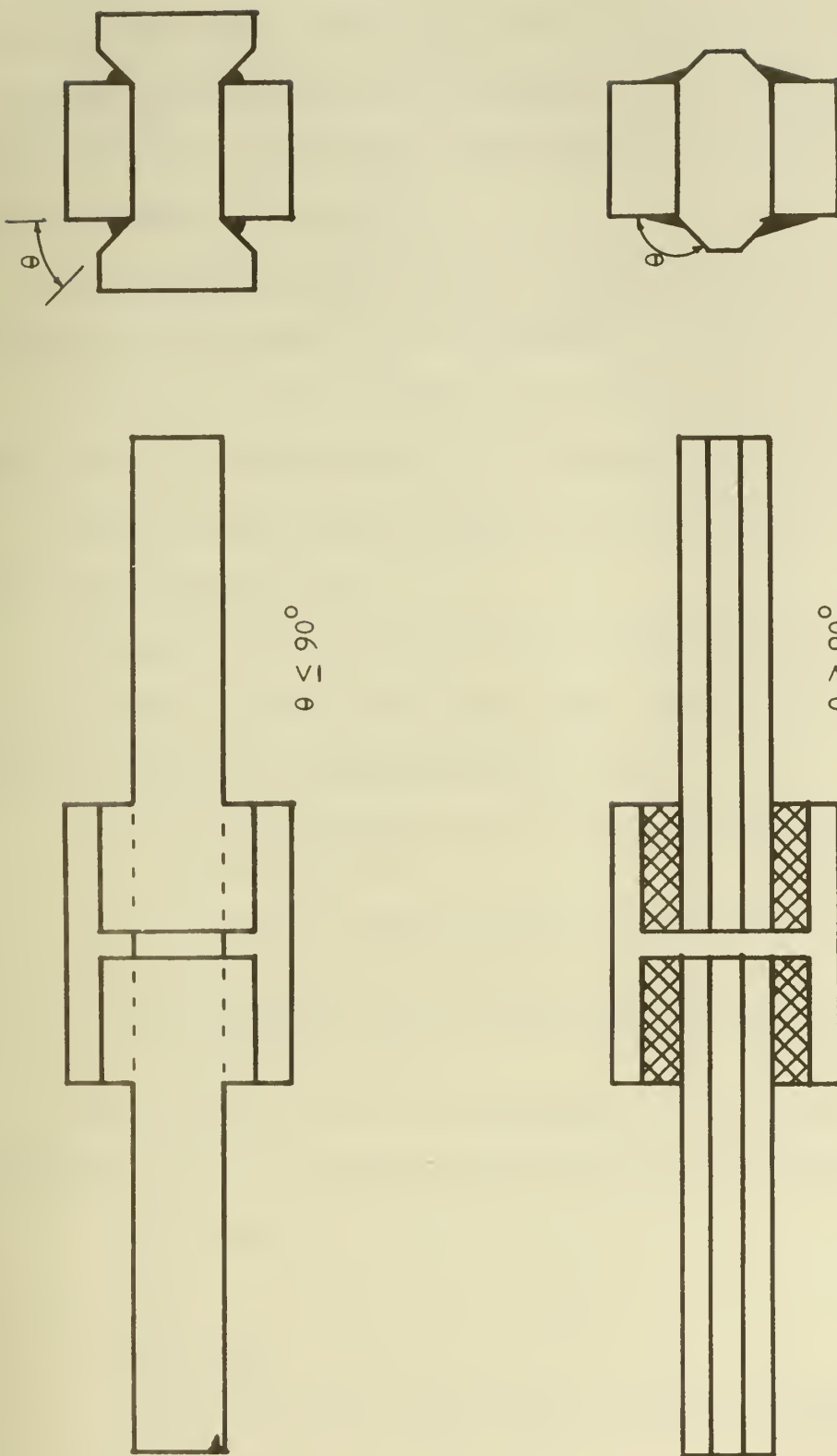


FIGURE 2.9. SHAPE OF E-TYPE TEST PIECES<sup>5</sup>



The investigators compared the strength of welds at various angles to the standard  $90^\circ$  angle which is widely used. A plot of the angle of intersection and the breaking stress extent ratio is shown for both the theoretical throat depth and for actual throat depth in Figures 2.10 and 2.11.

The strength of welds at angles of greater than  $120^\circ$  will be completely satisfactory if the workmanship is of good quality.

Ductility was also checked and the experimenters concluded that the welded specimens for  $\theta > 120^\circ$  had sufficient ductility.

Nishida, et al, also performed tests on test pieces that are shown in Figure 2.12.

They also worked out some formulas based upon maximum principal stress theory, maximum shear stress theory, and shear strain energy theory. The following assumptions were made:<sup>5</sup>

1. Breaking takes place on one plane which passes along the root.
2. Stress in breaking times is distributed uniformly on the breaking section.
3. The shape of the deformed fillet weld is as shown in Figure 2.13.

When the acting force  $P$  is decomposed to normal force  $N$  and shear force  $T$  on the breaking section of the fillet weld, we have

$$N = p \sin r$$

and

$$T = p \cos r$$

and the overall section area of breaking section is

$$a l \sec \left( \frac{\theta}{2} - r \right)$$



FIGURE 2.10  
RELATION BETWEEN INTERSECTING ANGLE  
AND THE UNIT BREAKING STRESS  
(THEORETICAL THROAT DEPTH)

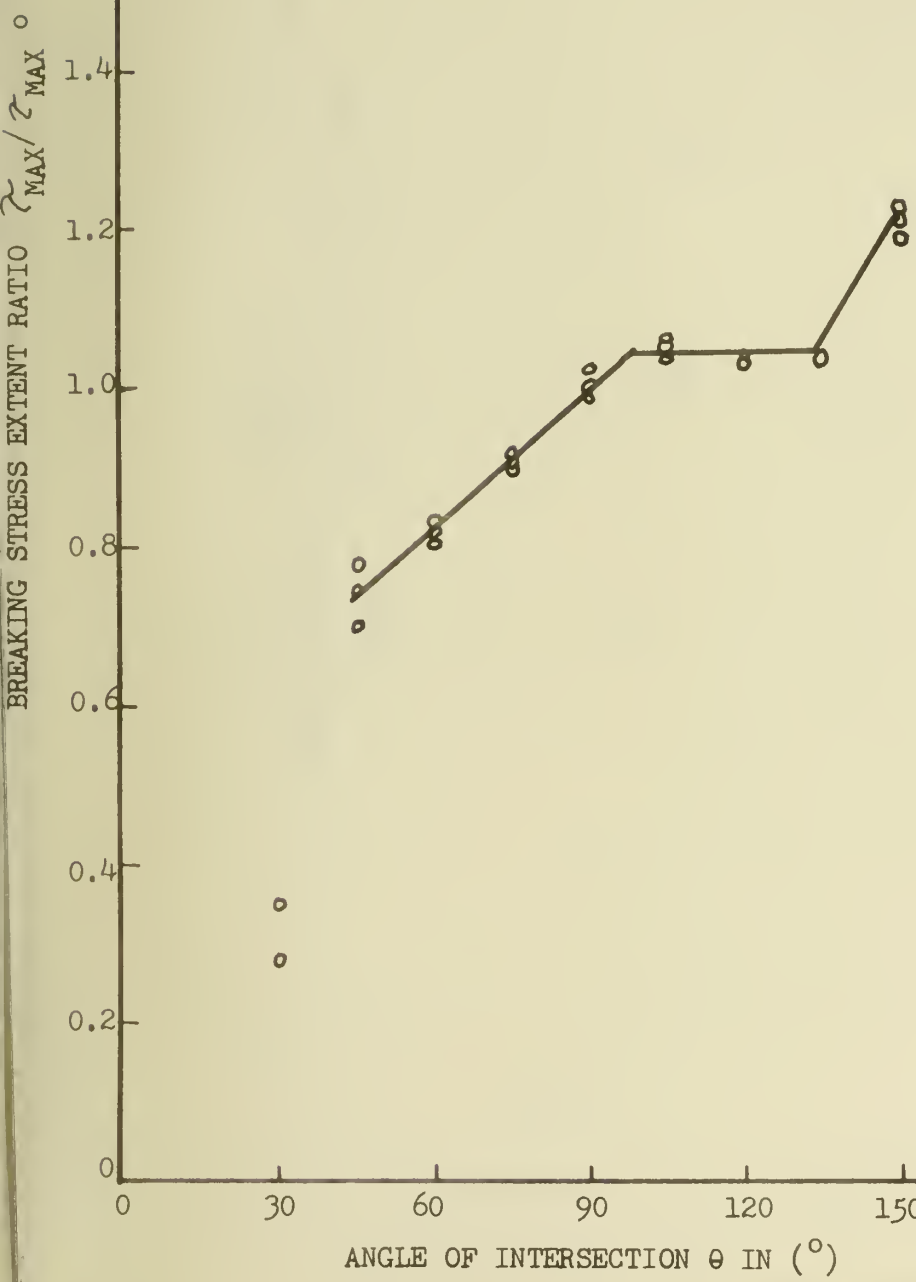




FIGURE 2.11.  
RELATION BETWEEN INTERSECTING ANGLE AND THE UNIT  
BREAKING STRESS (ACTUAL THROAT DEPTH)

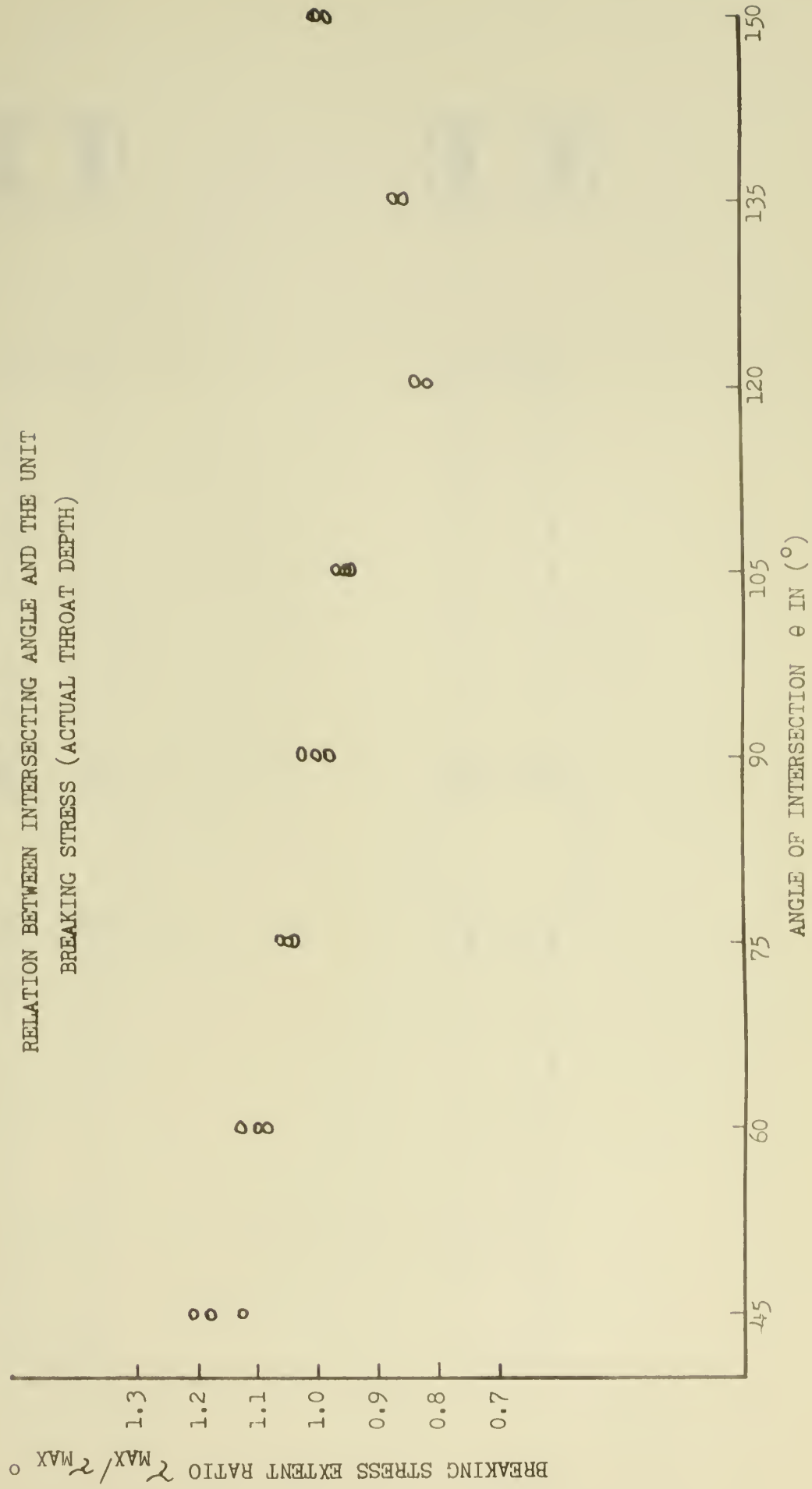
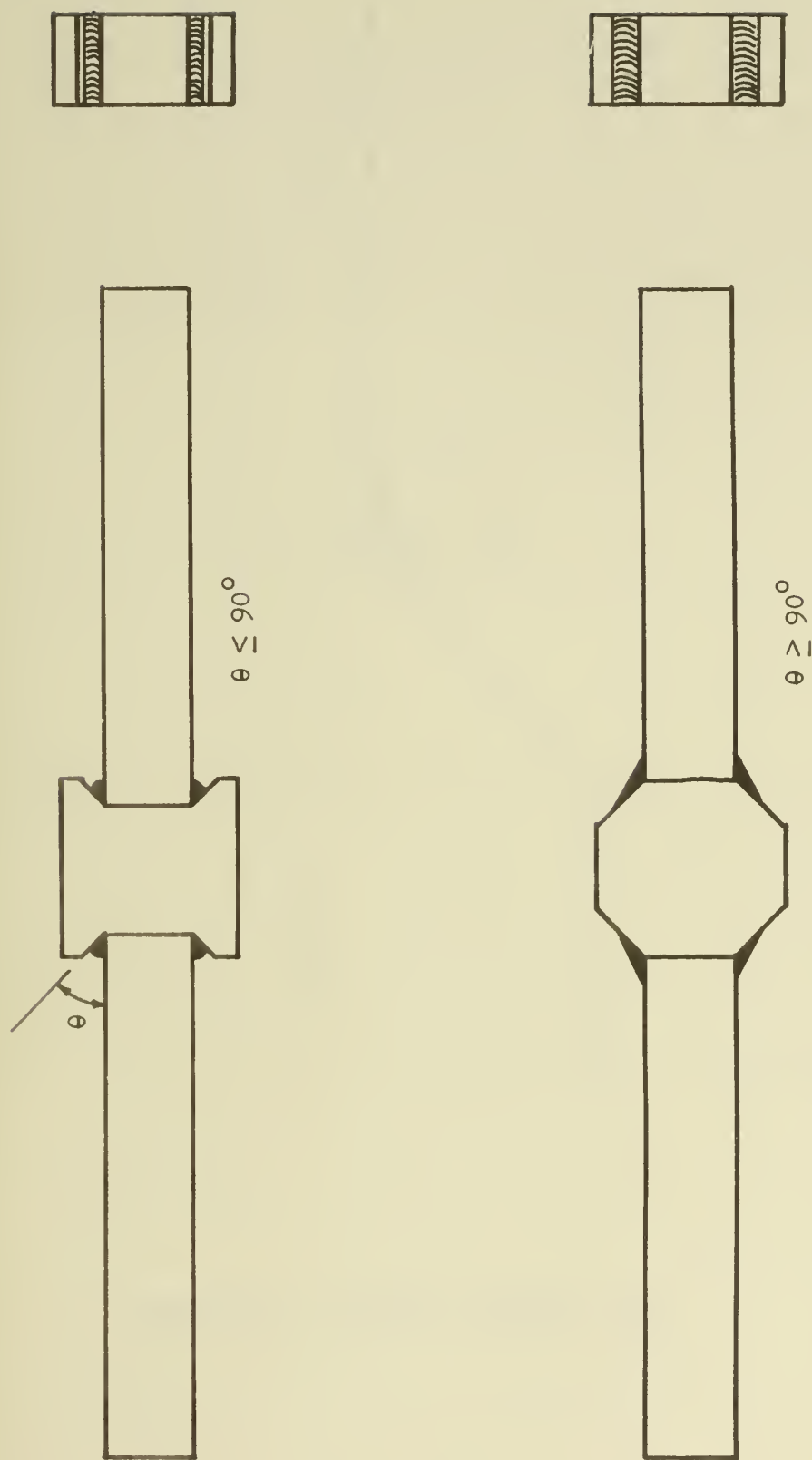




FIGURE 2.12. SHAPE OF F-TYPE TEST PIECES<sup>5</sup>



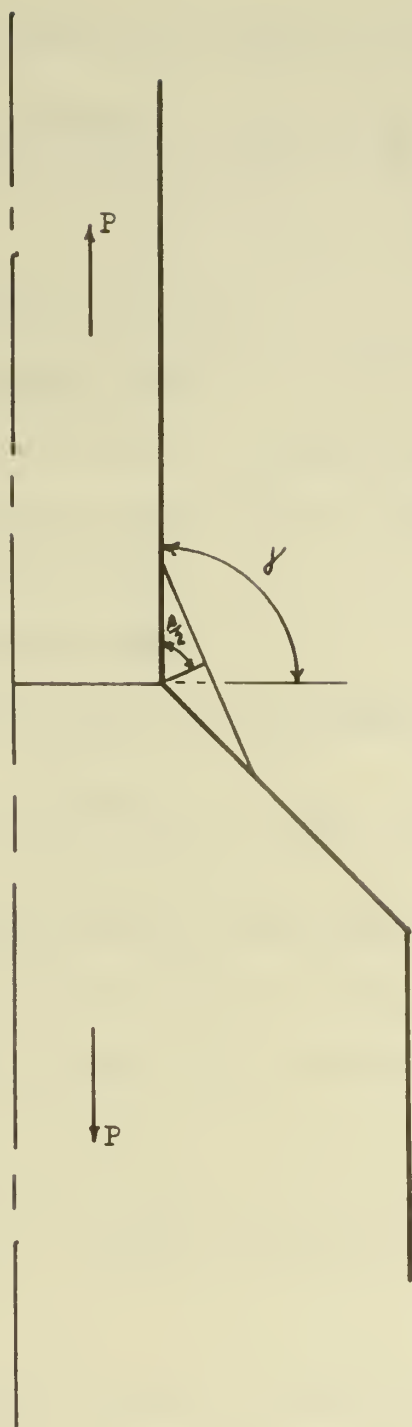


FIGURE 2.13. SHAPE OF DEFORMED WELD



Therefore, the normal unit stress on the breaking section is

$$\sigma_L = \frac{P \sin r}{a l \sec(\frac{\theta}{2} - r)} = \frac{P}{a l} \cos(\frac{\theta}{2} - r) \sin r$$

Where:

$\theta$  = intersecting angle

$r$  = breaking angle

$\sigma_L$  = normal stress to breaking section

$\sigma_{//}$  = parallel shear stress to breaking section

$a$  = throat depth

$l$  = welding length

The unit shearing stress on the breaking section is

$$\sigma_{//} = \frac{P \cos r}{a l \cdot \sec(\frac{\theta}{2} - r)} = \frac{P}{a l} \cos(\frac{\theta}{2} - r) \cos r$$

Using the maximum principal stress theory that assumes that breaking takes place when the amount of work spent to attain deformation reaches a definite value, the maximum stress in the throat section is

$$\frac{P}{a l} = 2 \sigma_w \times \frac{1}{\cos(\frac{\theta}{2} - 2) [\cos r + \sqrt{1 + 3 \cos^2 r}]}$$

Where:

$\sigma_w$  = tensile strength of welded metal

$r$  = has to be obtained from the following transcendental function

$$\frac{\sin(\frac{\theta}{2} - r)}{\cos(\frac{\theta}{2} - r)} = \frac{3 \cos r \sin r - \sqrt{1 + 3 \cos^2 r} \cdot \cos r}{1 + 3 \cos^2 r + \sqrt{1 + 3 \cos^2 r} \cdot \sin r}$$

Using the maximum shear stress theory which assumes that the



breaking takes place on a section in which the shear stress becomes maximum, the maximum unit stress per unit throat sectional area is

$$\frac{P}{a l} = \tau_w \cdot \frac{1}{\cos \left( \frac{\theta}{2} - r \right) \cos r}$$

Where:

$\tau_w$  = shearing strength of welded metal

And

$$r = \frac{\theta}{4} - \frac{n}{2} \pi \quad (n = -1, 0)$$

And using the shear strain energy theory which assumes that the breaking takes place when the amount of work spent to attain the deformation reaches a definite value  $\sigma_c$ , the maximum unit stress in the throat section is

$$\frac{P}{a l} = \sigma_c \times \frac{1}{\sqrt{1 + 2 \cos^2 r \cdot \cos \left( \frac{\theta}{2} - r \right)}}$$

Where:

$\sigma_c$  = is put equal to  $\tau_w$ , the tensile strength of the welded metal.

$r$  = has to be obtained from the following transcendental function

$$\tan \left( \frac{\theta}{2} - r \right) = \frac{\sin 2 r}{2 + \cos 2 r}$$

And using the theory proposed by I.I.W. 15<sup>th</sup> committee which has no relation to the other breaking theories, but, in which

$$\sigma = \sqrt{\sigma_{\perp}^2 + 1.8 \sigma_{\parallel}^2}$$

And the unit stress per unit throat sectional area at the time of breaking is

$$\frac{P}{a l} = \sigma_c \cdot \frac{1}{\cos \left( \frac{\theta}{2} - r \right) \sqrt{1 + 0.8 \cos^2 r}}$$



These investigators found that in the case of a deformed front fillet weld, the maximum principle stress theory is the most applicable theory. They also calculated the theoretical throat depth required to assure the same strength as a standard manual arc weld with 5 mm diameter welding rod, an intersecting angle of  $90^{\circ}$  and a theoretical throat depth of 5 mm (7.1 mm size).

This relation is presented in Figure 2.14.

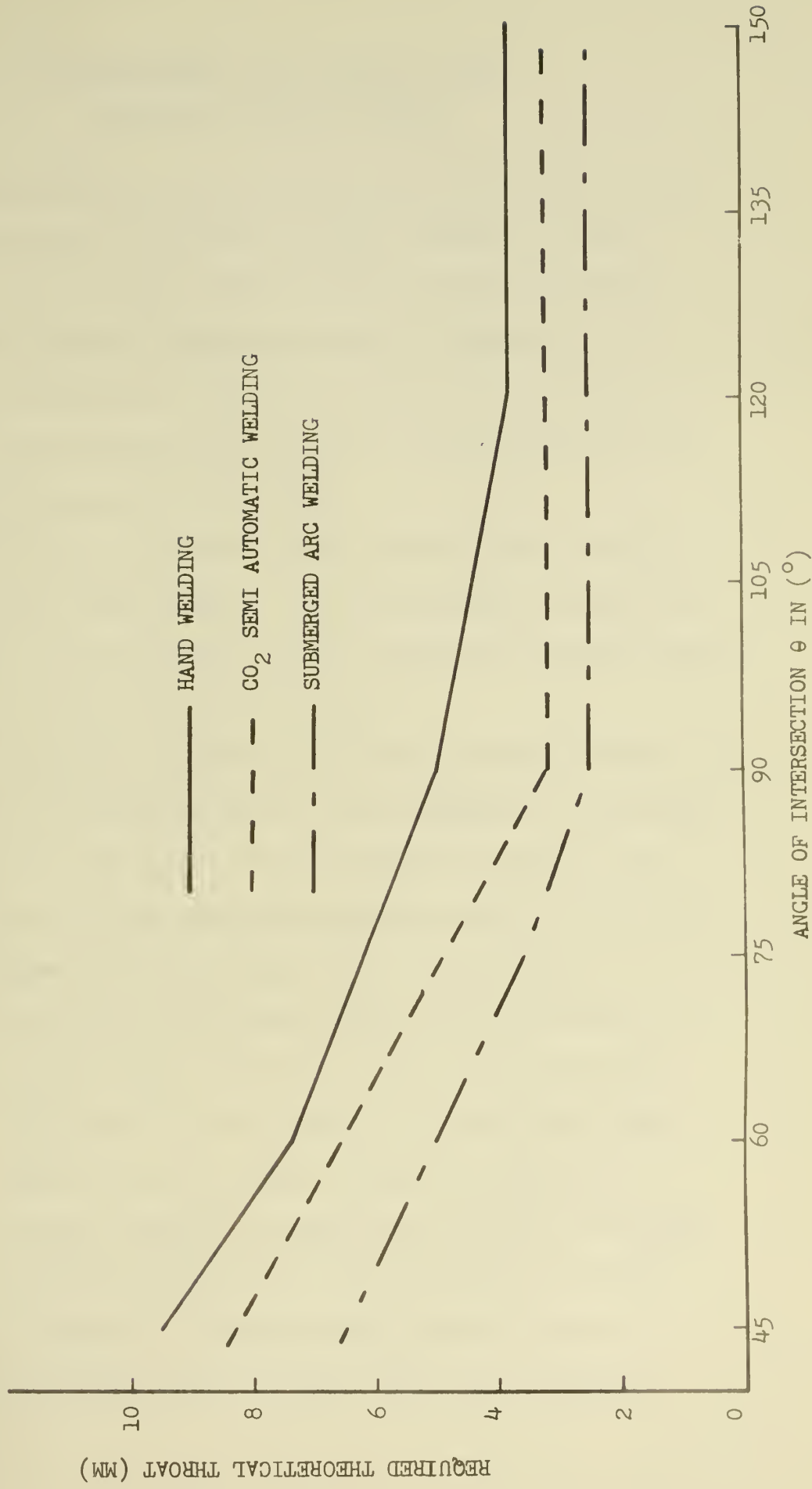
Nishida, Tanaka, and Tanaka drew the following conclusions from their work:<sup>5</sup>

1. The depth of weld penetration varies proportionately with the intersecting angle until a constant value is reached. However, a  $30^{\circ}$  intersecting angle yielded a weld with extreme deficiency of weld penetration for every welding method.
2. The weld strength of an intersecting angle of  $30^{\circ}$  was extremely low; however, the weld strength of angles above  $45^{\circ}$  was good.
3. Ductility tended to increase with an increasing intersecting angle; however, rigidity was scarcely influenced by a change in intersecting angle and remained almost constant.
4. In deformed fillet welds, the mean strength per unit throat sectional area increased as weld penetration increased; however, when the weld penetration reached a definite value, the mean strength became constant.

Now that we have looked at some of the results of work that has been done in the area of static strength of fillet welds, we will look at another area that deserves some serious consideration; that is the area of fatigue.



FIGURE 2.14.  
THEORETICAL THROAT DEPTH NECESSARY TO HAVE THE  
SAME STRENGTH AS A 5 MM 90° MANUAL ARC WELD





### III EXPERIMENTAL AND THEORETICAL WORK CONCERNING FATIGUE STRENGTH

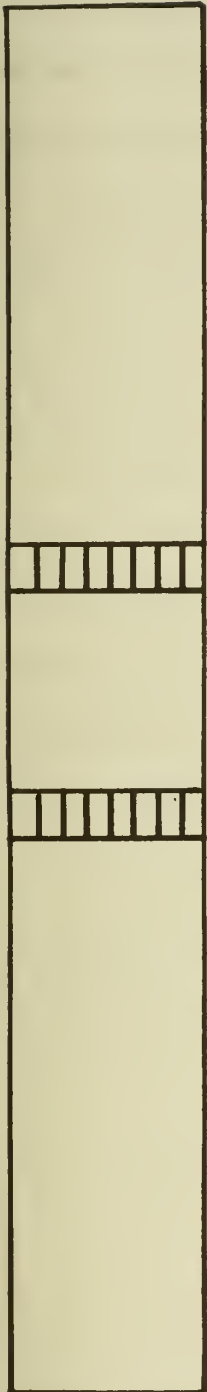
In this section, we will review some of the results of work that has been done in the area of fatigue strength of fillet welds. In one such study, Macfarlane and Harrison<sup>6</sup> performed experiments using test specimens as shown in Figure 3.1.

In the fabrication of these test pieces, all the welds were made using the downhand position, and the welding start and stop positions were removed by machining.

The specimens were tested using a pulsating axial loading in which the lower limit was zero. And the criterion of failure was the complete rupture of the test piece whether the failure occurred through the fillet weld or the base plate.

It is generally known that the fatigue strength of welded connections is independent of the tensile strength of the material employed in the connection. The investigators noted that when a weld failure occurred, the crack propagated from the weld root at right angles to the main plate until the final stages of propagation when the crack turned through  $45^{\circ}$  and proceeded through the weld throat. Therefore, in this study, the weld stresses were based on the leg size and not on the throat size which is usually the case in static strength investigations. Because it is very difficult to measure the weld size accurately, nominal weld sizes were used. This was estimated to introduce less than a 10% error. It became apparent that the ratio of weld size to the main plate thickness ( $2W/T$ ) is the deciding





A. COVER PLATE TYPE JOINTS



B. T-TYPE JOINTS

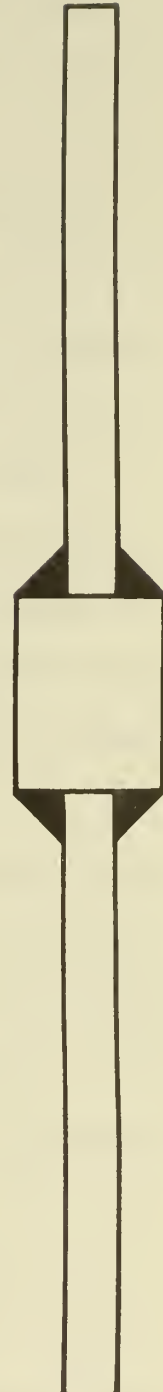


FIGURE 3.1. DIAGRAM OF TEST SPECIMENS<sup>6</sup>



factor as to where the failure will occur. If this value is low, the failure will propagate from the root of the weld; and, if the value is high, the failure will propagate from the toe of the weld. The optimum values of  $2W/T$  were found to be 1.5 for the cover type joints and 2.0 for the T-type joints.

Also, there is a relationship between joint geometry and failure location. This is demonstrated by the fact that the cover plate type joints had 88% of their failures in the weld; whereas, in the T-type joints, all of the failures occurred in the weld.

In another study, Solumsmoen<sup>7</sup> investigated the fatigue strength of specimens with holes, butt welds, and fillet welds. Included in the study were both mild and high tensile strength structural steels. The tests were performed in Det norske Veritas Laboratory. The test piece employed for fatigue tests of fillet welds is shown in Figure 3.2.

It was found that for fillet welded joints, both mild steel and high strength steel can be represented by the same S/N curve. Also the fatigue strength of double fillet welds does not increase significantly using basic iron powder electrodes instead of ordinary basic electrodes. For more detailed data, the reader is referred to reference 7.

Since fatigue strength is a major factor in fillet welds, and it is difficult to alter the design to either avoid fillet welds or place fillet welds in areas of low stress, there is much interest in methods that may improve the fatigue strength of joints.

The Welding Institute Research Laboratories<sup>8</sup> conducted some experi-



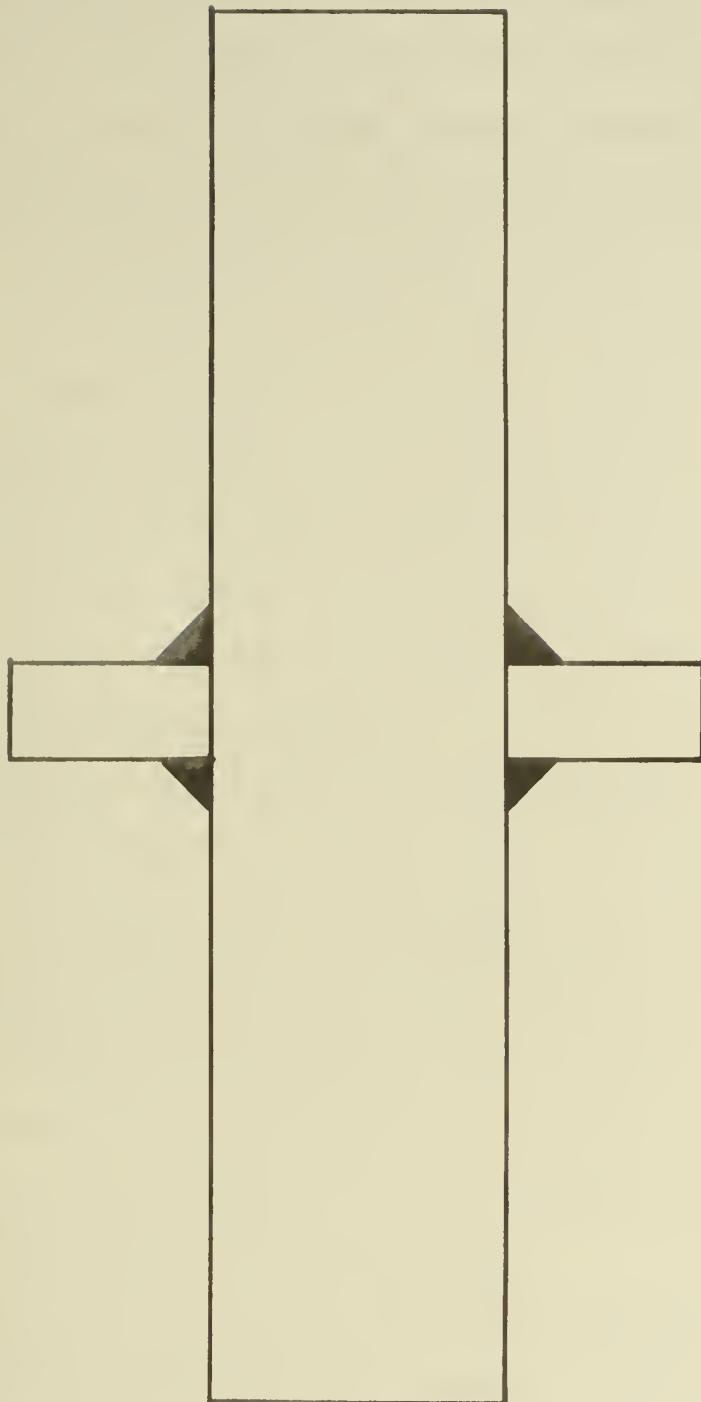


FIGURE 3.2. TEST PIECE OF A NON-LOAD CARRYING DOUBLE FILLET WELD?



ments to determine the effect of peening and grinding on the fatigue strength of fillet welded joints. The test pieces had non-load-carrying attachments fillet welded either parallel to or transverse to the direction of the applied stress. These specimens were fabricated in such a manner that the direction of stressing was parallel to the rolling direction of the material. A sample of the test pieces can be seen in Figure 3.3.

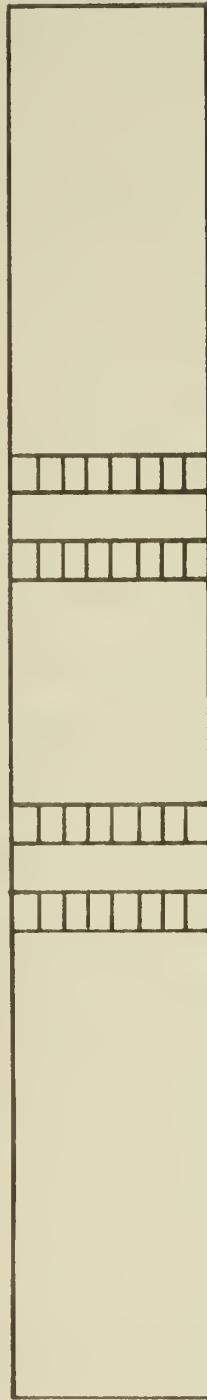
To study the effect of peening, the samples were peened with a pneumatic hammer fitted with a solid tool having a rounded end of approximately 1/2 inch diameter. This hammer was moved along the toe of the weld at a speed of approximately 18 inches per minute. Usually three runs of peening were required on each specimen to ensure that the whole length of the weld toe was subjected to the peening treatment.

Two types of local machining were also studied. The first consisted of grinding only at the weld toe. This grinding was carried out to ensure that the grinding marks were parallel to the direction of the stress. The second type of machining involved machining the whole weld to yield a concave profile and a smooth blend of the weld into the plate surface. The goal of this treatment was to obtain the maximum possible increase in strength that could result from machining.

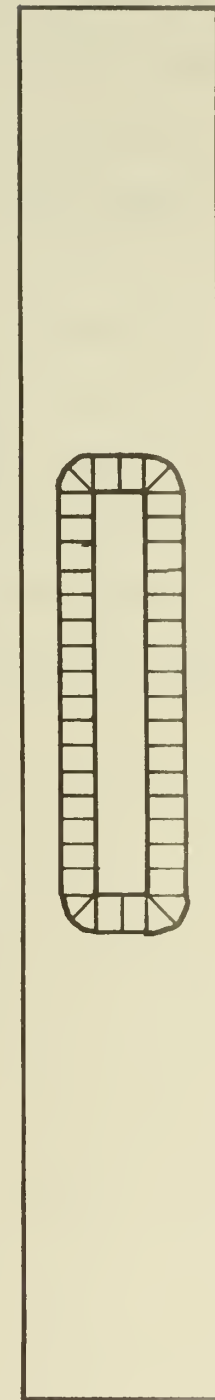
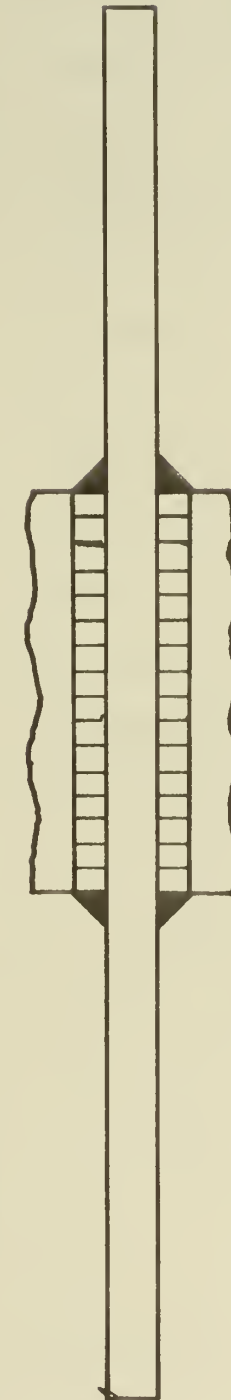
During the testing, all specimens were axially loaded with one of the following stress cycles. Either the test piece was loaded with a pulsating tension with a lower limit of zero or an alternating load with the minimum and maximum stresses equal



A. SPECIMENS WITH TRANSVERSE GUSSETS



B. SPECIMENS WITH LONGITUDINAL GUSSETS

FIGURE 3.3. DETAILS FOR TEST SPECIMENS<sup>8</sup>



in magnitude but opposite in sign. The criterion of failure was the complete rupture of the test piece.

Some of the samples were fabricated with welds around the ends of the gussets while others were left with the ends unwelded. It was found that the fatigue strength of these two types of samples were the same for the non-load-carrying longitudinal fillet welds. The fatigue strength of samples was found to increase for both the peening treatment and local machining. The increase in strength grew larger as the life increased for the case of peening; whereas for the local machining operation, the increase was about the same for the whole range examined. The test results showing the effects of grinding and peening for mild steel specimens with longitudinal and transverse gussets are shown in Figures 3.4 and 3.5 respectively.

In the tests employing pulsating tension, it was found that peening increased the fatigue strength by about 75%, while with both pulsating tension and alternate loading, the full local grinding operation increased the fatigue strength by about 50% in all cases except that of mild steel specimens with transverse fillet welds which yielded nearly 100% improvement over the as-welded condition. Even though this is less increase than that obtained from peening, the difference in the slope of the S/N curves for peened and ground specimens accounts for the fact that grinding was found to be more effective than peening for tests in which the number of cycles were less than about 50,000. Full grinding of the test pieces with longitudinal fillet welds



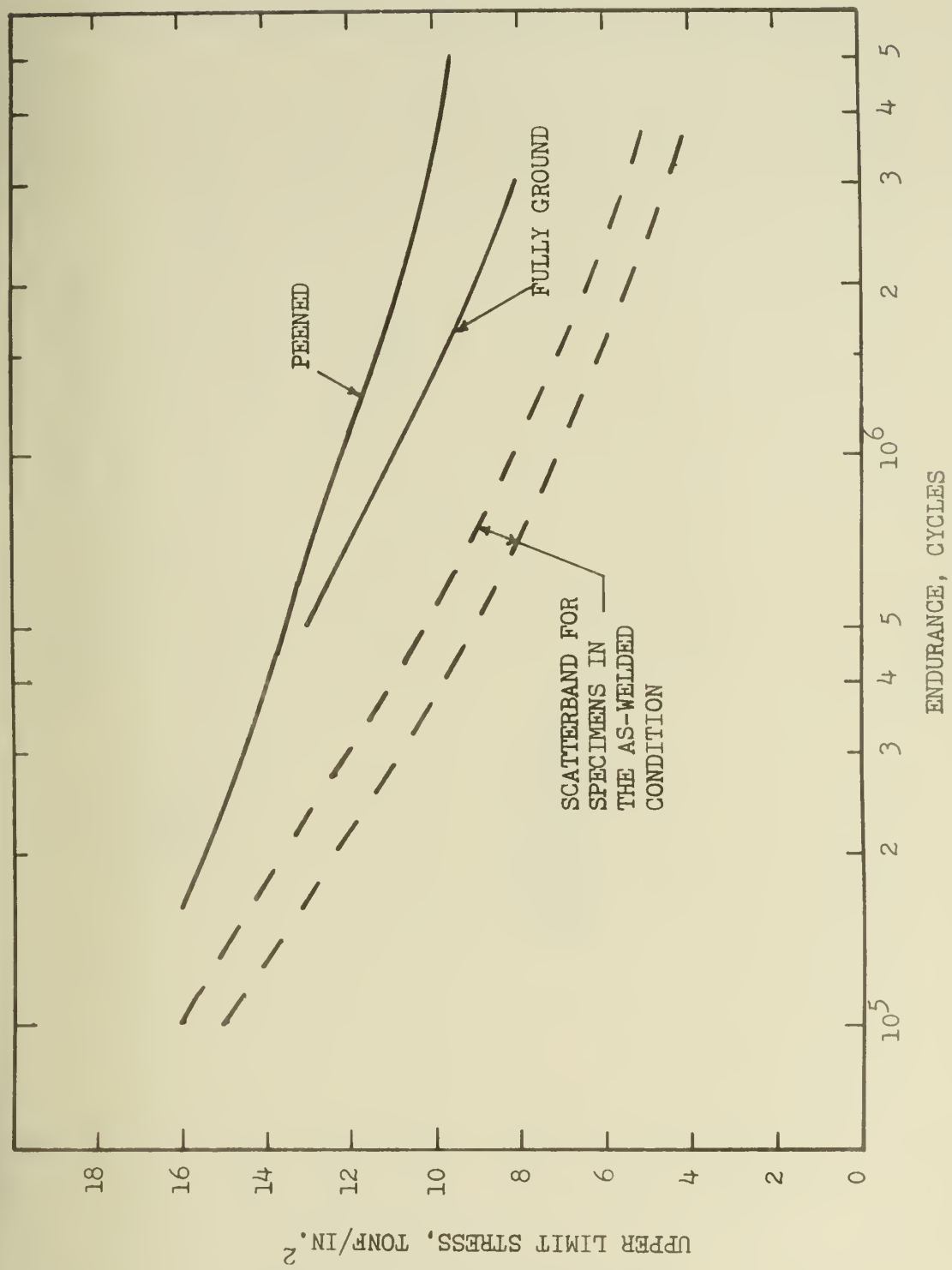


FIGURE 3.4. FATIGUE TEST RESULTS FOR MILD STEEL SPECIMENS WITH LONGITUDINAL GUSSETS SHOWING THE EFFECTS OF GRINDING AND PEENING.  
8



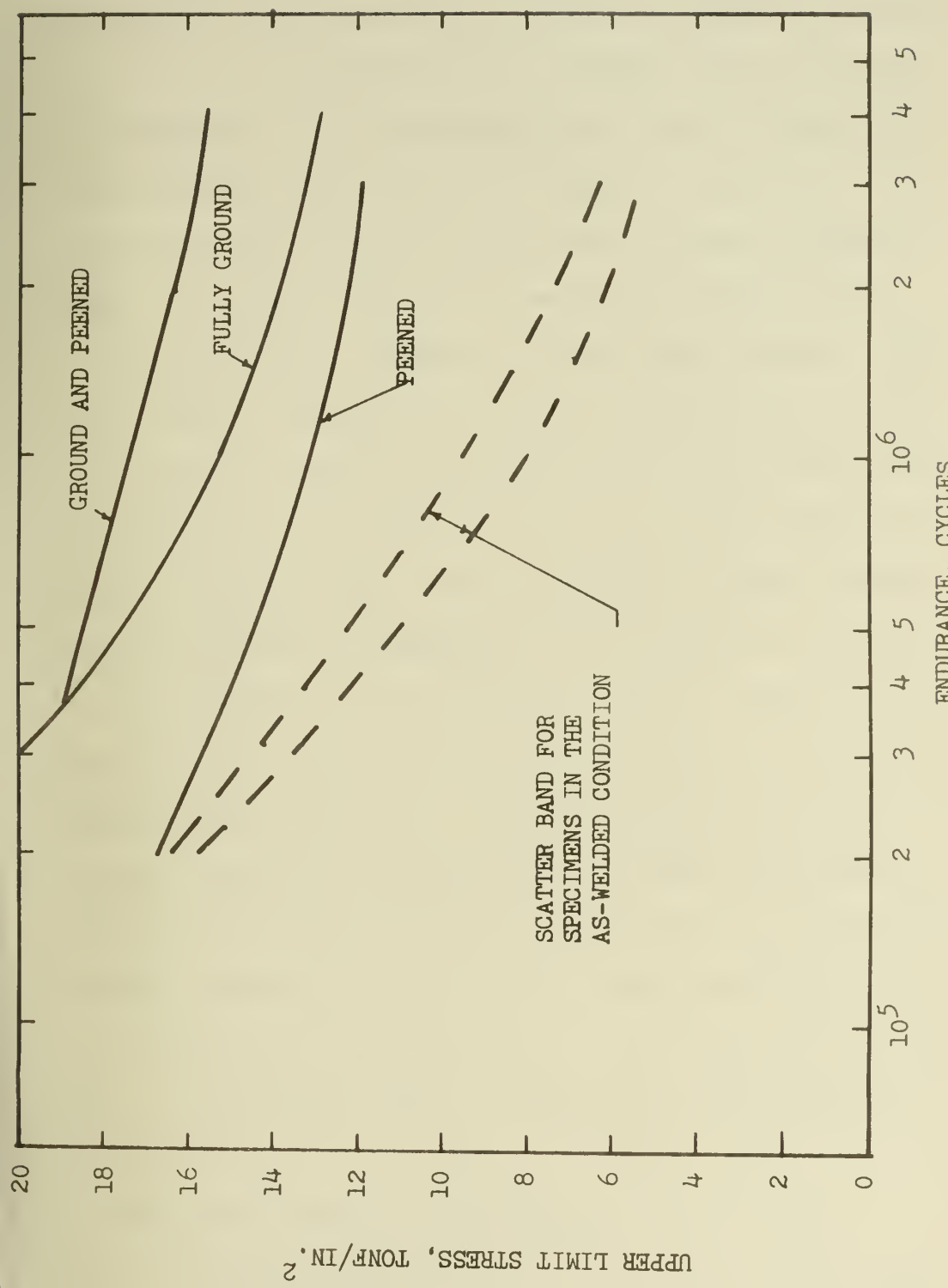


FIGURE 3.5. FATIGUE TEST RESULTS FOR MILD STEEL SPECIMENS WITH TRANSVERSE GUSSETS SHOWING THE EFFECTS OF GRINDING AND PEENING.<sup>8</sup>



normally failed as a result of initiation at the root of the weld. In the case of light grinding at the weld toe, the improvement was found very variable. This is assumed to be related to the fact that it is very difficult to control the degree of grinding. This technique is considered to be unreliable and is, therefore, not recommended. It is interesting to note that in tests performed on samples with transverse gussets, it was found, if the samples were fully ground and also peened, fatigue strengths as high as the parent material could be obtained (Figure 3.5).

Several years ago, Maddox<sup>9</sup> analyzed fatigue cracks in fillet welds. While the results of this work are not of direct concern to our present problem, a brief description of his work is useful in pointing out a direction for future work in the field of fatigue strength of fillet welds. This investigator collected various proposed solutions that appeared in the literature and adapted them, where possible, to the particular case of a semi-elliptical surface crack at the toe of a fillet weld. This is the mode of failure in most of the lower fatigue strength welded joints. It was found that the two features of this problem which received little attention were the shallow crack shapes (low  $a/2c$  values) which are relevant to fatigue cracks in most welded joints and the external stress concentration due to the shape of the weld. Figure 3.6 demonstrates what is meant by the semi-elliptical surface crack.

The general form of the solution is

$$K = \sigma (\pi a)^{1/2}$$



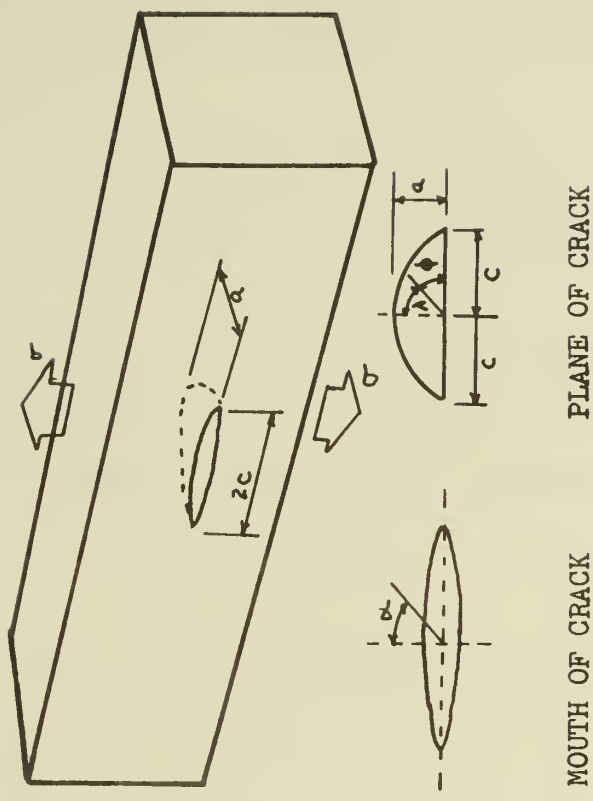


FIGURE 3.6. SEMI-ELLIPTICAL SURFACE CRACK IN A PLATE IN TENSION<sup>9</sup>



However, in most cases correction factors are used to account for the geometry of the crack and the cracked body. Irwin<sup>7</sup> suggested that the solution should be modified as follows:

$$K = \frac{M_s M_t M_p}{\Phi_0} \sigma (\pi a)^{1/2}$$

Where:

$M_s$  = a correction factor to allow for the effect of free surface at the mouth of the crack. It depends on the crack depth to width ratio  $a/2c$  and the position around the crack front as defined by  $\phi$ .

$M_t$  = a correction factor to allow for the presence of a free surface ahead of the crack which depends on the crack depth to plate thickness ratio  $a/B$  and the crack front shape  $a/2c$  (sometimes referred to as the back-surface correction).

$M_p$  = a correction factor to allow for the crack tip plasticity and depends on the size of the crack tip plastic zone.

$\Phi_0$  = the complete elliptic integral defined as

$$\Phi_0 = \int_0^{\pi/2} \left[ 1 - \left( 1 - \frac{a^2}{c^2} \right) \sin^2 \phi \right]^{1/2} d \phi$$

For details of each of these correction factors as well as solutions for special cases which have been used to approximate the general solution, the reader is referred to reference 9.

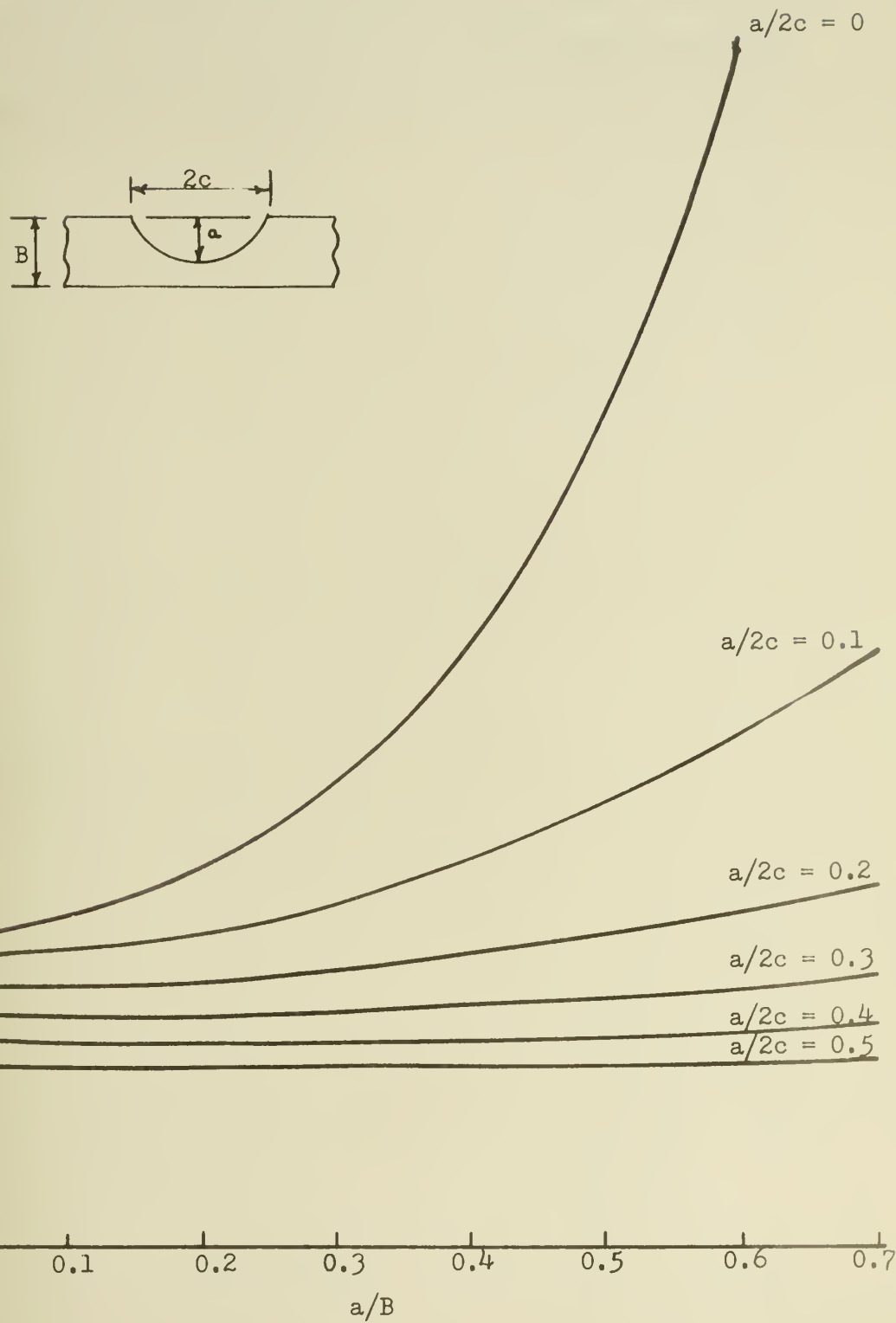
It is interesting to look at the variation of the total correction term  $(M_s M_t)/\Phi_0$  with crack depth ( $a/B$ ) for particular  $a/2c$  values. As demonstrated by Figure 3.7, because we see that for fatigue cracks in which  $a/2c > 0.3$ , we can use, for practical purposes, the following expression for  $K$  at any crack depth.

$$K = \sigma (\pi a)^{1/2}$$



FIGURE 3.7.

VARIATION OF  $(M_s M_t / \Phi_0)$  WITH CRACK DEPTH  
FOR VARIOUS SHAPES  $(a/2c)^9$





This work may be of great help in future studies in connection with the strength of fillet welds as welded. Statistical studies may predict the largest probable crack in a weld given a certain result of quality assurance inspection. This might lead to a set of specifications with more detail as to what imperfections can be accepted by the inspector.



## IV EXPERIMENTAL AND THEORETICAL WORK CONCERNING SHEAR STRENGTH

In this section, we will review some of the experimental and theoretical work that has been done in the area of shear strength of fillet welds. Swannell<sup>11</sup> conducted an experimental program designed to measure the deformations that occur in the weld metal itself.

In order to perform experimental tests, a simplified test piece shape was needed to ensure that the weld carried a uniform shearing intensity throughout its length. This was especially important because it is analytically extremely difficult to determine the shearing intensity distribution along the length of a fillet weld in any conventional joint. In these joints, it becomes necessary to determine an empirical "load-pick-up" curve, and, thus, the gradient of this curve yields the intensity distribution. The load-pick-up curve is very difficult to obtain in that it requires very accurate experimentation in order to obtain satisfactory results.

By choosing a special joint geometry in which the manner of loading and the symmetry of the test piece are such as to produce uniform shearing intensity, one can obtain intensity deformation relationships for the weld metal. A symmetrical test-piece implies a uniform toe displacement characteristic from cross section to cross section along the length of the weld as well as uniform intensity.

The test piece employed by Swannell<sup>11</sup> is shown in Figure 4.1. It can be seen that this test piece would obtain a uniform shearing



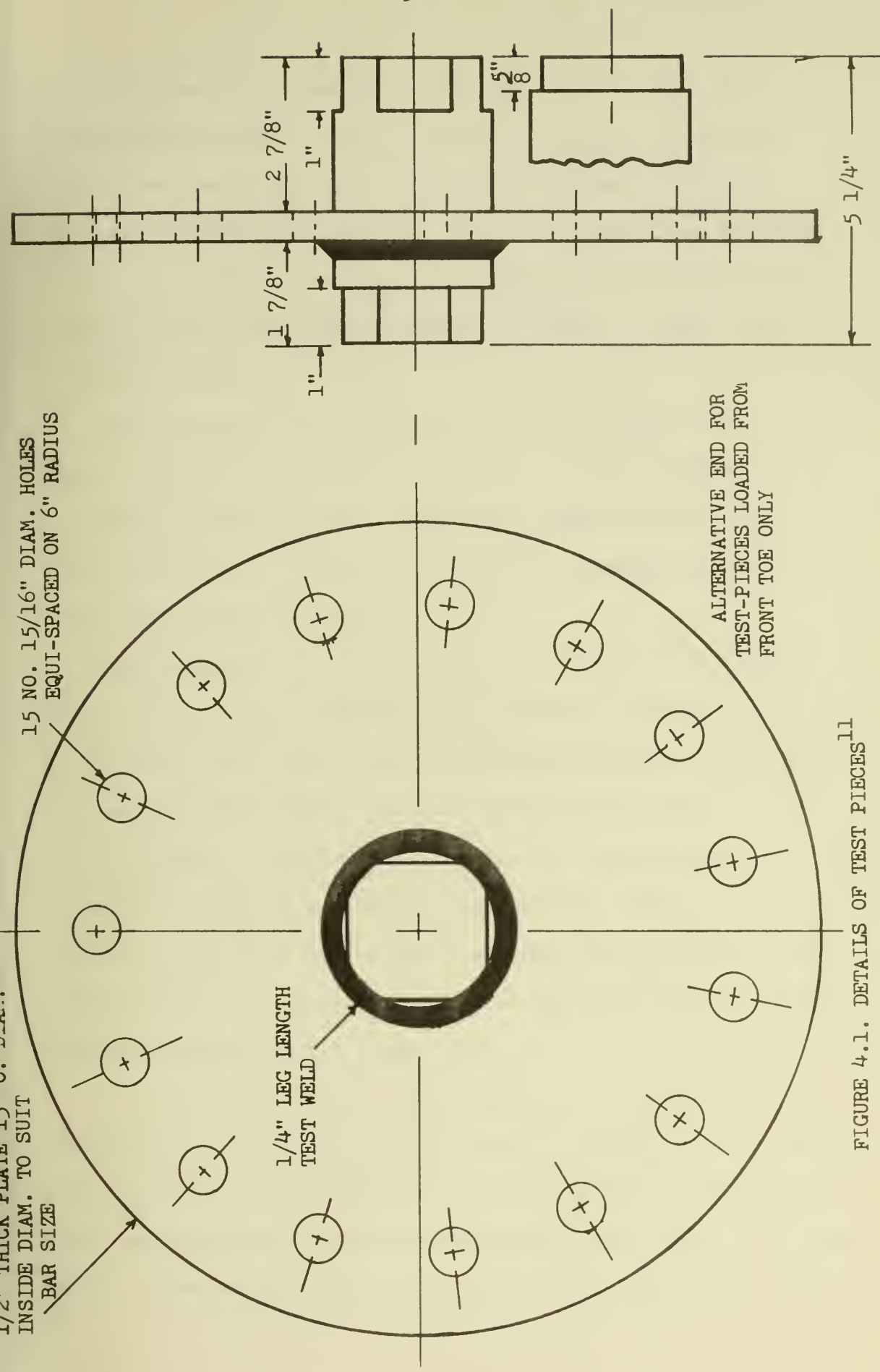


FIGURE 4.1. DETAILS OF TEST PIECES<sup>11</sup>



intensity when the circumferential fillet weld is subjected to shearing stresses that produce a reactant torque. The ends of the bar were machined square so that they were an exact fit in the seating collars through which the applied torque was delivered. When it was desired to apply the load solely at the toe or at the heel, one or the other square ends was replaced by a free-running circular bearing.

The welds were made on one side of the main plate with 8 s.w.g. electrodes, and they were machined back from 5/16 inch to a nominal 1/4 inch leg size. Upon visual inspection of the completed test pieces, it was not possible to detect the starting point of the welding process.

This test series was made up of fifteen test-pieces. Two of these test pieces were loaded only at the end of the bar adjacent to the test weld. These samples were designated MS.T. because the load was delivered entirely to the front toe of the weld.

In another sample designated MS.H., the load was applied to the end of the bar at a distance from the weld, thereby being delivered to the heel of the weld. A comparison of the MS.T. and MS.H. samples can be seen in the plot of shearing intensity versus apparent surface strain in Figure 4.2.

It can be seen that the joint stiffness is a function of the applied load. Table 4-1 gives the details of tests for each sample. After inspecting the samples that were fractured, the investigators found that there was very little root penetration in any of the test welds. It was found that the gradients of the "unload/load" loops



FIGURE 4.2. RELATIONSHIP BETWEEN  
APPARENT SURFACE STRAIN AND  
SHEARING INTENSITY<sup>11</sup>

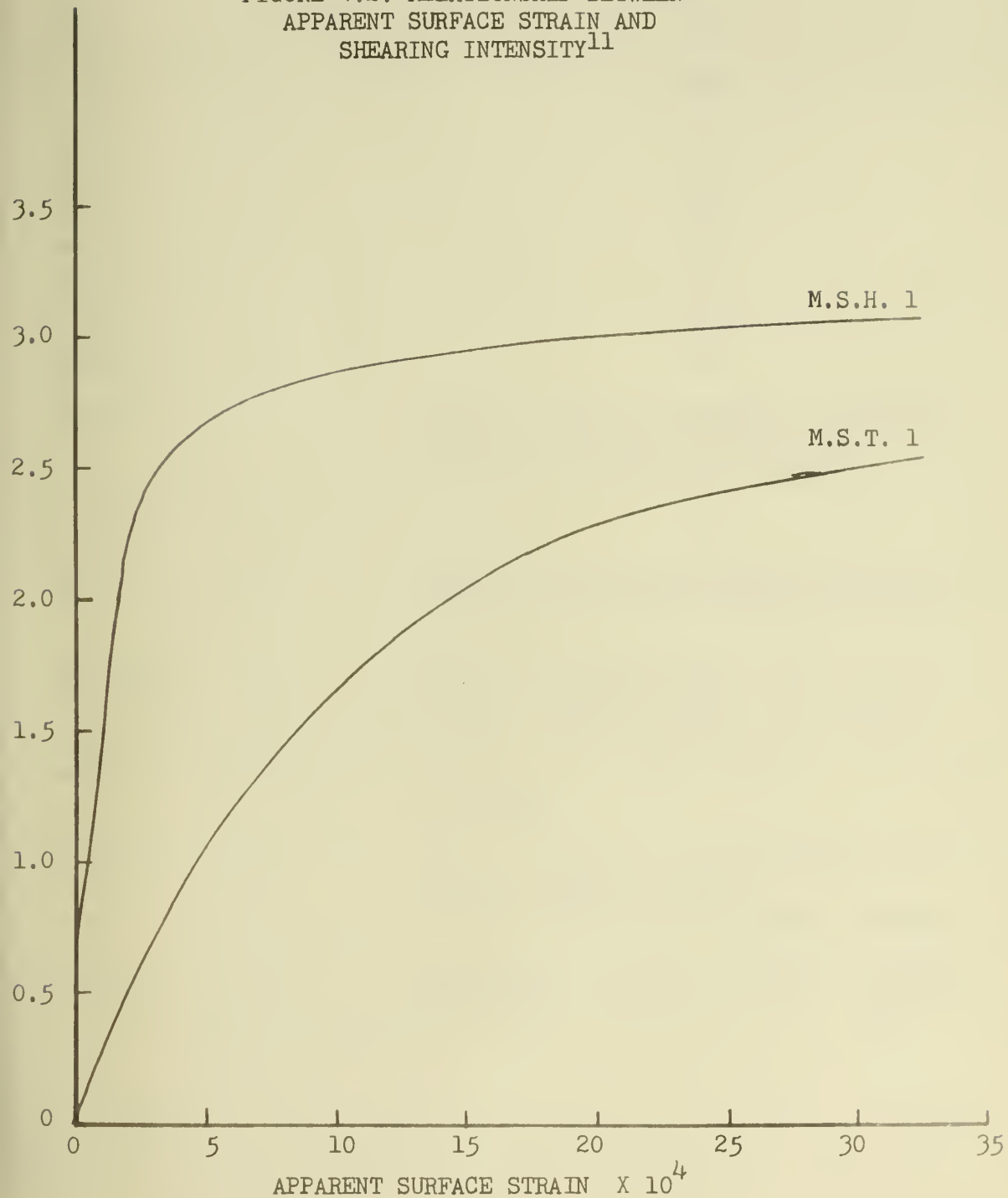




TABLE 4-1. Details of Tests<sup>11</sup>

Ref. No.	Nominal Dia., in.	Description of Test Loading
MS.B 1	3	Loading continuously from zero to failure. No cycling.
MS.B 2	3	Do.
MS.B 3	3	Do.
MS.B 4	3	Do.
MS.B 5	3	Do.
MS.B 6	3 $\frac{1}{2}$	Do.
MS.B 7	4	Do.
MS.B 8	4 $\frac{1}{2}$	Do.
MS.B 9	3	Variable loading as defined by following load per jack (lb): 0-400-0-800-0-1,200- 0-1,600-0-2,000-0-2,400-0-failure
MS.B 10	3	Do.
MS.B 11	3	Variable loading as defined by following load per jack (lb): 0-2,800-0-failure
MS.B 12	3	0-500-0-1,000-0-1,500-0-2,000-0-2,500-0 Reverse test-piece then: 0-500-0-1,000-0-1,500-0-2,000-0-failure
MS.T 1	3	Loading continuously from zero to failure. No cycling.
MS.T 2	3	0-500-0-1,000-0-1,500-0-2,000-0-2,500-0 Reverse test-piece then: 0-500-0-1,000-0-1,500-0-2,000-0-failure
MS.H 1	3	Loading continuously from zero to failure No cycling.



progressively decrease as the upper limit of the loading was increased. The investigators suggested that these decreasing gradients can be accounted for by cracking at the weld root.

While a theoretical analysis of an actual weld mass with varying joint geometry along both the length and width of the fillet weld and with essentially three-dimensional stress distribution, it is possible to obtain an elastic solution in an idealized geometry employing a numerical technique.<sup>11</sup>

However, it should be noted that this solution is not a general solution, but it is also limited by the assumptions concerning the elastic module of the weld metal throughout the weld length.

Swannell<sup>11</sup> reached the following conclusions as a result of his investigation:

- "1. The results do not represent a full description of the behavior of a conventional longitudinal fillet weld, but they do show the effect of joint stiffness and manner of load application on the deformations.
- "2. Stiffness is determined by many parameters, including neighboring parent member geometry, weld size, amount of root penetration, manner of load application, and metallurgical considerations.
- "3. Joints which are initially very stiff remain stiff under increasing load.
- "4. The whole question of the influence of residual stress and their tendency to produce premature failure can only be answered in the context of whether, in a good weld metal like mild steel, they are of significance compared with the unavoidable high stress peaks in the primary stress distribution."

In another study concerning shear strength, Kassov<sup>12</sup> presented some test results on strap and flange joints that were subjected to



shear stresses, and he also recommended some safe limiting stresses which can be used in fillet weld calculations. More than fifty sample test-pieces were employed to allow varying such parameters as grade of steel, electrode type, plate thickness, and fillet weld length.

In the past, the permissible shear stresses for welded joints were found by multiplying the safe limiting tensile stress for the parent metal by a factor of 0.6 - 0.65.

Some sources thought that this factor could be raised to 0.7 - 1.0. In the experimental work conducted, this factor  $X_i$  was found by dividing the breaking shear stress by the nominal tensile strength. The average of the factors obtained was 0.8365; however, through an approach employing the probability of random variables Kassov<sup>12</sup> concluded that there is a 93.7 - 87.1% probability that  $X_i = 0.6 - 0.65$  is the correct figure.



## V DESIGN CONSIDERATIONS

In this section, we will examine some of the design considerations concerning fillet welds.

Boniszewski and Eldridge<sup>13</sup> discussed the problem of cracking of tube stub-header weldments in boilers of power plants. The geometry and crack location of a typical joint are shown in Figure 5.1. The failures were considered to be the result of a combination of creep rupture and high strain or thermal fatigue. In reviewing tube failures, it was found that the proportion of cracked tubes on a boiler header ranged from 2 to 50%. This is a serious problem since, at times, it is necessary to cut out good tubes to accomplish the repair of a tube which had failed. Some of the boiler tubes were modified in such a way as to remove the restraint which increased the stress in the joint. This modification did not work in every case.

The main problem seemed to result from an interaction between engineering design and welding workmanship. It was found a good weld profile, the regular 45° with well blended toes and free from under cut, could absorb the effect of the restraint by distributing the strain away from the weldment.

Upon investigation, it was also found that in some failures the dressing of the weld led to the sharpening of the angle and with this came the increase in stress concentration. The relation between stress concentration factor and the angle of the weld profile is shown in Figure 5.2. These stress concentrations are probably optimistic because in the real weld there are sometimes toe



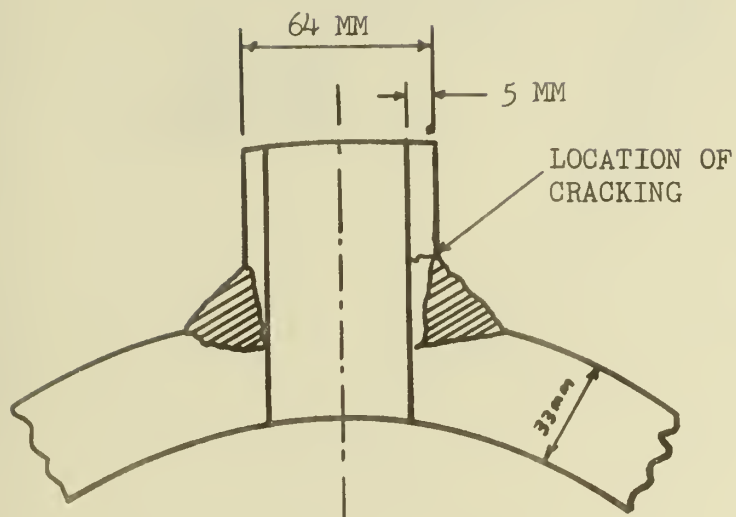


FIGURE 5.1. THE GEOMETRY OF A TYPICAL JOINT<sup>13</sup>



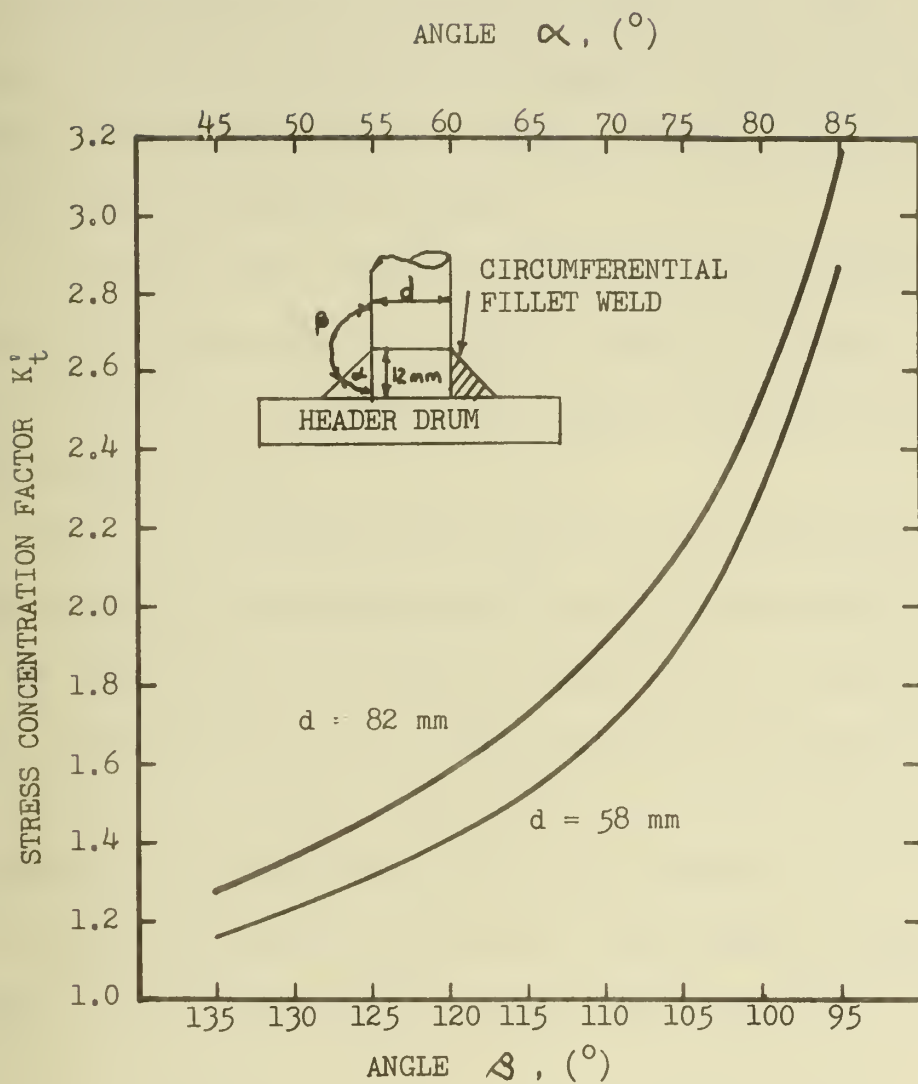


FIGURE 5.2. STRESS CONCENTRATION FACTOR AT THE FILLET WELD TOE ADJACENT TO THE TUBE<sup>13</sup>



imperfections which cause the stress concentration to be higher than the predicted value.

Boniszewski and Eldridge<sup>13</sup> recommended that the fillet weld profile must be controlled to  $45^\circ \pm 5^\circ$ . If the welds are dressed, this operation must be done in such a manner as to ensure that the overall fillet weld profile is not degraded. In any engineering design, it is important that unnecessary notches not be introduced by the lack of attention to detail.

In another study, Clark<sup>14</sup> reviewed some of the research and some of the design codes in an effort to give the designer a better tool to enable him to estimate the strength and performance of fillet-welded joints.

Due to the complexity of the geometry and stresses in a fillet weld, simplifying assumptions were made to overcome such facts as at the root of the weld the material must take on a finite displacement by straining over a very small distance and that the fillet weld can sustain residual stresses which are of the same order of magnitude as the yield stress of the weld material.

The fillet weld force system for a weld loaded at right angles to its longitudinal axis can be that as described in Figure 5.3.

Various stress theories have been used to predict the strength of a fillet weld. In some cases the yield stress is replaced with the ultimate stress for use in the equations resulting from principle stress, maximum shear stress, and strain energy theories. These theoretical approaches tend to underestimate the true strength



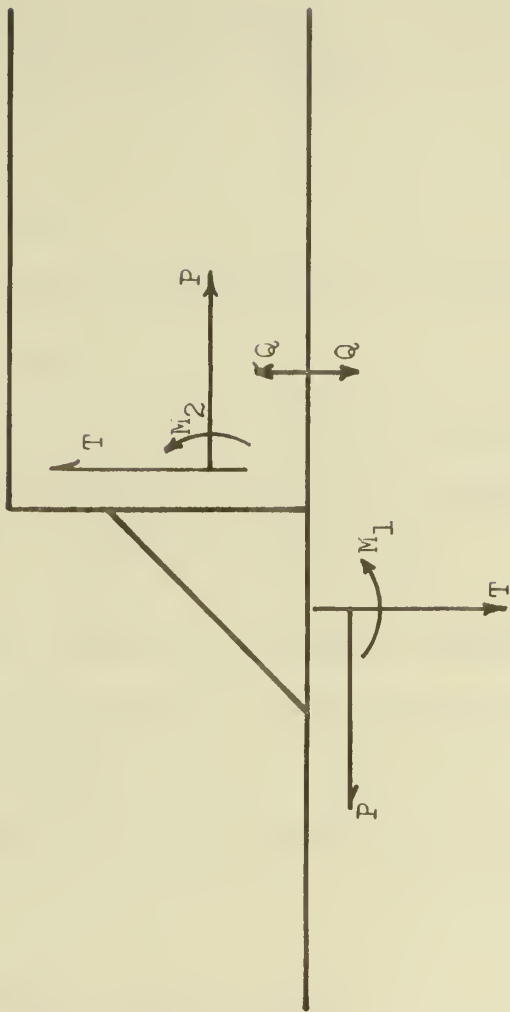


FIGURE 5.3. FORCE SYSTEM OF A FILLET WELD LOAD AT RIGHT ANGLES  
TO ITS LONGITUDINAL AXIS<sup>14</sup>



of the fillet weld.

Also several practical strength formulae have been used or recommended for use. The Von Mises equivalent stress formula, which is well known to designers, states that:

$$\sigma_e = \sqrt{\sigma^2 + 3(\tau_{\perp}^2 + \tau_{\parallel}^2)}$$

A modification of this becomes:

$$\sigma_e = \sqrt{\sigma^2 + \lambda(\tau_{\perp}^2 + \tau_{\parallel}^2)}$$

Where:

$$\lambda = 1.8$$

This modification developed from the statistical analysis of experimental data.

Another equation developed by the Stevin Laboratory<sup>15</sup> which retains the original form of the Von Mises equation states that:

$$\sigma_e = 0.7 \sqrt{\sigma^2 + 3(\tau_{\perp}^2 + \tau_{\parallel}^2)}$$

Clark<sup>14</sup> states that the most logical approach to design would be to use either modification of the Von Mises equation along with appropriate load factors.

A total load factor against weld failure under known loading becomes<sup>14</sup>

$$\frac{3}{2} \times \frac{\text{ultimate stress of plate}}{\text{yield stress of plate}} \times$$

$$\frac{\text{true strength of weld deposit}}{\text{specified strength of parent plate}} \times$$

$$\frac{\text{true weld strength}}{\text{weld strength predicted by equation}}$$

The reader is directed to reference 14 for further comparison of various design codes and load factors as determined by the above



equations.

There seems to be two different approaches to design. In one case lower safety factors are used by employing comprehensive rules for designing welds. The other approach uses a higher factor of safety to cover the approximations involved in very simple design rules.

Another design equation that has been used by the American Bureau of Shipping<sup>16</sup> states that:

$$\sigma_c = \sqrt{k_1 \sigma_1^2 + k_2 3(\tau_1^2 + \tau_{\parallel}^2)}$$

Where:

$\sigma_c$  = allowable design stress intensity in weld, numerically equal to allowable design stress intensity in plate. For transverse member = 0.85 X minimum tensile yield strength, for longitudinal member = 0.75 X minimum tensile yield strength.

$k_1$  = factor reflecting the minimum tensile strength of fillet weld metal relative to that of ABS normal strength steel.

$$= \left[ \frac{\text{minimum ultimate tensile strength of ABS normal strength steel}}{\text{minimum ultimate tensile strength of weld metal}} \right]^2$$

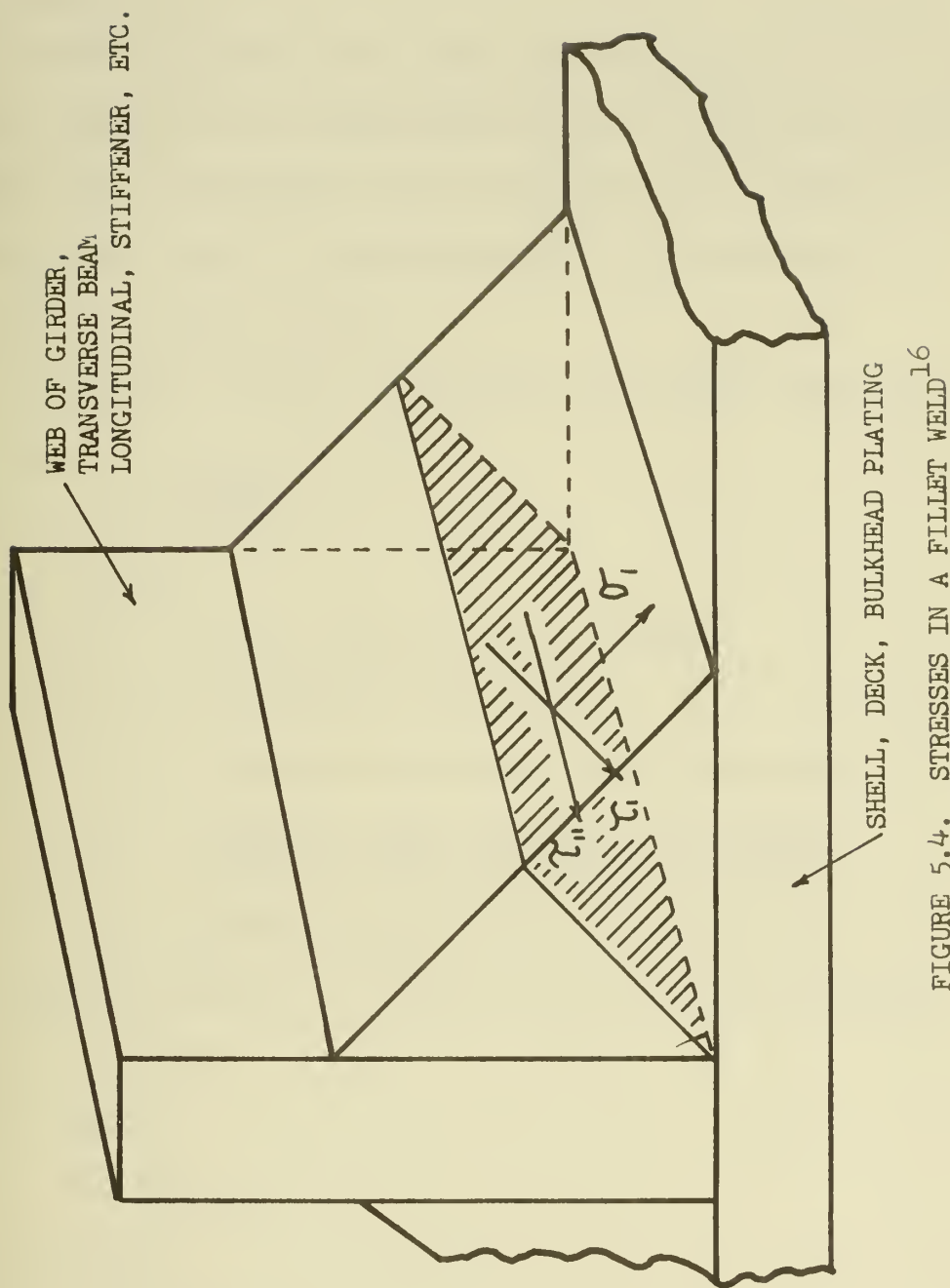
$k_2$  = factor reflecting the minimum ultimate shear strength of the fillet weld metal relative to that of ABS normal strength steel.

$$= \left[ \frac{\text{minimum ultimate shear strength of ABS normal strength steel}}{\text{minimum ultimate shear strength of weld metal}} \right]^2$$

$\sigma_1$  = tensile or compressive stress in fillet weld (see Figure 5.4) based on assumed local loading conditions given in 22.27.3 of ABS Rules.

$\tau_1$  = shear stress in plane of fillet weld throat in direction perpendicular to the plate being attached based on same loading conditions.







$\gamma_{II}$  = shear stress in plane of fillet throat in direction parallel to the plate being attached, based on the same loading conditions.

As one can readily see, this also is a modification of the Von Mises equation.

We will now discuss the method used to determine the weld size that is required by the United States Navy for a continuous double fillet weld. This subject will be discussed in more detail in Section VIII; however, a brief mention of it is necessary to complete this design section.

The equation employed to determine the required weld size is<sup>17</sup>

$$S = \frac{e T_1 R_1}{1.414 R_2}$$

Where:

$S$  = Fillet weld size (leg) in inches

$e$  = Efficiency of the joint

$T_1$  = Thickness of the weaker member in inches

$R_1$  = Ultimate tensile strength of the weaker member in pounds per square inch (psi).

$R_2$  = Shear strength of the weld metal in psi.

The above equation is a result of the following derivation:

$$F_1 = F_2$$

Where:

$$F_1 = R_1 A_1$$

and

$$F_2 = R_2 A_2$$

therefore,

$$R_1 A_1 = R_2 A_2$$



Where:

$$A_1 = T_1 L$$

and

$$A_2 = 1.414 S L$$

therefore,

$$R_1 T_1 L = 1.414 R_2 S L$$

$$R_1 T_1 = 1.414 R_2 S$$

And, therefore, for joint efficiency of 100%

$$S = \frac{R_1 T_1}{1.414 R_2}$$

The joint efficiency term,  $e$ , is introduced into the equation so that the equation can be used for joints of various joint efficiencies. Figure 5.5 demonstrates the model of the continuous double fillet weld.

This approach is believed to have come from the design of riveted joints.

To show the similarity between this method and that of riveted joint design, we will briefly look into riveted joint design. Before welding became commonplace in the construction of ships, ships were fabricated using riveted joints. There are various modes by which a riveted joint can fail and, in order to achieve an acceptable design, the engineer must check all possible modes and ensure that the critical loads for all modes of failure are higher than any load that the structure may have to sustain throughout its useful life.

A few of the possible modes of failure in riveted joints are:



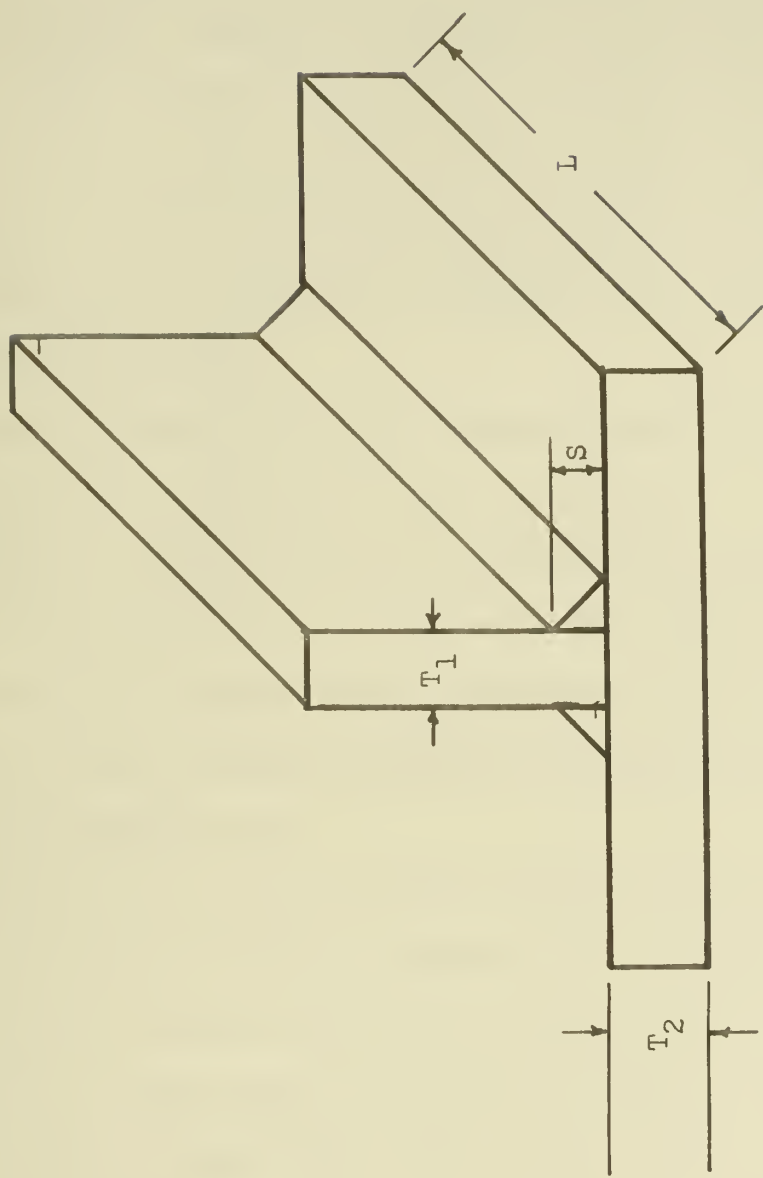


FIGURE 5.5. A CONTINUOUS DOUBLE FILLET WELDED T JOINT



1. Failure of the plate in front of the rivets
2. Crosswise tearing of a plate through a row of rivets
3. Failure of the rivets in tension
4. Shearing of all rivets

Each of these modes of failure can be prevented by proper design of a structure. Failure of the plate in front of the rivets often results because the rivets are relatively large and are either too close to the edge of the plate or have an excessive bearing pressure. By following various design codes in relation to rivet spacing and the diameter to thickness ratio, this mode of failure can be prevented.

The crosswise tearing of a plate through a row of rivets can usually be prevented by the proper spacing of rivets.

The failure of rivets in tension has been known to occur in machinery foundations where the combination of the initial tension in the rivets and the additional load increases the tensile stress in the rivets. This is normally prevented by setting the allowable working stress relatively low.

This brings us to the mode of failure which is caused by the shearing of all rivets. This is an important mode of failure, and, in many cases, the critical load for this mode is lower than other modes of failure. This is where the similarity between riveted joint design and the design method used by the U. S. Navy for fillet welded joints is apparent.

To demonstrate this similarity, we will explore the calculation of the critical load and the joint efficiency of a simplified riveted



oint as shown in Figure 5.6.

Once the maximum allowable shear stress is known, the maximum load can be obtained by multiplying this maximum value by the cross sectional area of the rivets. The joint efficiency can be determined by dividing the maximum load that can be carried by the rivets in shear by the maximum load that can be carried by the plate in tension.

An example might better demonstrate this.

**Example 5.1:**

Calculate the maximum permissible load that the riveted joint in Figure 5.6 can carry and the joint efficiency under the following conditions:

Allowable tensile stress = 22,000 psi  
 Allowable shear stress = 14,500 psi

$$\begin{array}{ll} d = 7/8" & b = 7.5 \\ t_1 = 3/4" & p = 3.5 \\ t_2 = 1/2" & c = 2.0 \\ n = 2 & \end{array}$$

In general the maximum load is:

$$P = \frac{n \pi d^2 \tau}{4}$$

In our case:

$$\begin{aligned} P &= \frac{(2) (\pi) (7/8)^2 (14,500)}{4} \\ &= 17,438 \text{ psi} \end{aligned}$$

The joint efficiency is:

$$e = \frac{\frac{n \pi d^2 \tau}{4}}{b t_{\min} \sigma}$$

In our case:



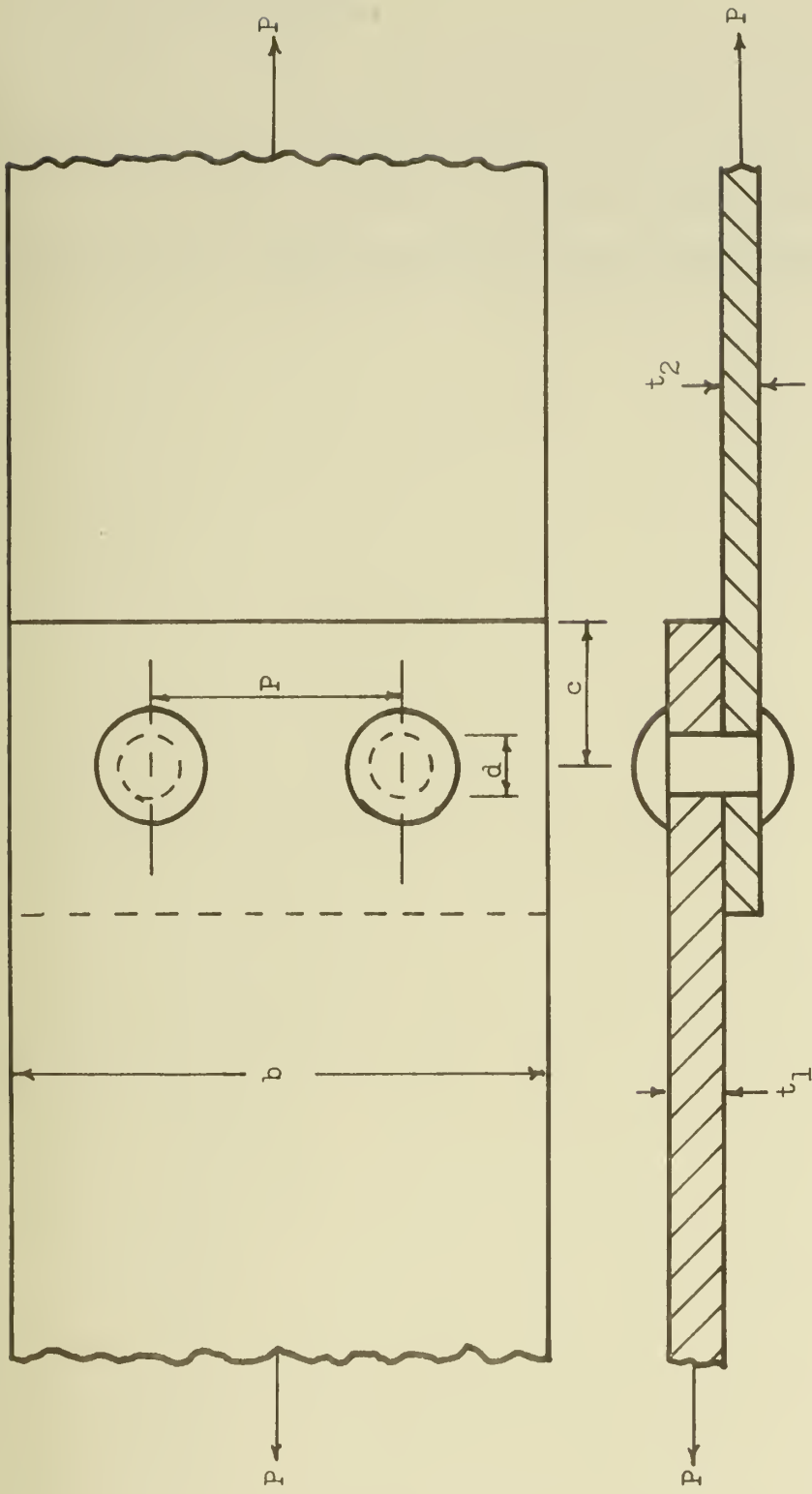


FIGURE 5.6. A SIMPLIFIED RIVETED JOINT



$$e = \frac{2 (7/8)^2}{7.5 (1/2)} \frac{14,500}{22,000}$$

$$= .211 \text{ or } 21.1\%$$

For further details on riveted joints see references 18 and 19.

We will take a closer look at joint efficiencies of fillet welded joints in Section VIII concerning current welding specifications.



## VI. FABRICATION CONSIDERATIONS

In this section, we will discuss some of the fabrication considerations involved in the design of welded joints with fillet welds. In the design of a welded joint, a model is used for strength calculations. A typical model for a continuous double fillet weld is shown in Figure 6.1. This is what the designer pictures the weld to be. However, the average joint as welded looks more like the one presented in Figure 6.2. While the designer cannot take into account poor workmanship when he determines a required weld size, he should at least be aware of some of the differences between his model of the welded joint and the actual finished welds. Details of specifications will be discussed in Section VIII; however, at this time we will look into a few of the variations from the ideal continuous double fillet weld.

One such variation is convexity. Usually there is a maximum allowed value of convexity which will still permit the weld to be accepted. Figure 6.3 demonstrates how convexity is measured.

Another variation is the re-entrant angle. Normally if the re-entrant angle is less than 90 degrees, the weld is unacceptable. Figure 6.4 demonstrates the meaning of re-entrant angle.

Another variation from the ideal joint as modeled is the skewed tee joint. Two different types of skewed tee joints are shown in Figures 6.5 and 6.6. Normally skewed joints with angles of less than 60 degrees are unacceptable (See reference 20).

One other variation that should be pointed out is a fillet welded joint with a gap. This variation is demonstrated in Figure 6.7 and will be discussed in more detail in Section VIII which talks about



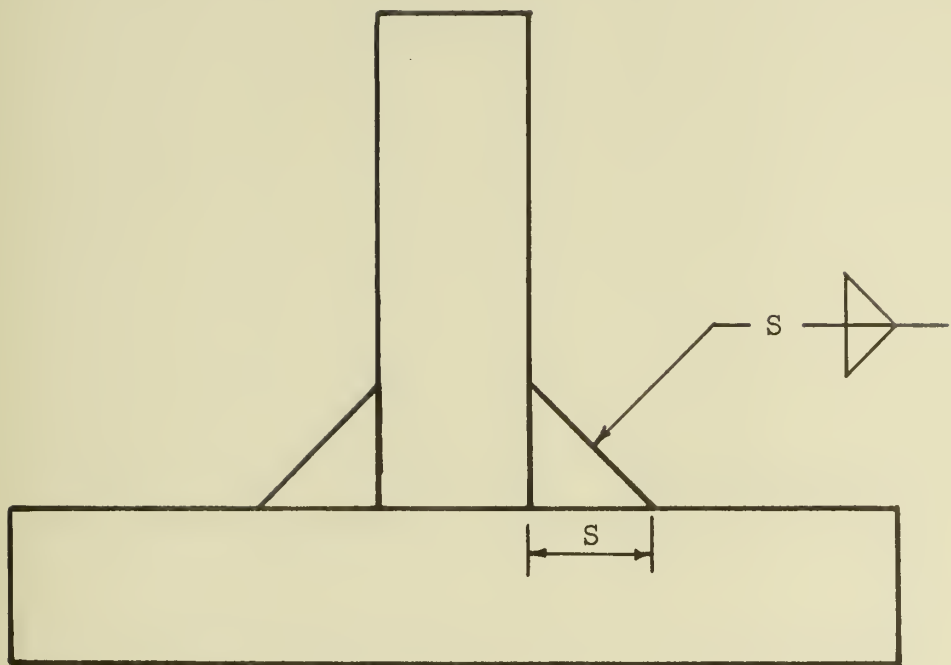


FIGURE 6.1. A TYPICAL MODEL OF A CONTINUOUS  
DOUBLE FILLET WELD



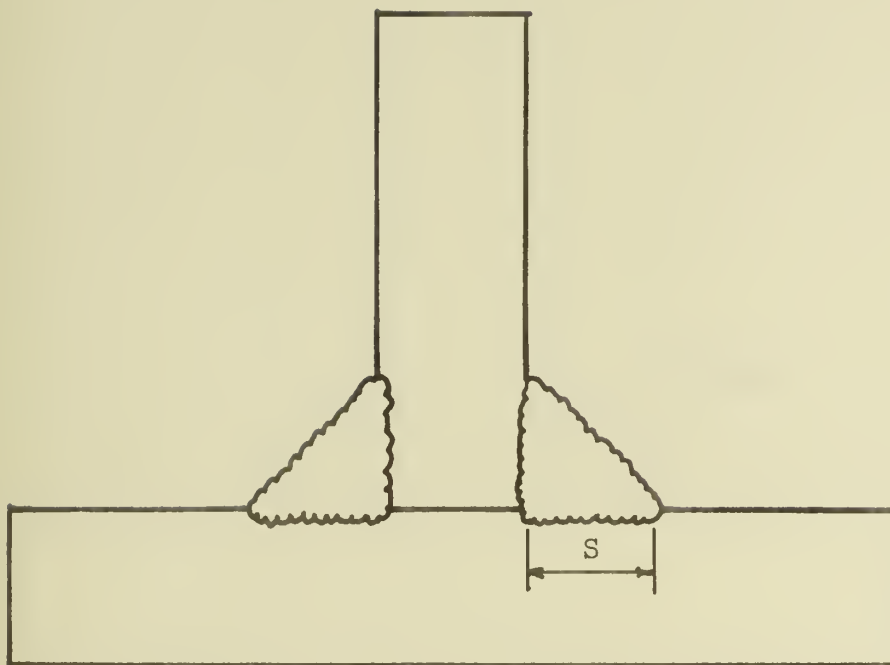


FIGURE 6.2. AVERAGE DOUBLE FILLET JOINT  
AS WELDED



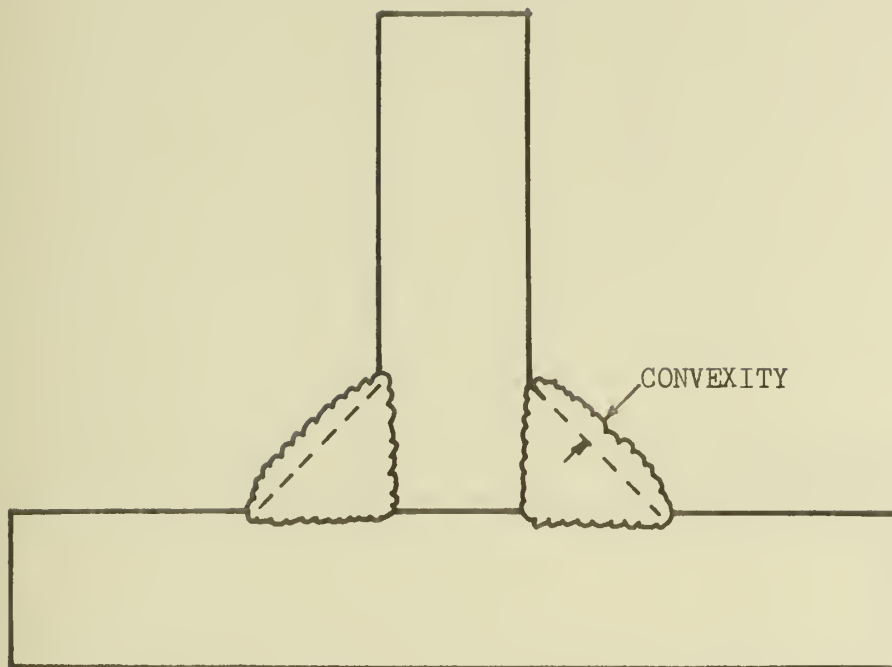


FIGURE 6.3. A TYPICAL CONVEX DOUBLE FILLET WELD



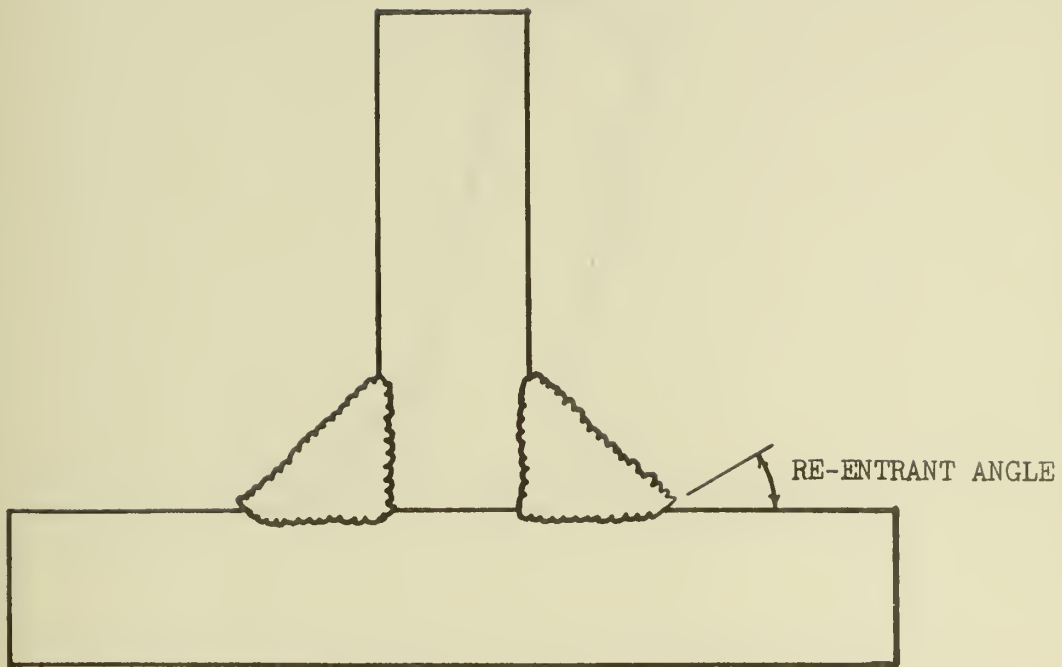


FIGURE 6.4. A FILLET WELD WITH AN UNACCEPTABLE  
RE-ENTRANT ANGLE



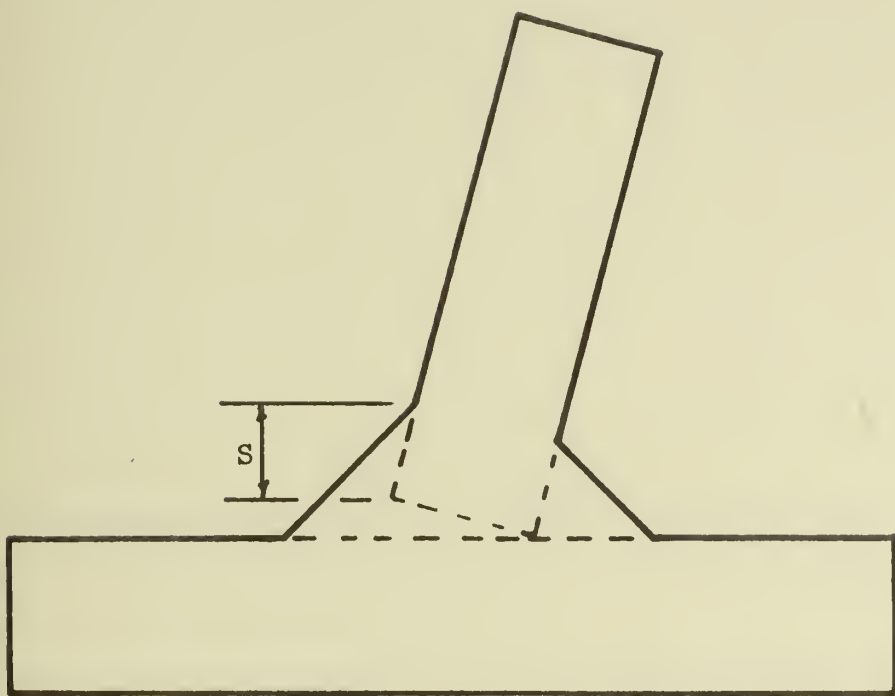


FIGURE 6.5. A SKEWED FILLET WELDED TEE JOINT



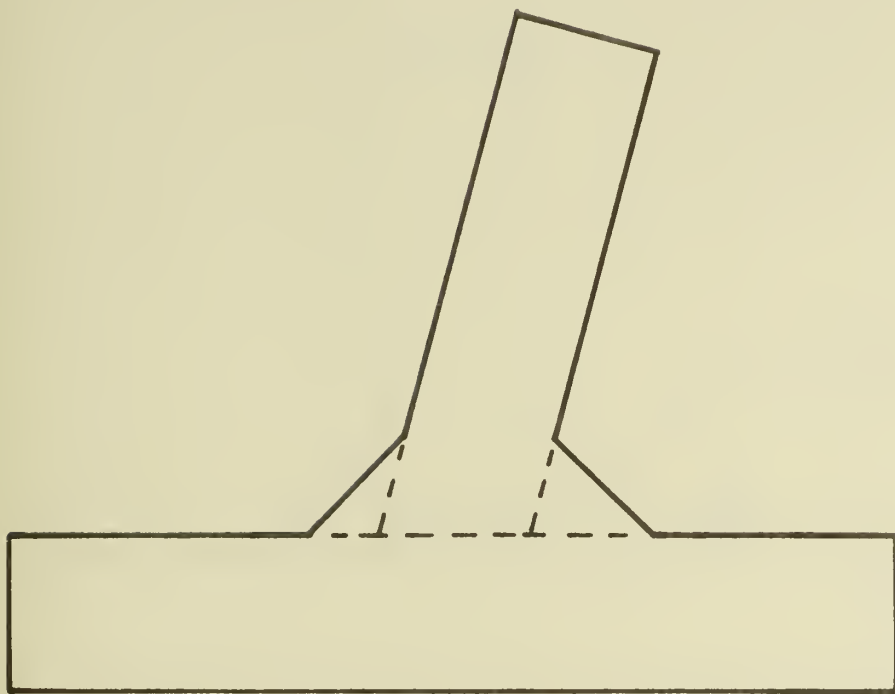


FIGURE 6.6. ANOTHER SKEWED FILLET WELDED TEE JOINT



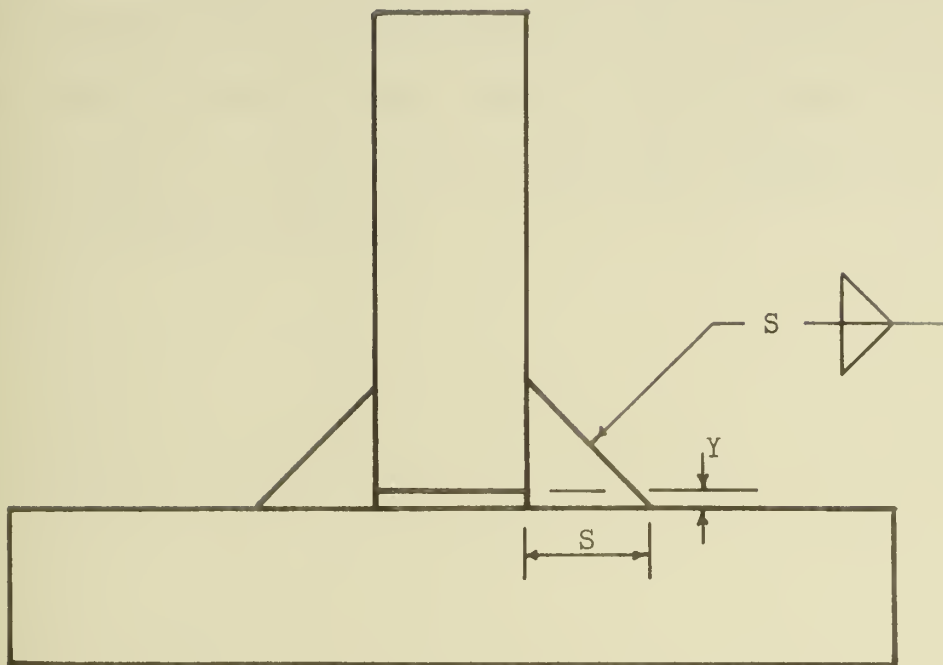


FIGURE 6.7. A DOUBLE FILLET WELDED JOINT WITH A GAP ( $Y$ )



current specifications.

The preceding discussion gives the reader a brief look at a few of the variations from a typical model that are found in the industrial environment. There are, of course, others; however, this section should give the reader an idea of some of the considerations that the designer ought to be aware of while carrying out his work.

Other areas which might be of interest to the designer are welding inspection techniques, weld qualification procedures, and weld test procedures. While a review of these areas is beyond the scope of this study, they all play an important role in the design, planning, and fabrication of a complex structure.



## VII A PROPOSED SYSTEM FOR ANALYZING FILLET WELD STRENGTH

Now that we have considered most of the factors that are involved in estimating the strength of fillet welds, it is apparent that a system of analysis is needed to combine these factors and to indicate what size fillet weld is needed to ensure a given strength of a tee joint. The reason for discussing such a system at this point, before discussing the current welding specifications for ship construction, is to avoid being too strongly influenced by current practices. This is not to say that current standards are worthless; but, in a study such as this, it is important to consider all the facts at face value and then apply good judgement as to what direction to go.

Looking to the future, it seems that an analysis system that can be computerized is desirable. One such system employs algorithms. In this system, the final weld size,  $D$ , would be the sum of increments,  $d_i$ .

Thus:

$$D = \sum_{i=1}^n d_i$$

Each  $d_i$  would be the incremental increase in weld size that is required for each of the factors that might affect the strength of a fillet welded joint.

Within each category, the value of  $d_i$  could vary from zero to some maximum value depending on the conditions of the particular joint in question. The joints would be classified by type. For instance, a joint on an auxiliary ship in the midship section between a transverse bulkhead and the ship's hull may be classified



as A-7. This classification would take into account the required joint efficiency, possible different requirements of different classes of ships and the location of the joint in a given ship. A matrix would be set up to give the value of  $d_i$  for different joint classifications (see Table 7-1).

At the present time, this system is envisioned to have ten elements each of which would have its own  $d_i$  as demonstrated in Table 7-2. In the future, each category would be a subroutine of the entire system. The inputs to this system would be the thickness of the structural members to be joined, the design loads and other information required by the subsystems or subroutines. The ultimate output of this system would be the required fillet weld size for the joint in question under the conditions specified by the input.

While the development of this entire system is beyond the scope of this study, values for the  $d_i$ 's for one of the typical joints discussed in section IX will be estimated and presented in section XV. These estimates might be somewhat rough, but it will give the reader a better understanding of the proposed analysis system and hopefully give direction for future studies.



TABLE 7-1.  $d_i$  Values for Different Joint Classifications



TABLE 7-2. Fillet Weld Analysis System Elements

Category	$d_i$	Method of Determination
Static Strength	$d_1$	Computer FEM
Fatigue Margin	$d_2$	Experimental Results
Fabrication or Workmanship	$d_3$	FEM
Welding Method	$d_4$	Experimental Results
Conditions of Welding	$d_5$	Industrial Data
Environmental:		
Corrosion (general)	$d_6$	Calculation-Experimental Results
Corrosion (local)	$d_7$	Experimental Results
Quality Control		
Ability to Detect Defects	$d_8$	Industrial Data
Test Procedure Required	$d_9$	Specifications
Design Method	$d_{10}$	Judgement



## VIII CURRENT WELDING SPECIFICATIONS FOR SHIP CONSTRUCTION

In this section, we will first compare the U.S. Navy welding specifications for fillet welds with other welding specifications that are currently being used in construction of ships throughout the world. This will give an overview of where the U.S. Navy specifications are with respect to the most conservative as well as the most liberal welding requirements. Then we will take a closer look at the U.S. Navy welding specifications for non-combatants.

A comparison of the U.S. Navy specifications to other welding standards is best demonstrated by a plot of the required weld size versus plate thickness for the various standards. The three joint types that were chosen for these plots are the joints between double bottom floors and shell plating, between web frames and shell plating, and between decks and shell plating. These plots can be seen in Figures 8.1, 8.2, and 8.3 respectively. We can readily see that Germischer Lloyd<sup>21</sup> is the most conservative followed by the American Bureau of Shipping<sup>22</sup> and the U.S. Navy<sup>23</sup>; while Bureau Veritas<sup>24</sup>, Lloyd Register<sup>25</sup> and Det Norske Veritas<sup>26</sup> are the most liberal requirements. Also, it is very apparent that there is a wide range between the most conservative rules and the most liberal rules. In fact, there is over a factor of two difference in some cases. This difference may not be as large as it seems because the specifications may be based upon slightly different models or include or exclude different considerations. For instance, one may include a corrosion and another may tell



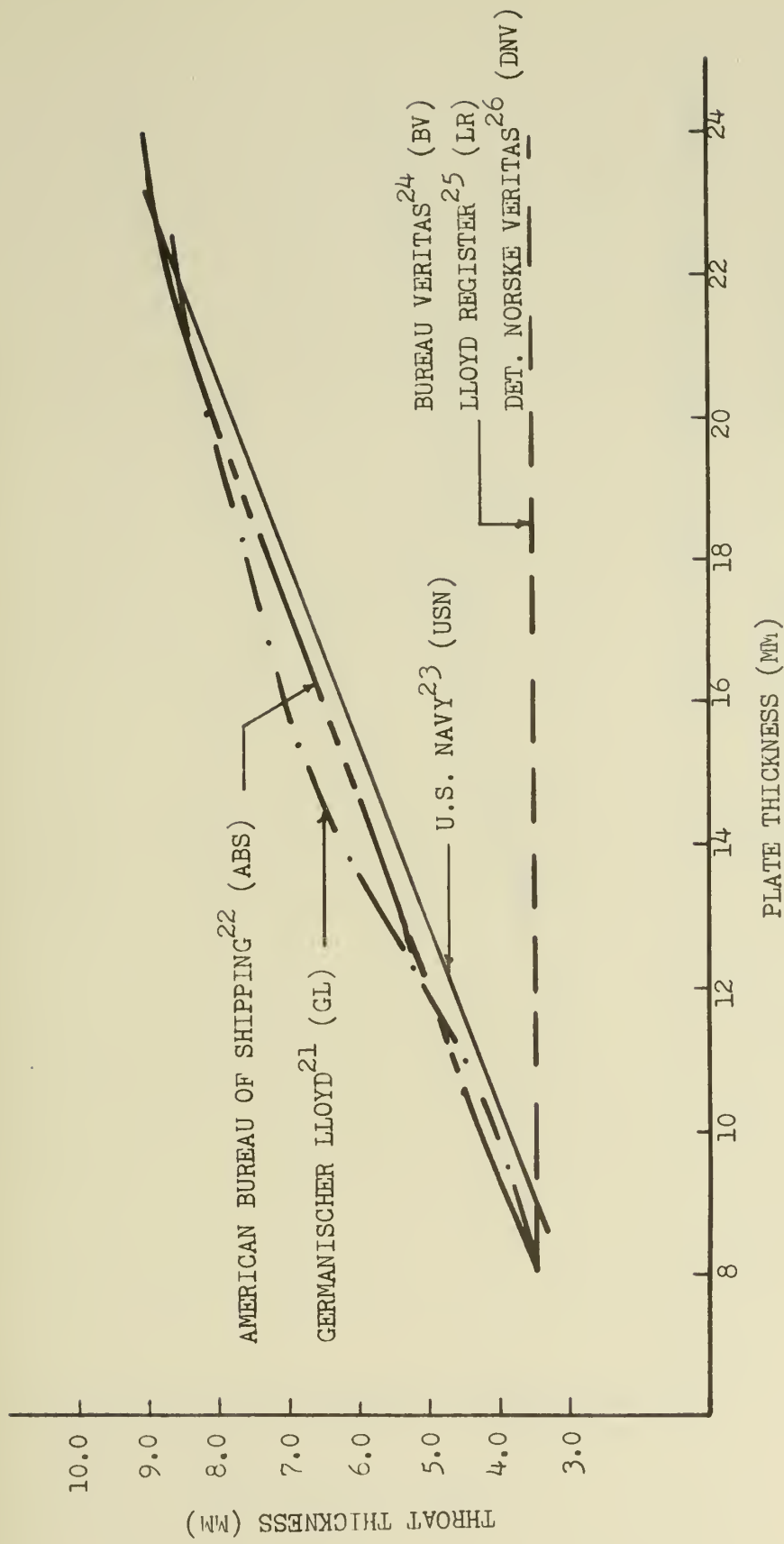


FIGURE 8.1. CURRENT WELDING SPECIFICATIONS FOR JOINTS BETWEEN DOUBLE BOTTOM FLOORS AND SHELL PLATING



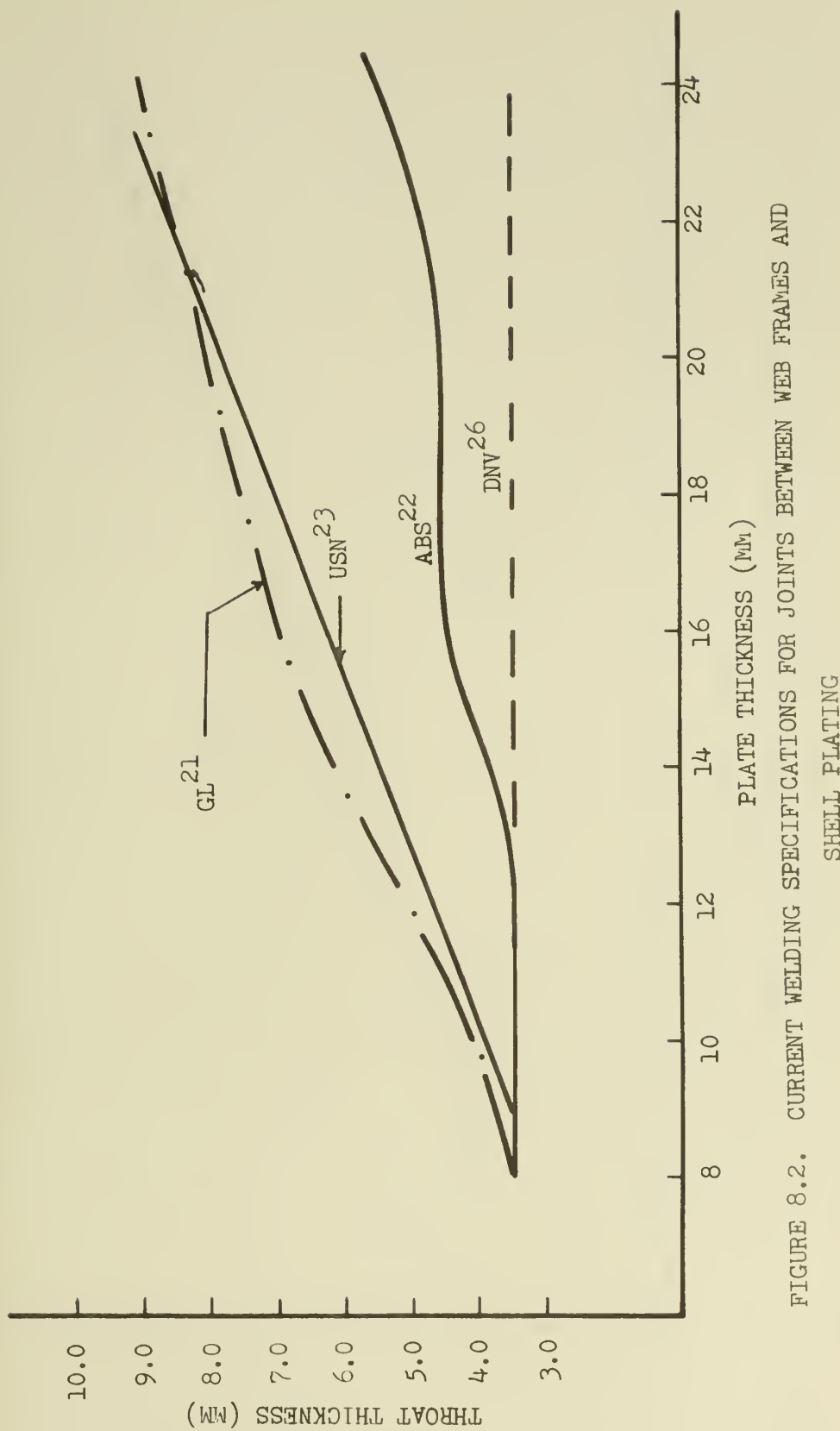


FIGURE 8.2. CURRENT WELDING SPECIFICATIONS FOR JOINTS BETWEEN WEB FRAMES AND SHELL PLATING



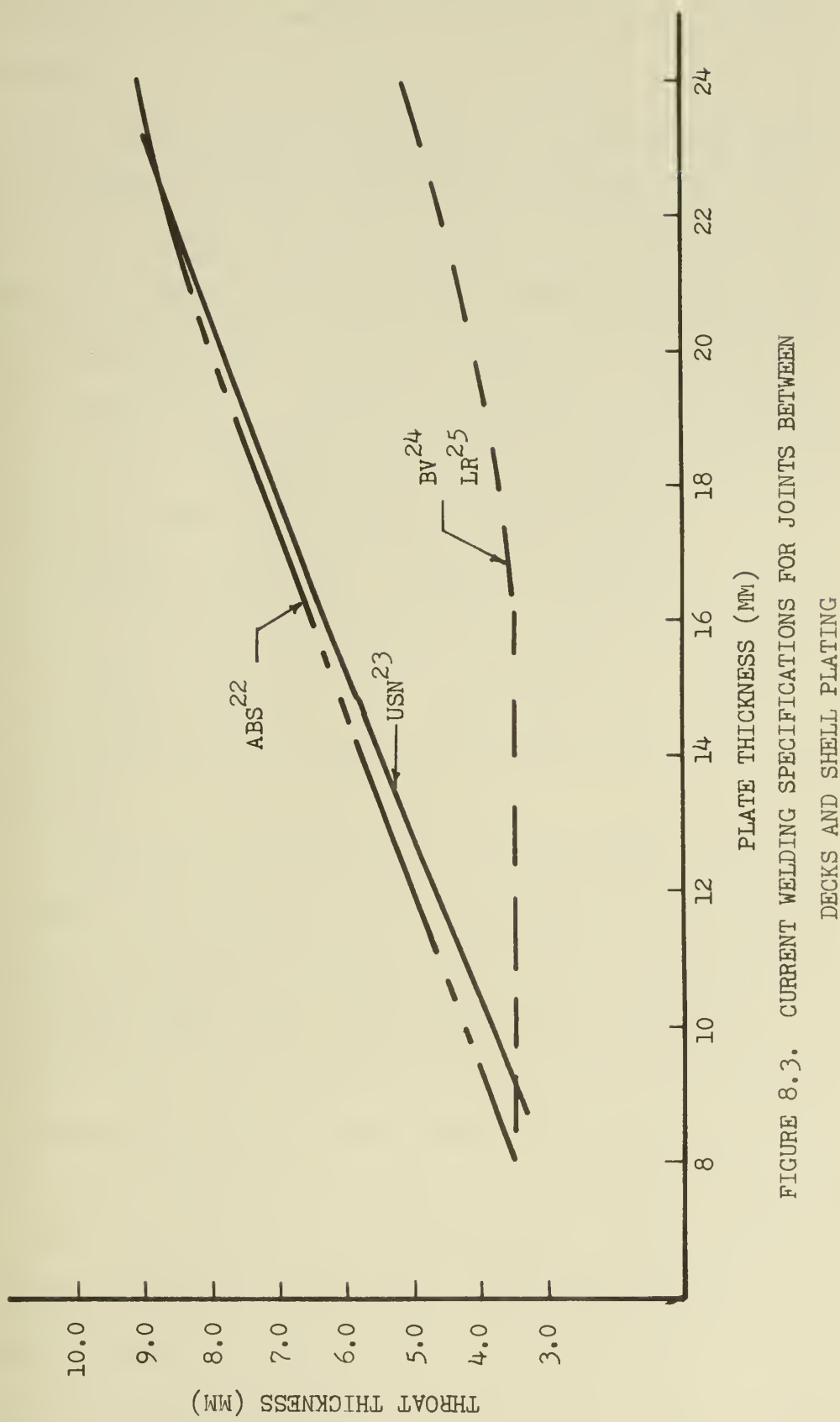


FIGURE 8.3. CURRENT WELDING SPECIFICATIONS FOR JOINTS BETWEEN DECKS AND SHELL PLATING



the designer to add on a margin in addition to what is required by the chart.

We will now proceed to review the U.S. Navy specifications for non-combatants. While a presentation of the entire set of specifications is not warranted, a brief presentation of the basic format and use of the requirements is considered worthwhile. The U.S. Navy specifications use the weld leg size in inches rather than the throat size in millimeters as is used by other standards. Also the U.S. Navy standards give the plate thickness as a function of pounds per square foot rather than in millimeters.

The required weld sizes are presented in graphical form of a plot of plate thickness versus joint efficiency with constant required weld size curves. There is a different plot for each different combination of materials from which a joint can be constructed.

The graph for a continuous double-fillet welded tee joint made between medium steel (U.T.S. 60,000 psi) made with MIL-6011 electrodes is presented in Figure 8.4. There are other graphs for tee joints made between high tensile steel (H.T.S.) and medium steel for a given electrode, and tee joints made between high tensile steel and high yield steel HY-80 for a given electrode, and for other combinations of construction materials and electrodes used. The joint efficiency can be calculated using the method presented in section V. Rather than use a different graph for various locations in the ship as was done in Figures 8.1, 8.2, and 8.3, the U.S. Navy specifies the locations in the ship. A partial



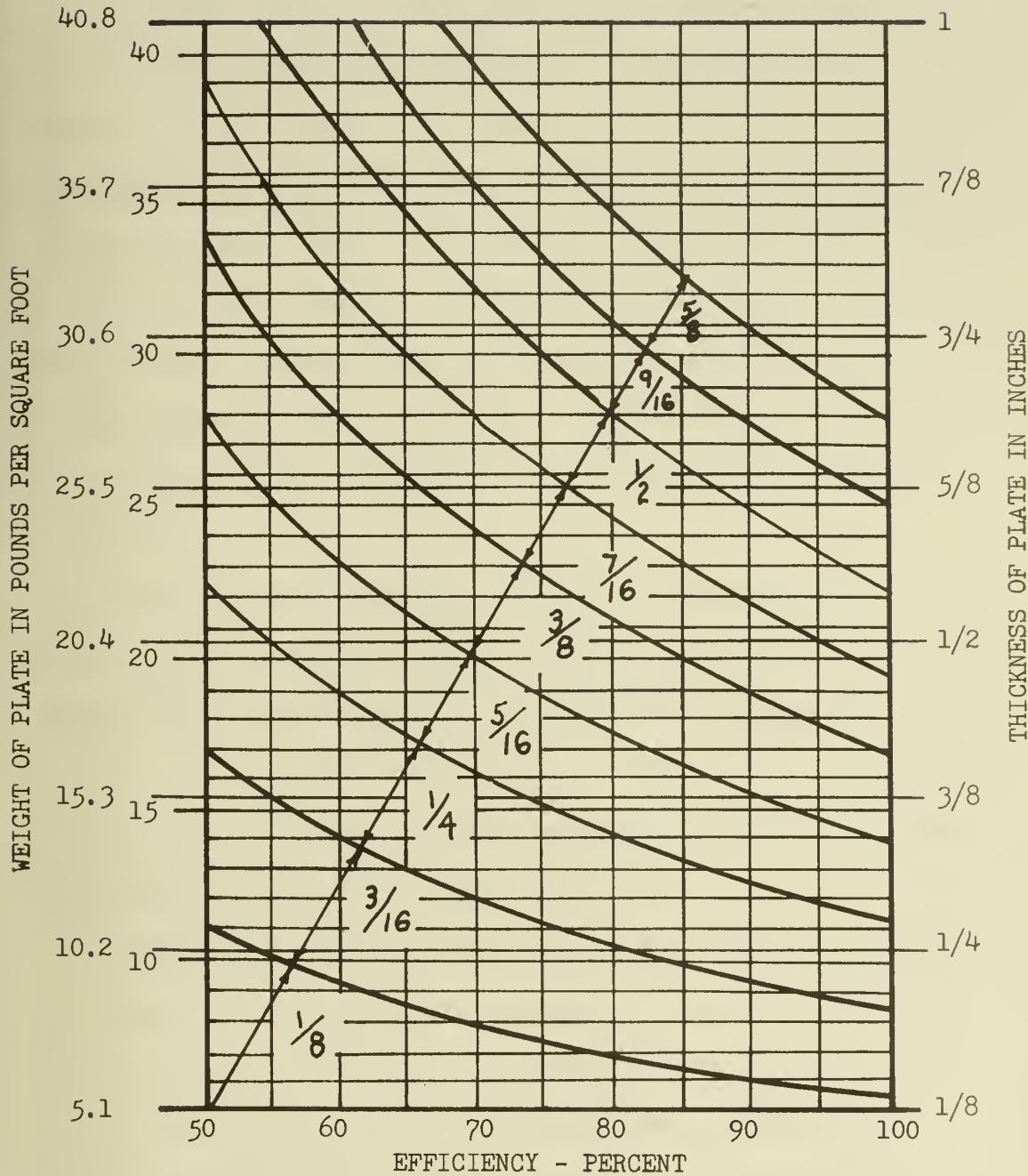


FIGURE 8.4. EFFICIENCY CHART FOR CONTINUOUS  
DOUBLE-FILLET WELDED TEE JOINTS MADE BETWEEN MEDIUM STEEL MADE WITH  
MIL-6011 ELECTRODES <sup>23</sup>



listing of the required joint efficiency is given in Table 8-1. For a complete listing see reference 23.

Now that we have discussed the basic format and the use of the U.S. Navy welding specifications, it will be worthwhile to examine a few of the details contained in the specifications. The required weld size is given in terms of fillet weld leg size. In an ideal model there is no mistake of what this means; however, in actual welds, there may be some confusion. The weld size of actual welds is demonstrated in Figures 8.5 and 8.6. The maximum allowable convexity for fillet welds varies with the weld size as shown by Figure 8.7. The tolerance on fillet weld sizes is as follows:<sup>23</sup>

"Fillet welds up to and including 3/8-inch size shall not vary below the specified size by more than 1/16-inch, and any such variance shall not extend for a total distance greater than 1/4 of the joint length nor for more than 6-inches at any one location. Fillet welds, 7/16-inch size and larger, shall not be less than the gage limits for their respective sizes."

Another point that has been discussed in section VI is that in fabrication a gap is often introduced as shown in Figure 8.8. The maximum gap that is allowed without increasing the weld size is 1/16-inch. If the gap (Y) is greater than 1/16-inch, the required weld size (S) is equal to the normal required size plus Y. The maximum permitted gap even with increasing the weld size is 1/16-inch.

The U.S. Navy specifications include many more details



TABLE 8-1. Required Joint Efficiencies for Various Fillet Welded Joints<sup>23</sup>

Item	Connection	Joint Efficiency (Per Cent)
Bilge Keels	Connections to shell	75
Bulkheads, Longitudinal and Transverse	Main subdivision bulkheads	100
Decks and Platforms	Longitudinal	75
	Transverse	
	With deck on only one side	75
	With deck on both sides	100
	Shell and interbottom	75
Foundations	Gun Foundations	100
Framing, Longitudinal and Transverse	Connections to flanges or faceplates around lightening holes	75
	End connections to intersecting members	
	Ordinary frames (less than 24-inches in depth)	100
Masts and Booms	All joints	100
Piping Penetrations	Shell plating and supports	100
Vertical Keel	Connections to flat keel and rider plate	75



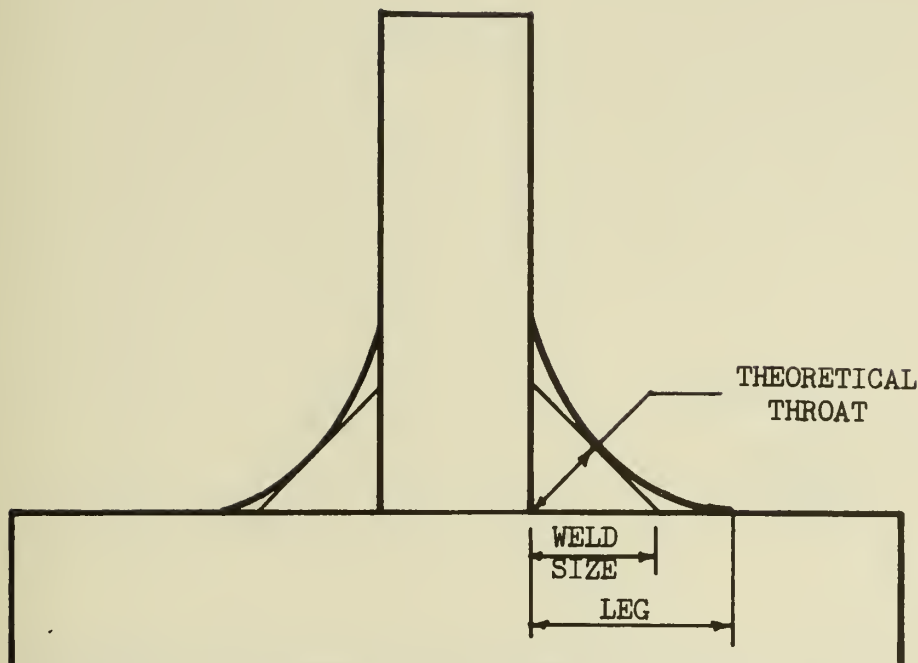


FIGURE 8.5. WELD SIZE OF A CONCAVE FILLET WELD



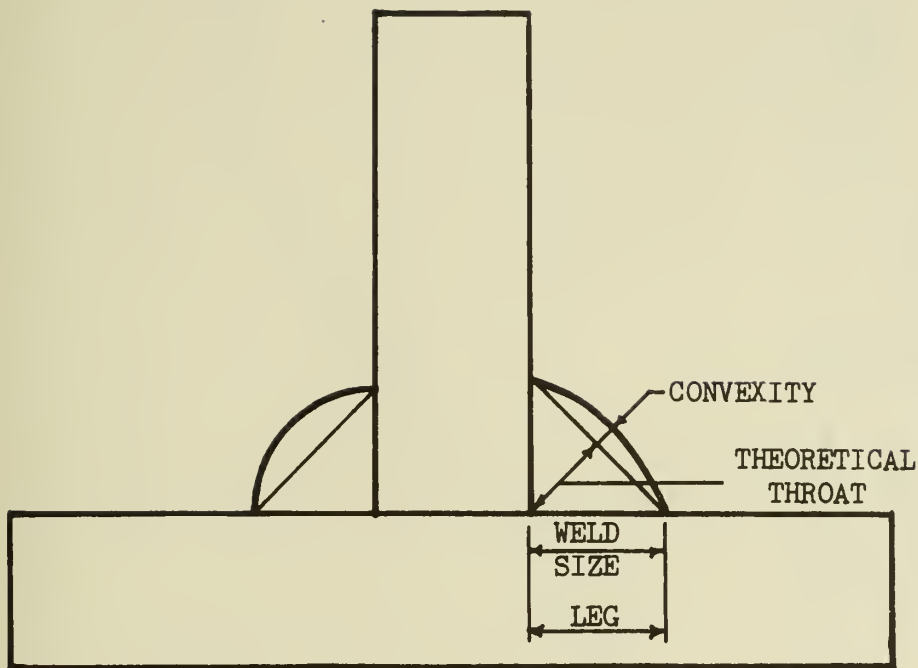


FIGURE 8.6. WELD SIZE OF A CONVEX FILLET WELD



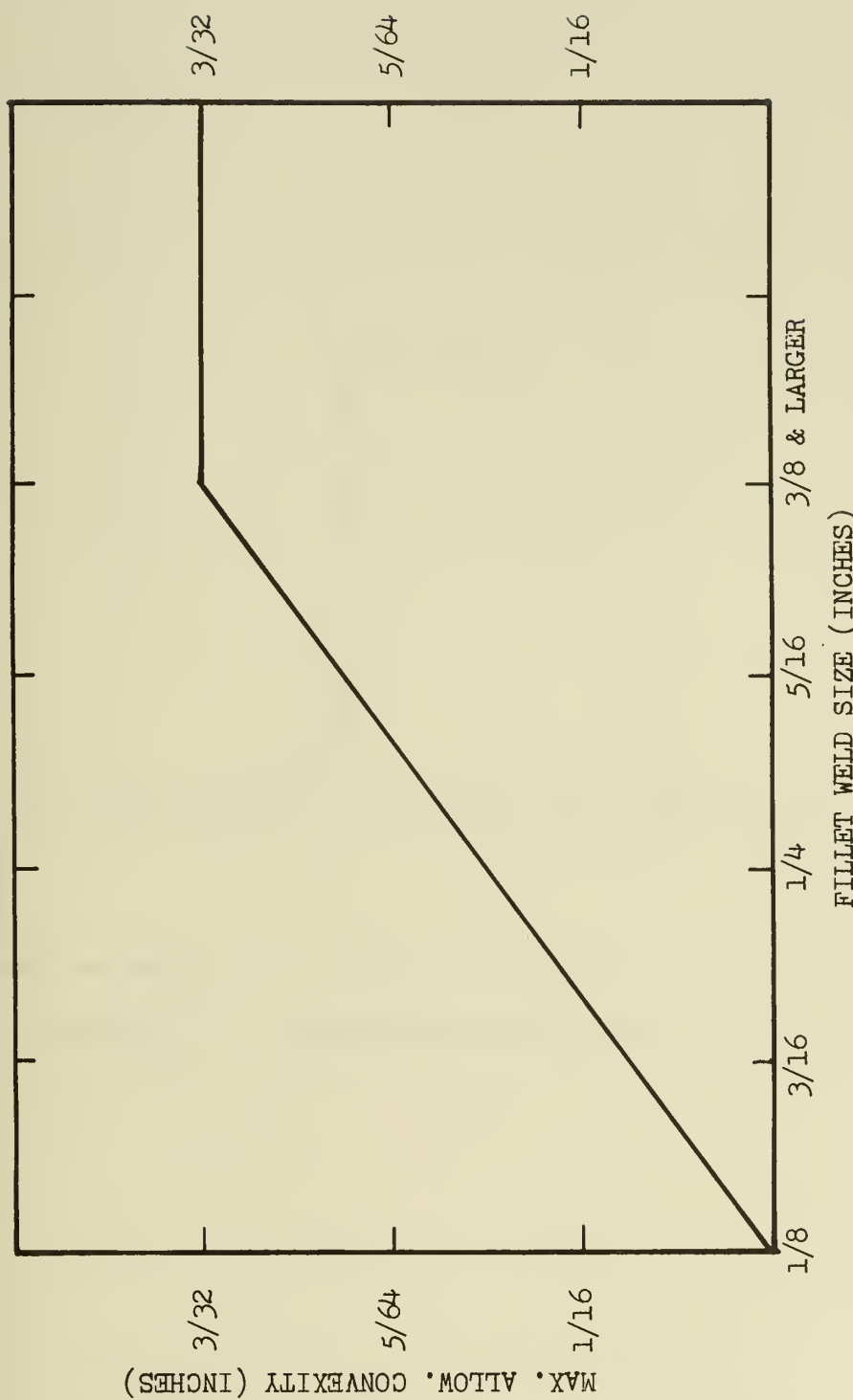


FIGURE 8.7. MAXIMUM ALLOWABLE CONVEXITY FOR FILLET WELD SIZES<sup>23</sup>



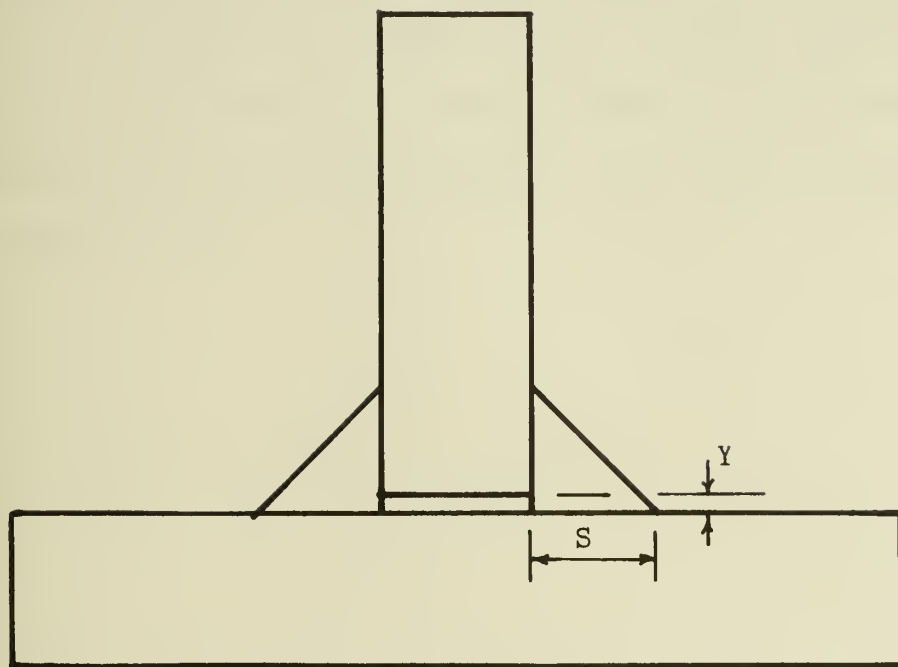


FIGURE 8.8. A DOUBLE FILLET WELD WITH A GAP (Y)



concerning inspection techniques, weld qualifications procedures, weld test procedures, and material certification procedures. For more information see references 17, 23, 27, 28, 29, 30, 31, 32, 33, and 34.

Now that we have review the current specifications and, in previous sections, the experimental and theoretical work that has been done in the field of fillet weld strength, we will next look at some of the typical tee joints that are found on existing ships. This is the first step in our strength analysis of existing welded joints which will answer the question, "Are fillet weld requirements too conservative?"



## IX TYPICAL FILLET WELDED JOINTS

In this section, we will look at some of the typical fillet welded joints that have been used in existing naval ships. The two types of ships that will be studied are the destroyer tender, AD-37 class, and an oiler, AO-143 class. The reason that these two ships were chosen is that they are U.S. Navy ships, but, yet, they are similar to commercial ships.

We will now look at a few of the principle characteristics of these two ships as given in reference 35.

The destroyer tender, AD-37 class, has a full load displacement of 22,260 tons and has an overall length of 643 feet with a beam of 85 feet and a draft of 22.5 feet. This ship was designed to "provide primarily maintenance and related towing and salvage services at advanced bases and at ports in the United States."<sup>35</sup>

The oiler or underway replenishment ship, AO-143 class, is a larger ship in that it has a full load displacement of about 40,000 tons (light load 11,600) and has an overall length of 655 feet with a beam of 86 feet and a draft of 35 feet. The cargo capacity of this ship is approximately 180,000 barrels of liquid fuels. This ship is much like an older tanker; however, it was designed to provide fuel to warships at sea.

Now that we have a rough idea of what the ships look like, we will next proceed to discuss what welded joints we want to examine in detail.

In order to choose a location in the ship that would be most beneficial to study, ship in-service performance reports were



reviewed. One such report is given in reference 36. The area of the ship that is most important is that of the midship section because the primary bending stress reaches a maximum in this location. Thus, the construction drawings pertaining to the midship section of these two ships were studied.

The two specific joints of primary concern are the joint between a transverse bulkhead and the ship's shell plating within the inner bottom and the joint between a longitudinal and the ship's shell plating also within the inner bottom.

Using the above guidelines, typical joints from each ship were chosen to be analyzed. Figure 9.1 shows the joint between a transverse bulkhead and the ship's shell plating of the destroyer tender. This transverse bulkhead is at frame 69 1/2, which is in the midship section of the ship, and the joint pictured in Figure 9.1 is typical of the structure from stringer number one outward within the inner bottom.

Figure 9.2 shows this same bulkhead as it joins the inner bottom floor. While this joint does not include the shell plating, it is a typical joint of a transverse bulkhead to an inner bottom floor in the midship section of the ship.

The next joint we will look at is that of a longitudinal and the shell plating of the destroyer tender. This member is longitudinal number seven, and it is located approximately eighteen feet outboard of the center vertical keel. This is still within the inner bottom. This structural member can be seen in Figure 9.3.

The last joint we will look at of the destroyer tender is that



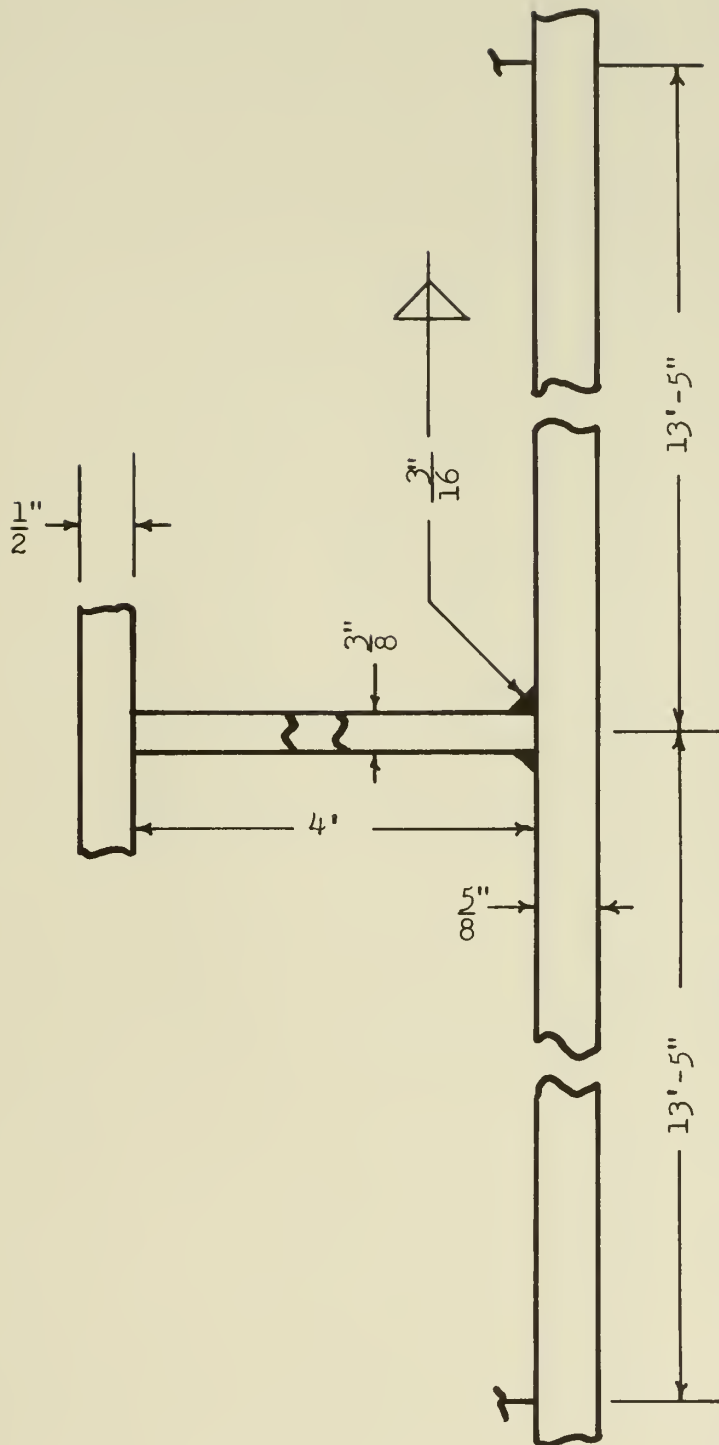


FIGURE 9.1. TYPICAL JOINT BETWEEN A TRANSVERSE BULKHEAD AND THE SHELL PLATING OF THE AD-37

CLASS SHIP. 37, 38, 39



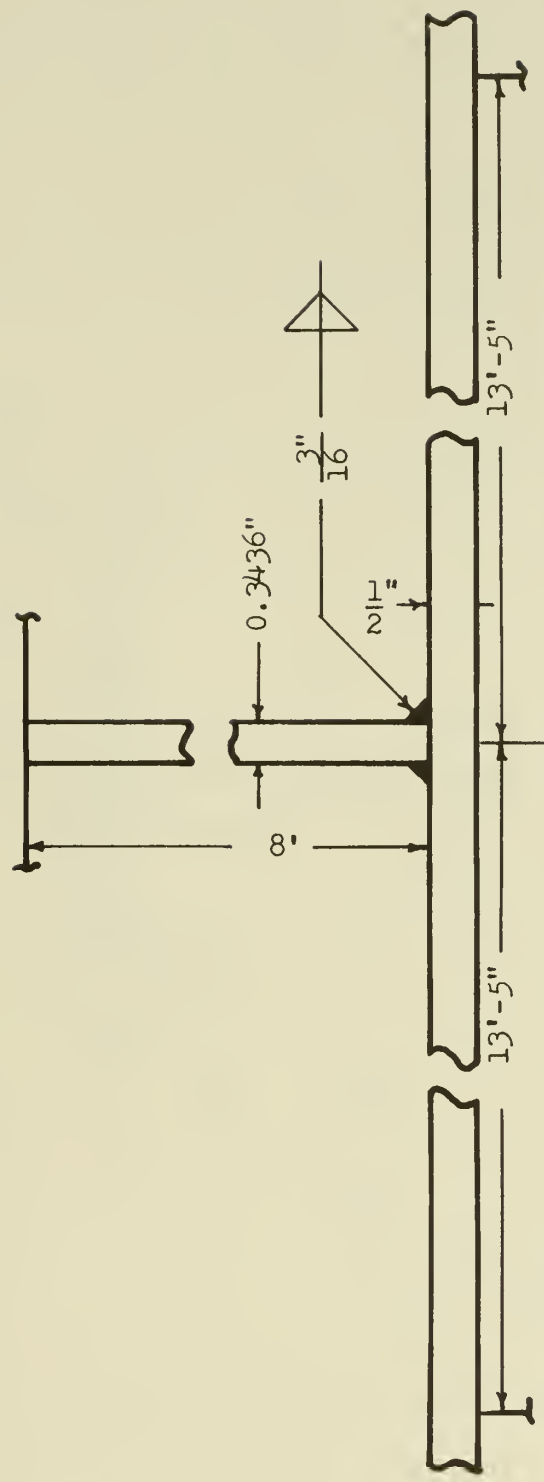


FIGURE 9.2. TYPICAL JOINT BETWEEN A TRANSVERSE BULKHEAD AND THE INNER BOTTOM FLOOR OF THE AD-37  
CLASS SHIP. 37, 38, 39



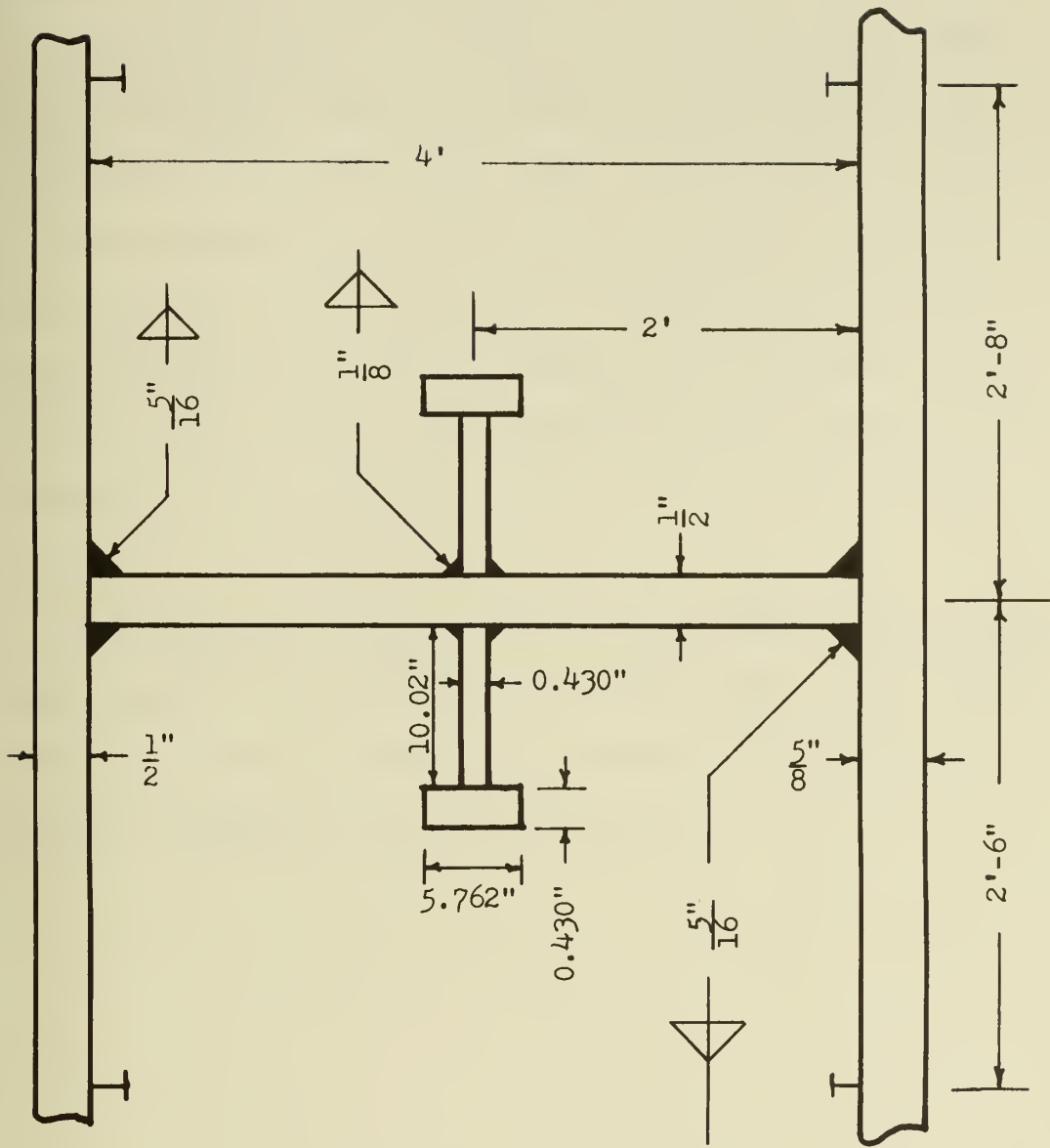


FIGURE 9.3. TYPICAL JOINT BETWEEN A LONGITUDINAL AND THE SHELL PLATING OF THE AD-37 CLASS SHIP. 37, 40, 41



between stringer number nineteen and the shell plating. This member is a longitudinal member located almost three feet above the third platform or about fifteen feet above the base line. The details of this joint can be seen in Figure 9.4.

We will now examine two typical joints of the oiler. The first joint is that between longitudinal number thirty and the shell plating. This structural member is approximately ten feet off the center line of the ship near the base line. Figure 9.5 shows a typical view of the joint in the midship section of the ship. The second joint is that between oil tight bulkhead number 80 and the shell plating. This bulkhead is in the midship section of the ship, and the details of this joint can be seen in Figure 9.6.

Now that we have examined several of the typical fillet welded joints employed in non-combatant U.S. Naval ships, we will proceed to the next section in which we will analyze the loading in the structural members of a few of these joints.



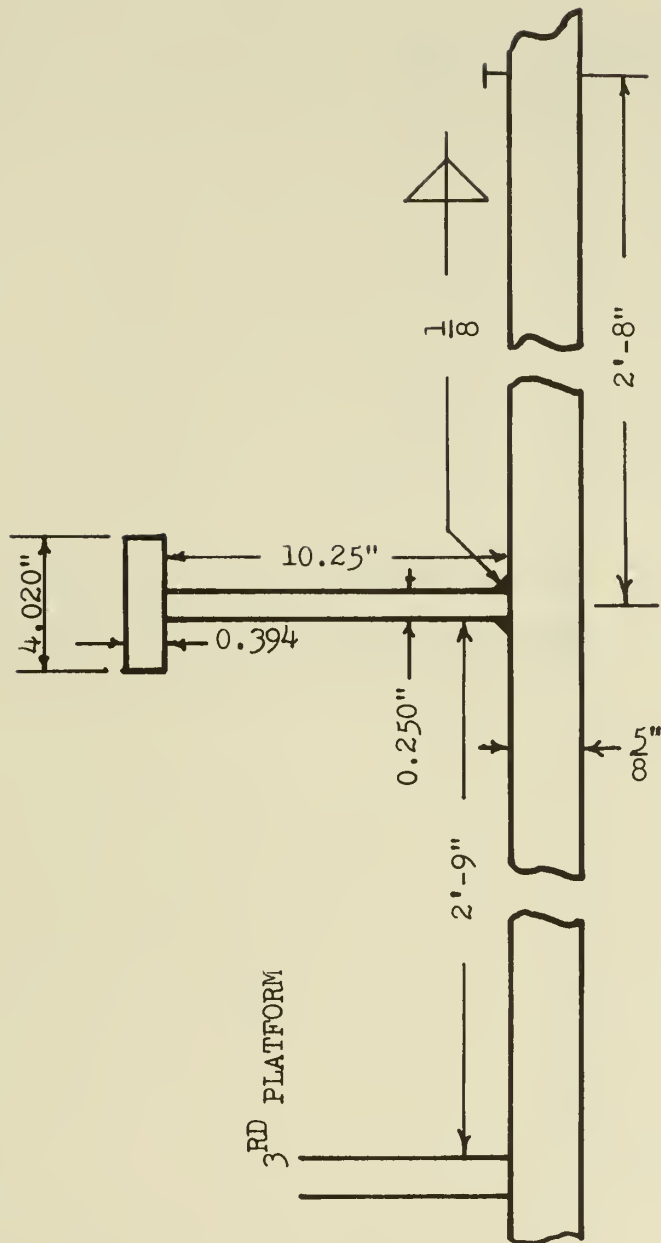


FIGURE 9.4. TYPICAL JOINT BETWEEN A STRINGER AND THE SHELL PLATING OF THE AD-37 CLASS SHIP. 37, 42, 43



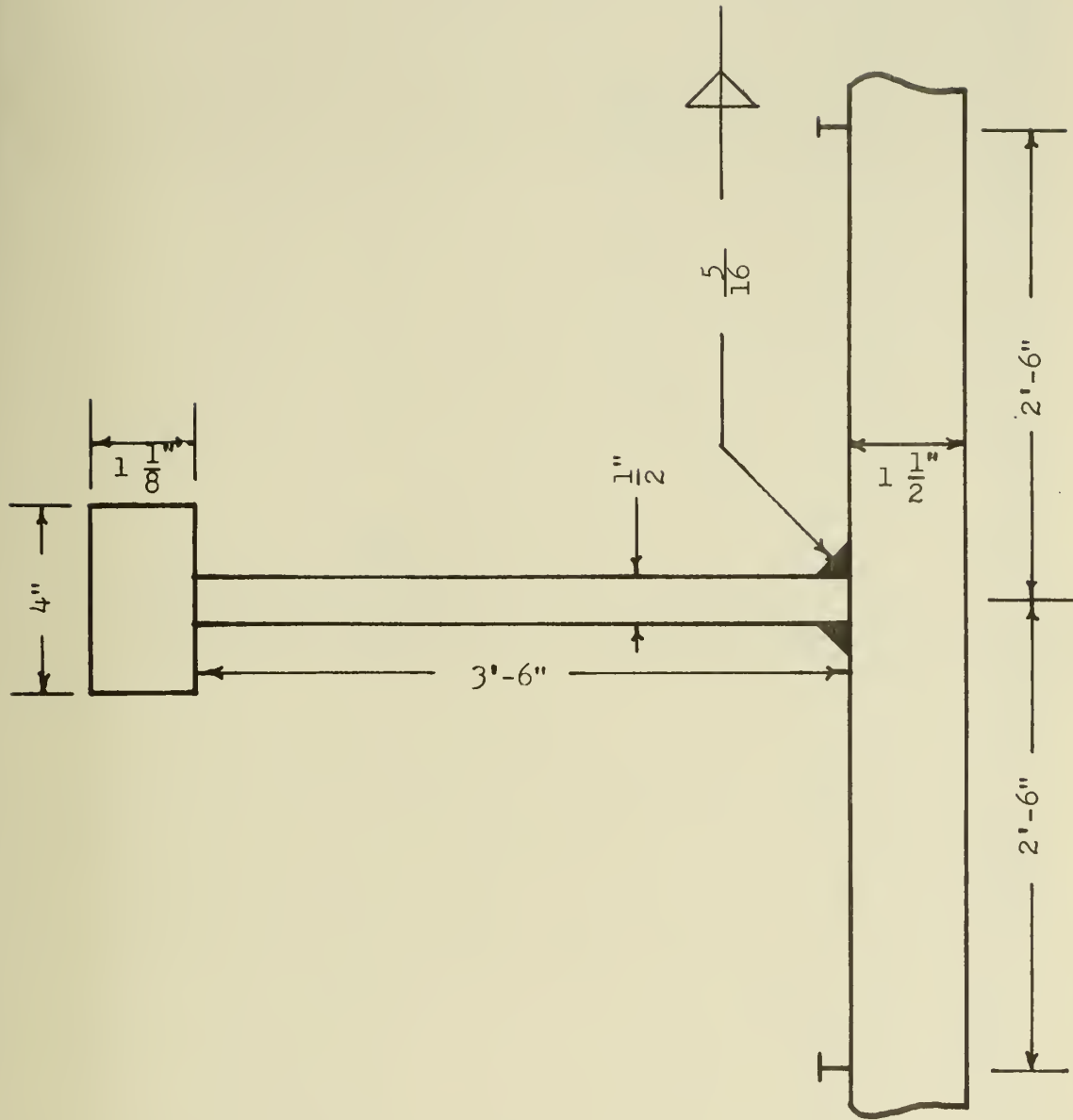


FIGURE 9.5. TYPICAL JOINT BETWEEN A LONGITUDINAL AND THE SHELL PLATING OF THE AO-143 CLASS SHIP. <sup>44,45</sup>



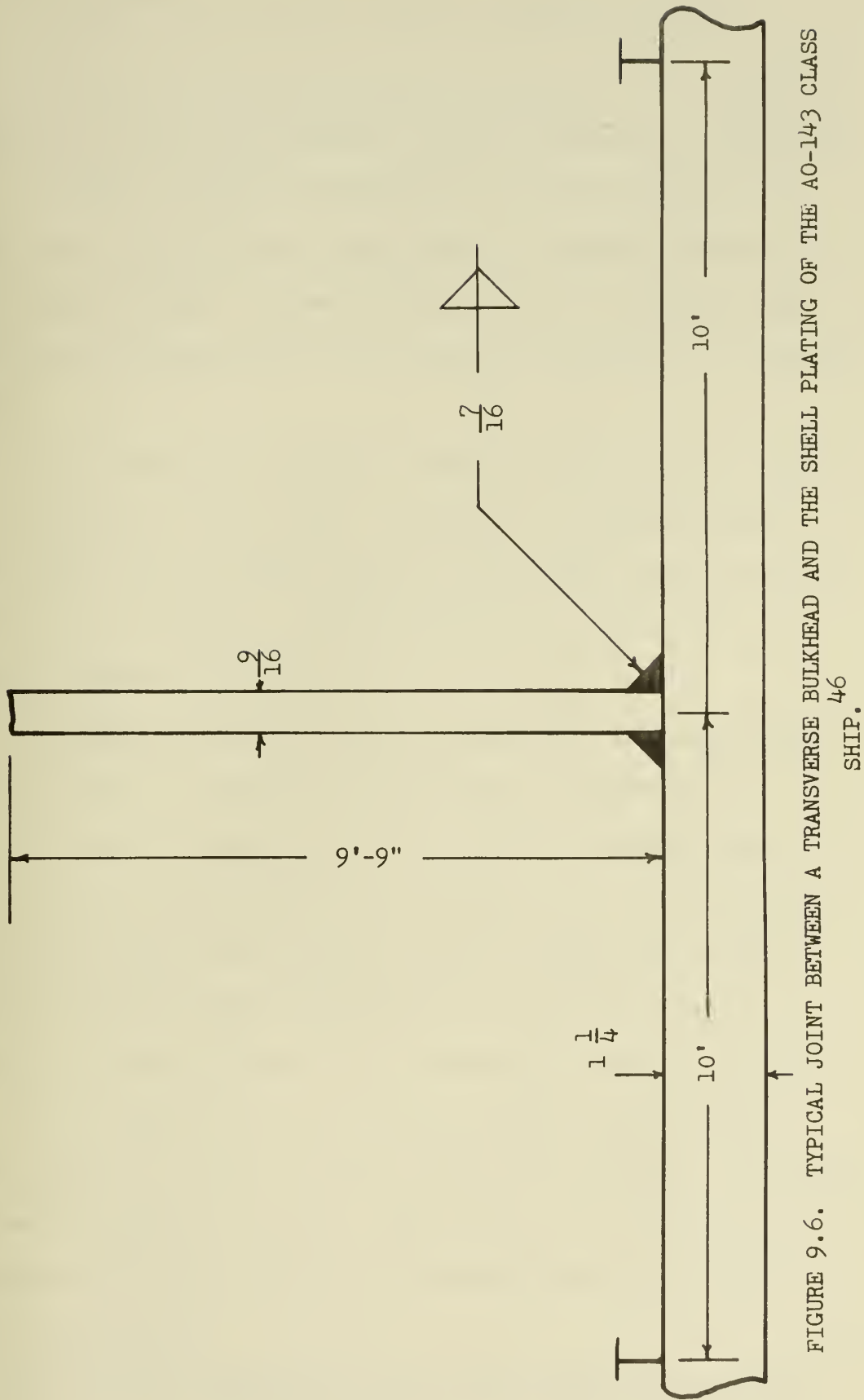


FIGURE 9.6. TYPICAL JOINT BETWEEN A TRANSVERSE BULKHEAD AND THE SHELL PLATING OF THE AO-143 CLASS SHIP.

46



## X STRUCTURAL ANALYSIS OF LOADING IN SELECTED MEMBERS

In this section we will analyze the loading in the structural members for a few of the typical joints as presented in section IX.

In order to analyze the stresses in structural members, we must rely on the structural theory that is presently employed in the design of ships. The basic concepts will be reviewed before we proceed to analyze some of the structural members in the typical joints.

The stresses of a structural member of a ship can be thought of as coming from three levels. These are the primary stress or area stress, the secondary stress or line stress, and the tertiary stress or point stress. A drawing showing the three levels of stress is shown in Figure 10.1.

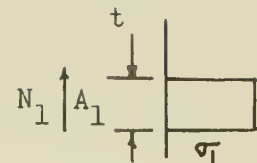
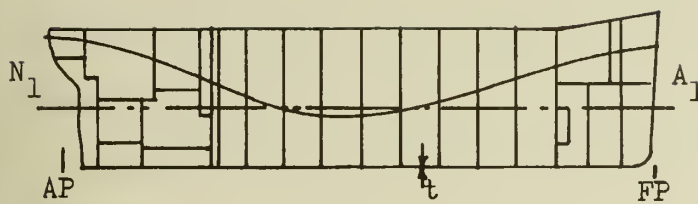
The following will be a brief discussion of the theory and procedure that is presented in more detail in reference 47.

The primary stress,  $\sigma_1$ , is the ship's hull bending stress. This is normally calculated by assuming the ship's hull acts like a beam, and, thus, this stress is directly proportional to the distance from the ship's neutral axis. This stress is also basically constant throughout the thickness of the ship's plating.

The secondary stress,  $\sigma_2$ , is the stiffener bending stress which results from the reaction of the plating stiffener combination to design loading of the ship. This stress in the plating has a maximum value at the stiffener and diminishes as you move away from the stiffener.

The tertiary stress,  $\sigma_3$ , is the plate bending stress which





HULL BENDING STRESS

TYPICAL BOTTOM STRUCTURE

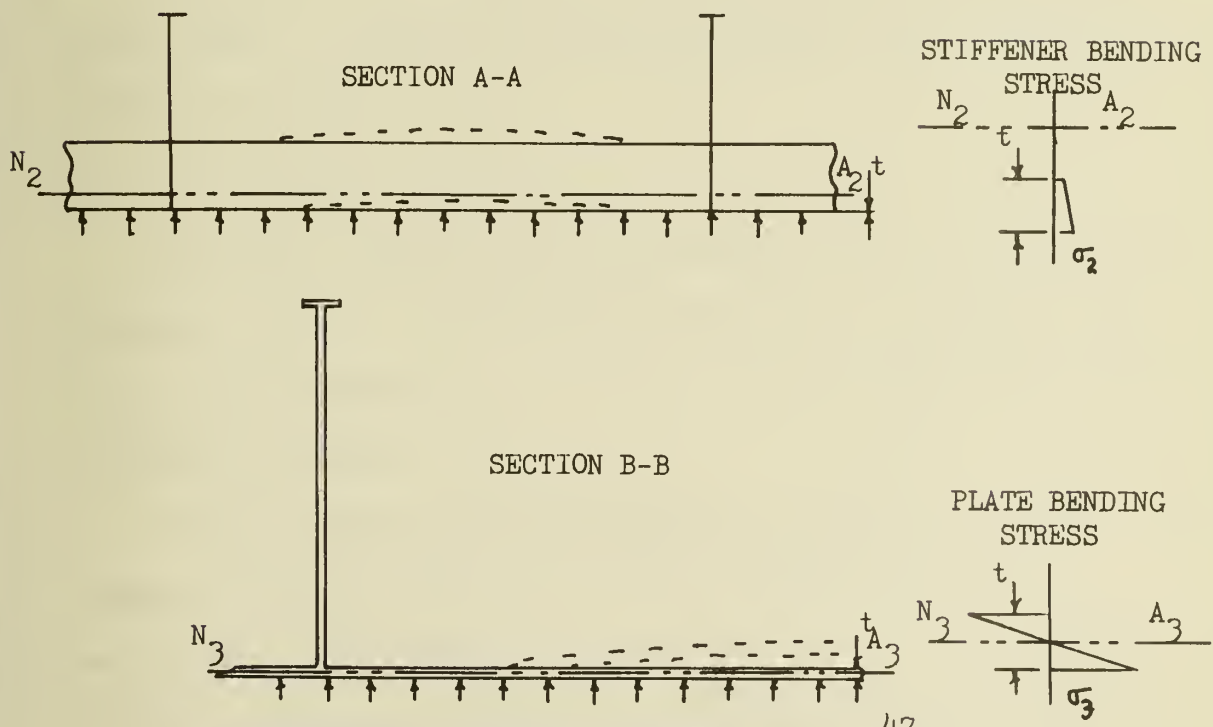
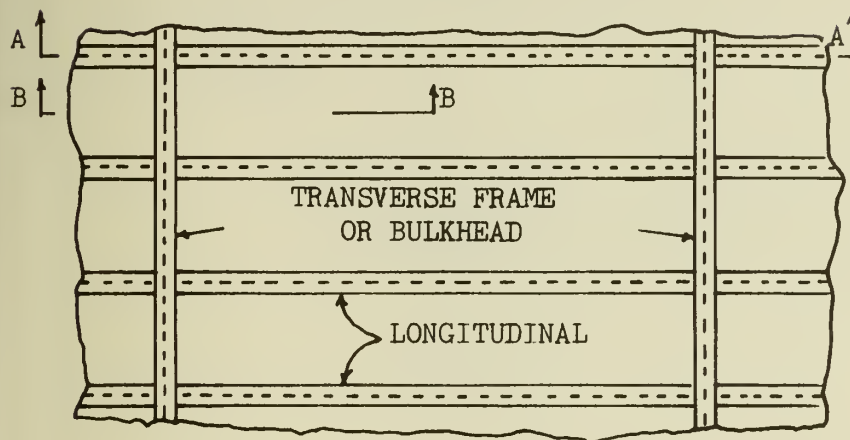


FIGURE 10.1. BENDING STRESSES IN SHIPS 47



results from a panel of plate, that is supported on all four edges, reacting to a lateral load. This load may be caused by hydrostatic pressure.

An expression for plate panel bending stress under a uniform hydrostatic load is<sup>47</sup>

$$\sigma_3 = \frac{1}{2} K_L \rho h \left(\frac{b}{t}\right)^2 \frac{1}{144} \text{ psi}$$

Where:

$\sigma_3$  is the plate panel bending stress

$K_L$  is a modifying coefficient varying with panel aspect ratio (see Figure 10.2)

$\rho$  is the density of the loading medium ( $\text{Lb}/\text{ft}^3$ )

$h$  is the pressure head (ft.)

$b$  is the smaller panel dimension (in.)

$t$  is the thickness of the plate (in.)

The stress in a member can be calculated by combining these three levels of stress. In an adequate design, this combination should be such that

$$\sigma_1 + \sigma_2 + \sigma_3 \leq \sigma_y$$

The method described above is normally used in the design of new ships. That is, an allowable stress level is chosen and the above relationships are used to find the ship's scantlings, such as plating thickness.

We will, however, use this method to find the stress in a member knowing the scantlings of the two ships described in section IX. While this method may not be exact, it will provide us with a reasonable estimate of the stress in the structural



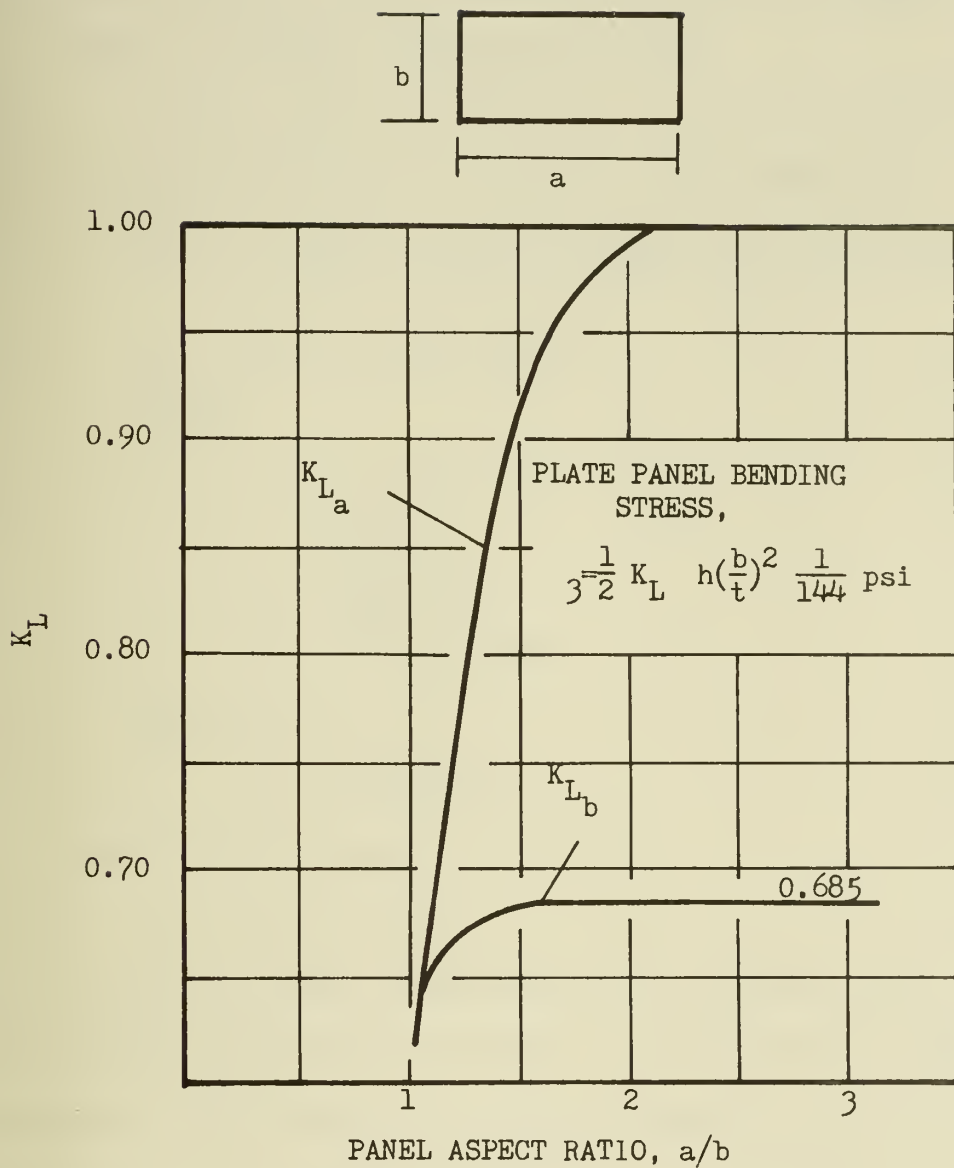


FIGURE 10.2. THE VARIATION OF  $K_L$  WITH PANEL ASPECT RATIO,  $a/b$  <sup>47</sup>



members in which we are interested.

The first typical joint that we will analyze is the transverse bulkhead to the ship's hull plating as described in Figure 9.1.

Case 1: Destroyer Tender (AD-37 class)

Joint: Transverse bulkhead to ship's shell plating

$$\sigma_1 = 7 \text{ tons/in}^2 = 15,680 \text{ psi} \text{ (see reference 48)}$$

$\sigma_2 = 0$  (Section shown in Figure 9.1 is not taken through a longitudinal; see Figure 10.3)

$$\sigma_3 = \frac{1}{2} K_L \rho h \left(\frac{b}{t}\right)^2 \frac{1}{144} \text{ psi}$$

Where:

$$\rho = 64 \text{ lbs/cu.ft.}$$

$$h = 24 \text{ ft.}$$

$$b = 2.5 \text{ ft.}$$

$$a = 13.42 \text{ ft.}$$

$$a/b = 5.367$$

$$K_L = 1.0 \text{ (see Figure 10.2)}$$

Therefore:

$$\sigma_3 = 12,280 \text{ psi}$$

Combining these stresses, we obtain

$$\sigma_1 + \sigma_3 = 27,960 \text{ psi}$$

We will now check the damaged case of this same joint. In this case the water head is assumed to be from the main deck, thus changing  $h$  from 24 feet to 67.5 feet. Therefore,  $\sigma_3$  becomes 34,538 psi. According to reference 48, when analyzing the damaged condition, one can eliminate the hull bending stress  $\sigma_1$ . Taking this into account

$$\sigma_1 + \sigma_2 + \sigma_3 = 34,538 \text{ psi} < 36,000 \sigma_y$$

This can be taken as the worst case, and this value will be used in section XI when we employ computer analysis to determine



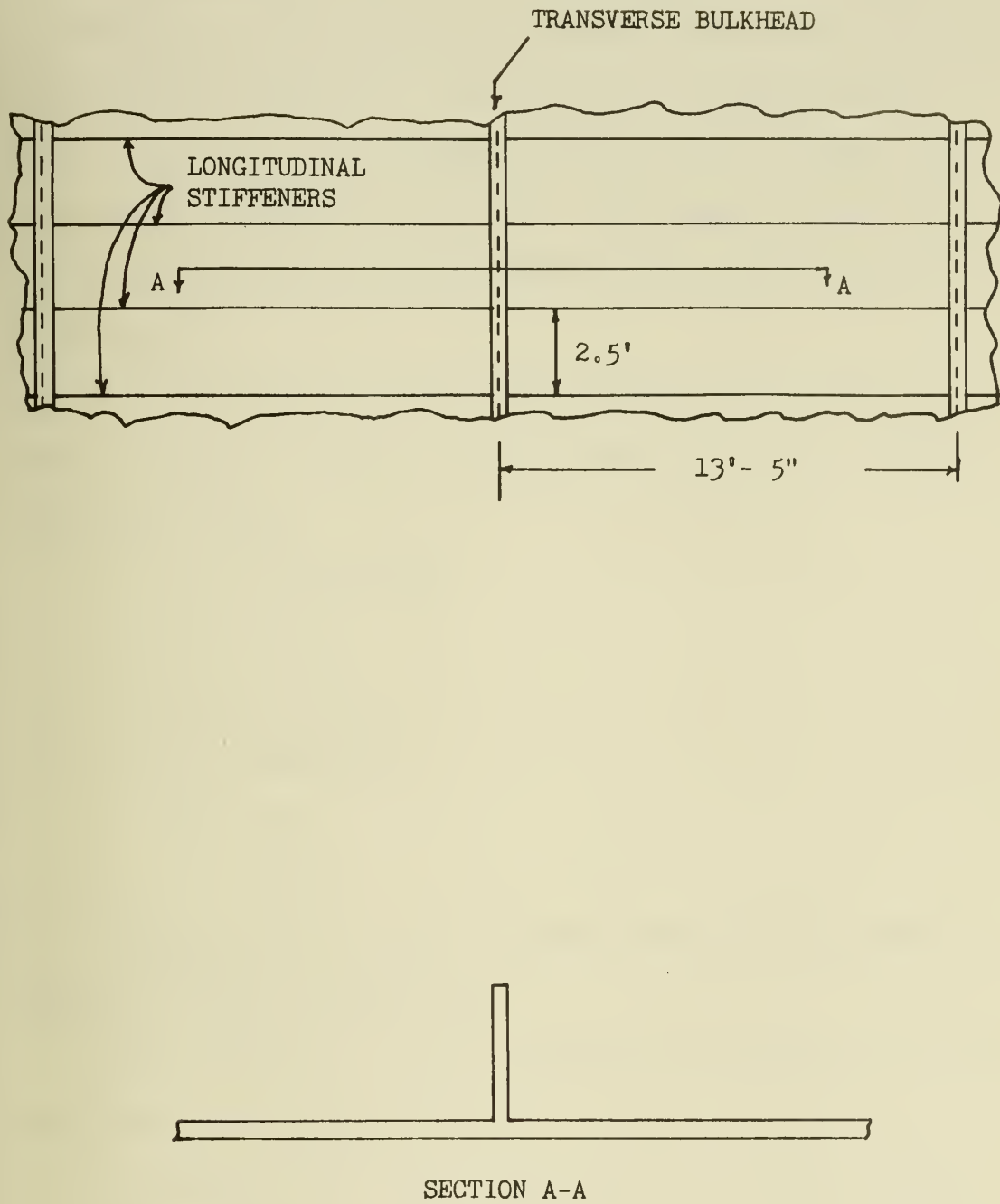


FIGURE 10.3. TYPICAL BOTTOM STRUCTURE OF AN AD-37 CLASS SHIP



the strength of the fillet welded joint as described by Figure 9.1.

The next typical joint that we will analyze is the one between a longitudinal and the ship's hull plating of the AD-37 class ship as described in Figure 9.3. The variation of ships principle bending stress,  $\sigma_1$ , with distance from the keel is plotted for the sagging condition in Figure 10.4. This figure is based on the assumption that the neutral axis is 0.45 times the depth of the ship.

Using the same procedure as was employed in case one, we find that  $\sigma_3$  is 14,016 psi. The following values were used to obtain this result:

$$\rho = 64 \text{ lbs/cu. ft.}$$

$$h = 24 \text{ ft.}$$

$$b = 2.67 \text{ ft.}$$

$$a = 13.42 \text{ ft.}$$

$$K_L = 1.0$$

$$t = 5/8 \text{ inch}$$

Combining these stresses, we obtain that  $\sigma_T$  of the shell plating is equal to 29,696 psi.

Again checking the damaged condition, we find that it is the worst case with a  $\sigma_T$  of 34,538 psi.

The stress in the longitudinal member is as shown in Figure 10.4.

The next typical joint that we will analyze is the one between a longitudinal and the shell plating of the AO-143 class ship as shown in Figure 9.5. In the sagging condition,  $\sigma_1$  at the keel is 14,134 psi, and it varies with the distance from the base line as shown in Figure 10.5. Again this figure is based upon the assumption



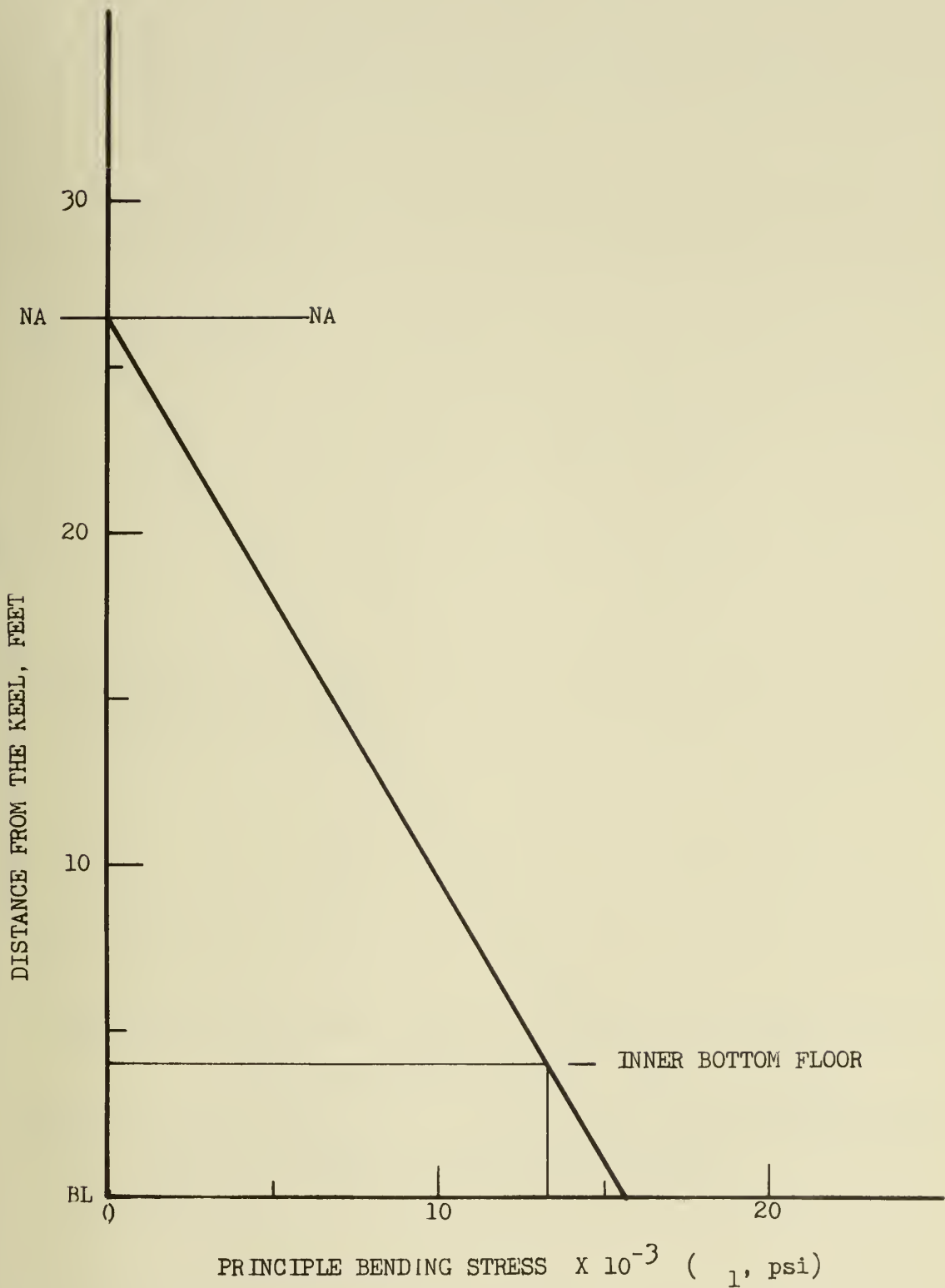


FIGURE 10.4. THE VARIATION OF  $\sigma_1$  WITH DISTANCE FROM THE KEEL OF THE AD-37 CLASS SHIP IN THE SAGGING CONDITION



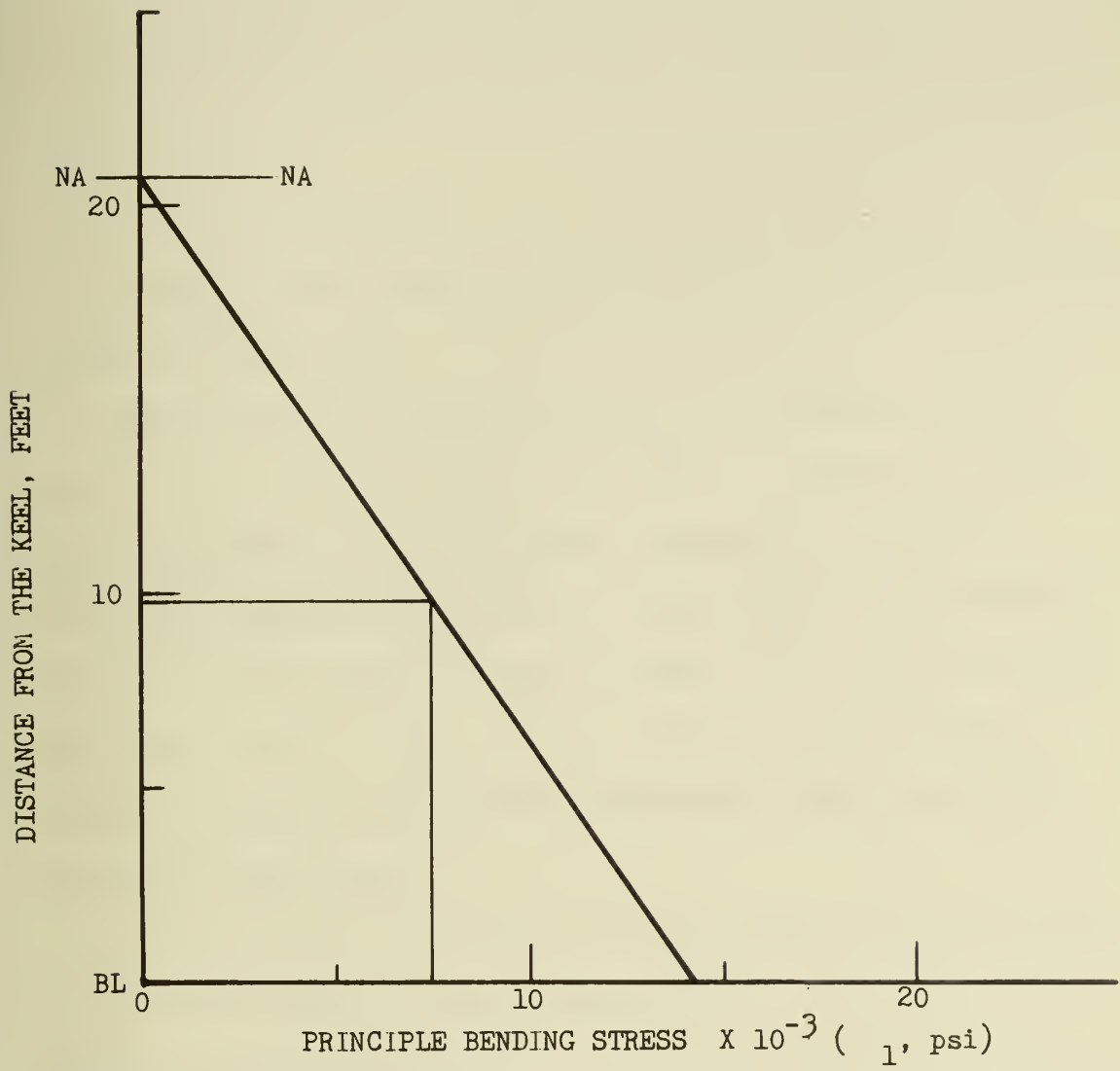


FIGURE 10.5. THE VARIATION OF  $\sigma_1$  WITH DISTANCE FROM THE KEEL OF THE AO-143 CLASS SHIP IN THE SAGGING CONDITION



that the neutral axis is located 45% of the distance from the keel to the main deck. In this case, we find that  $\sigma_3$  is 4,480 psi. The following values were used to obtain this result:

$$\rho = 64 \text{ lbs./cu. ft.}$$

$$h = 35 \text{ ft.}$$

$$b = 2.5$$

$$a = 10.0 \text{ ft.}$$

$$K_L = 1.0$$

$$t = 1.25 \text{ inches}$$

Combining these stresses, we obtain that  $\sigma_T$  of the shell plating is equal to 18,614 psi.

Again checking the damaged condition by changing  $h$  from 35 feet to 46 feet, we find that  $\sigma_3$  is equal to 5,888 psi. In this case, the combination of the sagging stresses and the normal hydrostatic membrane stresses is the worst case. This makes sense because the oiler has a lot less freeboard in the normal condition, and oilers have to be more concerned with hogging and sagging because they have the ability to change their loading condition by pumping fluid cargo.

The next typical joint that we will analyze is the one between a transverse bulkhead in the midship section of the ship and the shell plating of the AO-143 class ship as shown in Figure 9.6. In this case, the primary bending stress in the sagging condition,  $\sigma_1$ , is 14,134 while the tertiary stress,  $\sigma_3$ , is 4,480, which is based upon the following values.

$$\rho = 64 \text{ lbs./cu. ft.}$$



$$h = 35 \text{ ft.}$$

$$b = 2.5 \text{ ft.}$$

$$a = 10.0 \text{ ft.}$$

$$K_L = 1.0$$

$$t = 1.25 \text{ inches}$$

Combining these stresses, we obtain that  $\sigma_T$  is equal to 18,614 psi. The damaged condition again results in a  $\sigma_3$  of 5,888 psi.

As was the case for the longitudinal joint, the combination of the normal sagging stress and the hydrostatic membrane stresses is the worst case. For a summary of the stresses in the structural members of the joints we have discussed, see Table 10-1.

Now that we have analyzed the stresses in some of the typical joints discussed in section IX, we will use these stresses and the geometry of the joints as inputs to a finite element method computer model to determine the strength of these fillet welded joints.

The discussion of the computer model and results can be found in the following section.



TABLE 10-1. A Summary of Stresses in  
Structural Members of Joints

Ship	Joint (Figure)	Condition	$\sigma_1$	$\sigma_3$	$\sigma_T$
AD-37	Transverse Bulkhead (9.1)	Normal	15,680	12,280	27,960
		Damaged	--	34,538	34,538
AD-37	Longitudinal (9.3)	Normal	15,680	14,016	29,696
		Damaged	--	34,538	34,538
AO-143	Transverse Bulkhead (9.6)	Normal	14,134	4,480	18,614
		Damaged	--	5,888	5,888
AO-143	Longitudinal (9.5)	Normal	14,134	4,480	18,614
		Damaged	--	5,888	5,888



## XI COMPUTER ANALYSIS OF STRENGTH OF SELECTED FILLET WELDED JOINTS

In this section, we will discuss the results of the computer model that was employed for determining the strength of fillet welds. The model was developed at the Massachusetts Institute of Technology by Malliris<sup>49</sup> using the finite element method of an available library program. The program that was used in this case was ADINA which was developed in the Mechanical Engineering Department of MIT.<sup>50</sup> ADINA is a general purpose finite element program for linear and non-linear static and dynamic three dimensional analysis. The fillet weld model employed ADINA in the static and elastic-plastic mode following the Von Mises yield criterion. We will review a few of the details of the model that was used for the joint between a transverse bulkhead and the ship shell plating as shown in Figure 9.1. The boundary conditions and the applied load, which is a uniform tensile load, can be seen in Figure 11.1.

We will now look at the case of a 30% reduction in the specified weld size for the joint shown in Figure 9.1. The finite element mesh consists of 219 nodes and 72 elements and is best described by Figure 11.2. The loading function, which was derived from the structural analysis of section X, is comprised of two time steps and is plotted in Figure 11.3. And the resulting displacement of the toe element can be seen in Figure 11.4.

In order to determine the strength of a fillet weld, we need a general yielding criterion. We will define a yielding criterion,  $X$ , as:

$$X = \frac{\text{length of the yield plastic zone}}{\text{fillet weld leg size}}$$



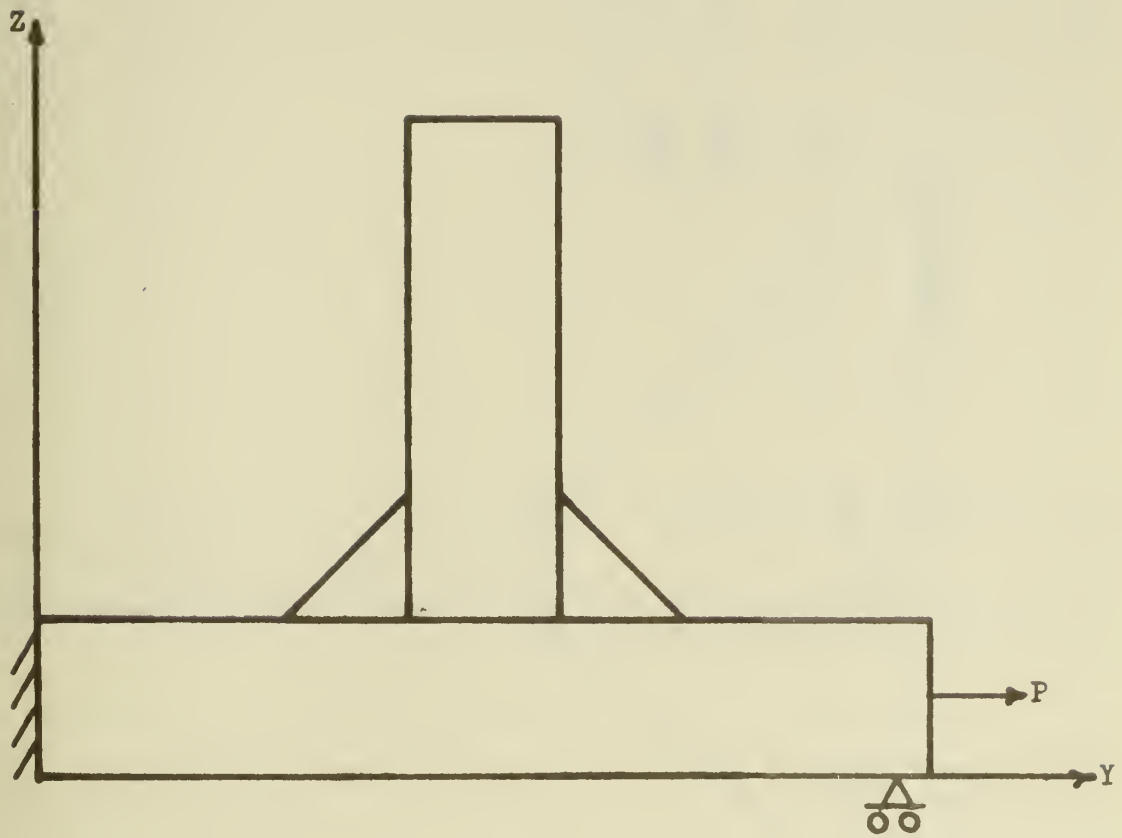
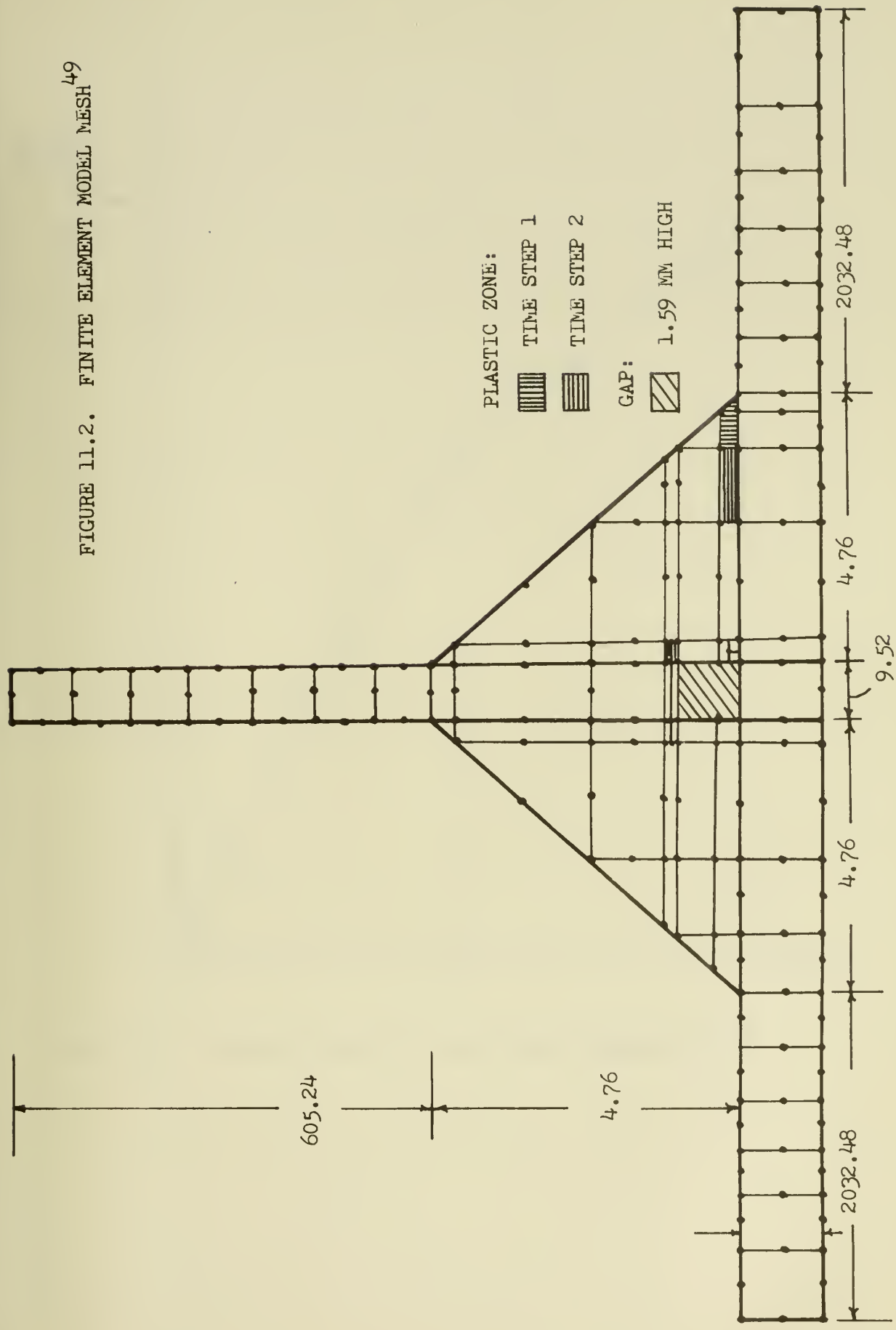


FIGURE 11.1. THE BOUNDARY CONDITIONS AND THE APPLIED LOADS OF THE FILLET WELD MODEL<sup>49</sup>



FIGURE 11.2. FINITE ELEMENT MODEL MESH 49





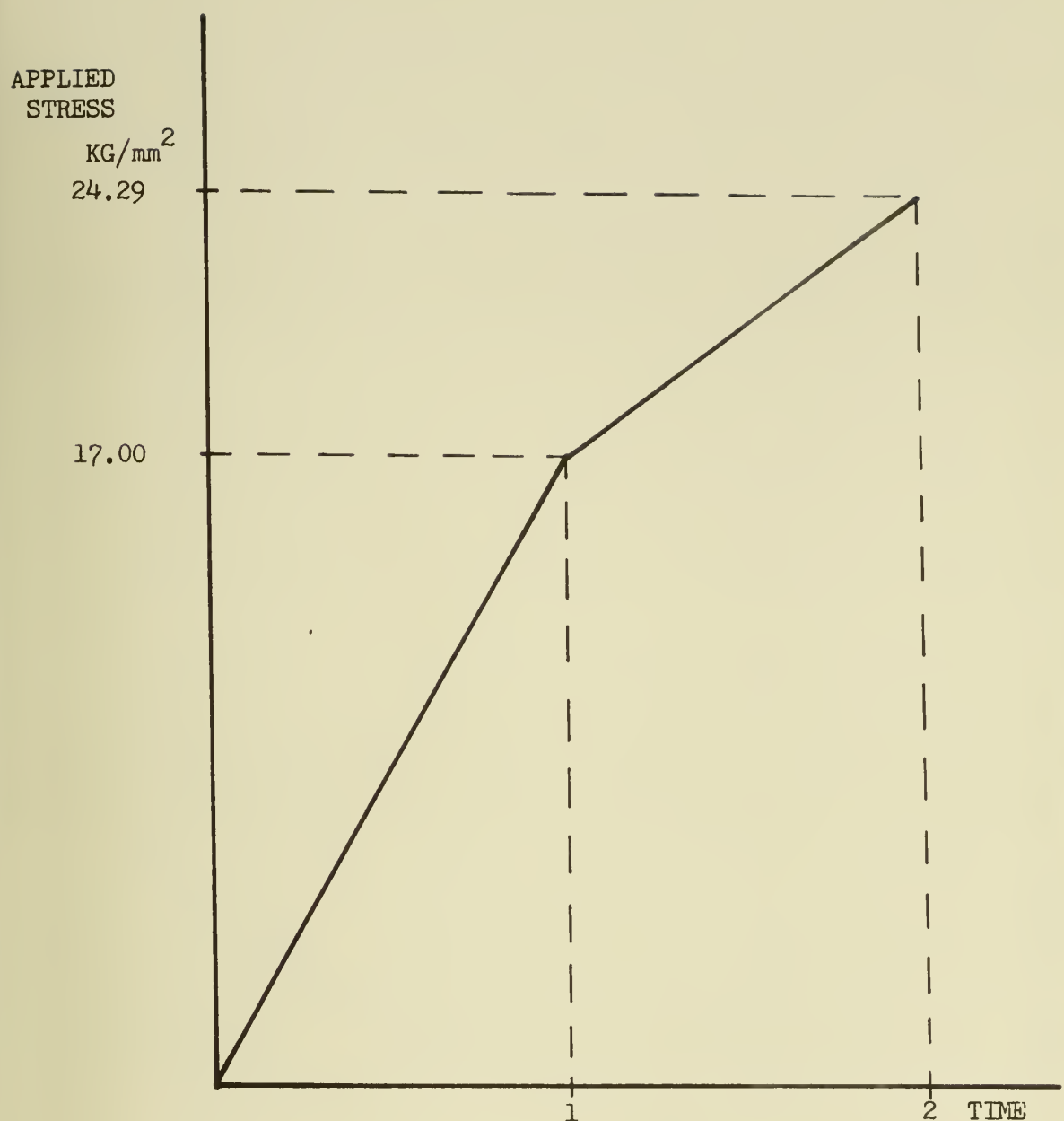


FIGURE 11.3. LOADING FUNCTION OF THE FINITE ELEMENT MODEL <sup>49</sup>



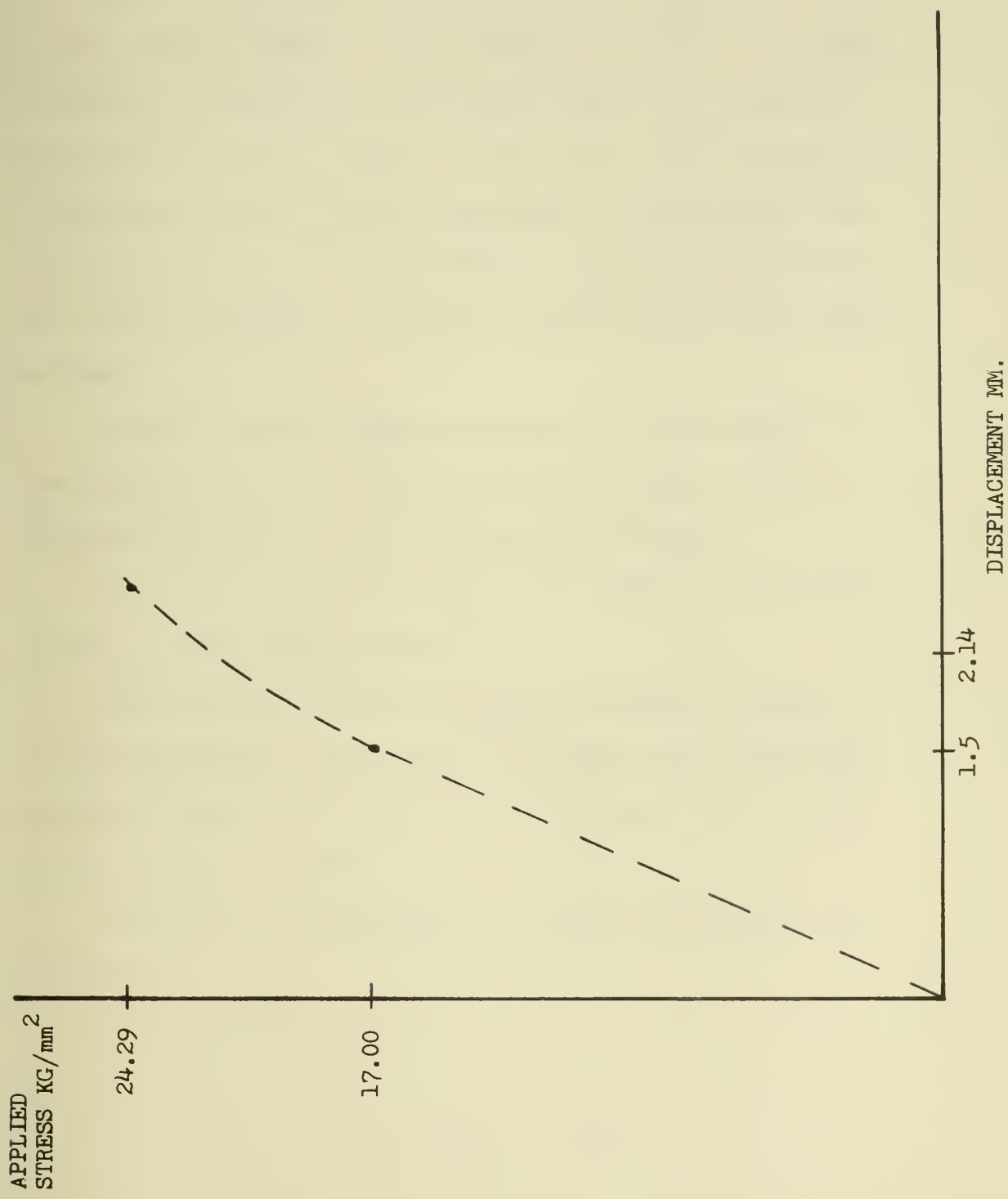


FIGURE 11.4. RESULTING DISPLACEMENT OF THE TOE ELEMENT<sup>49</sup>



It might be helpful to look at Figure 11.2, which shows the elements which make up the plastic zone and also the fillet weld leg size.

Using this general yielding criterion, we find that by starting with the required weld size for the transverse bulkhead joint as shown in Figure 9.1 and reducing this weld size by 10% increments, we obtain the relationship between the reduction in weld size and  $X$  that is shown in Figure 11.5. This indicates that a reduction of more than 30% is possible, but the required weld size was  $3/16$  of an inch and reducing a weld size below  $1/8$  of an inch seems meaningless at this time with the present day welding methods.

A sample computer output for the case of a 30% reduction of the specified weld size for the transverse bulkhead joint as described by Figure 9.1 can be found in the Appendix.

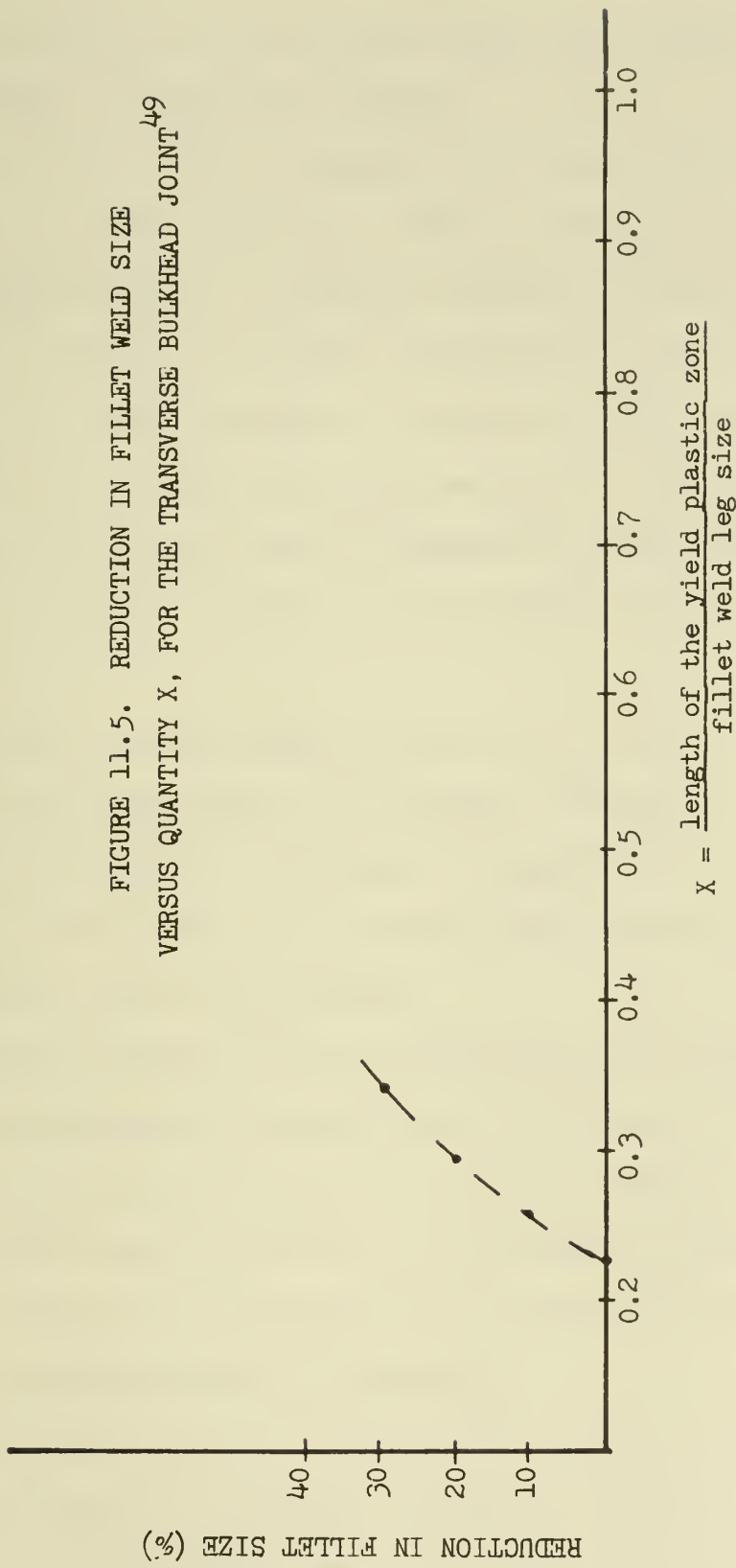
For a more detailed discussion of the model and the general yielding criterion see reference 49.

Future work in this area involves the computer analysis of the longitudinal joints which will require three dimensional analysis instead of the two dimensional analysis that was used for the transverse joints.

For further recommendations for possible future work, see section XV.



FIGURE 11.5. REDUCTION IN FILLET WELD SIZE  
VERSUS QUANTITY  $X$ , FOR THE TRANSVERSE BULKHEAD JOINT<sup>49</sup>





## XII CORROSION CONSIDERATIONS

In this section, we will examine some of the corrosion considerations concerning fillet welds.

There are many types of corrosion, but these types can be grouped into two main categories. These are general corrosion and localized corrosion. By general corrosion, we mean the uniform attack of a material--for example, the rusting of a steel plate in sea water. The steel corrodes at a relatively uniform rate of about  $0.005^{51}$  inches penetration per year (ipy). This is an average value that can be used in engineering calculations; however, the initial corrosion rate will generally exceed this value.

Localized corrosion means that the rate of corrosion is greater in some areas than it is in others. Pitting is an example of localized corrosion. In pitting, an appreciable attack is confined to a small area of the material which acts as an anode. This results in pits in the material.

A specific example of this is stainless steel in sea water. Pits usually initiate at crevices; and, in this case, the localized attack is called crevice corrosion. The most sensible way of combatting this type of corrosion is to eliminate crevices altogether. However, when this is not possible, the crevices can be widened so that the concentration cell is minimized.

Figure 12.1 shows the difference in the amount of corrosion before the failure of a structure with general and localized corrosion. It can be easily seen that usually a failure occurs in



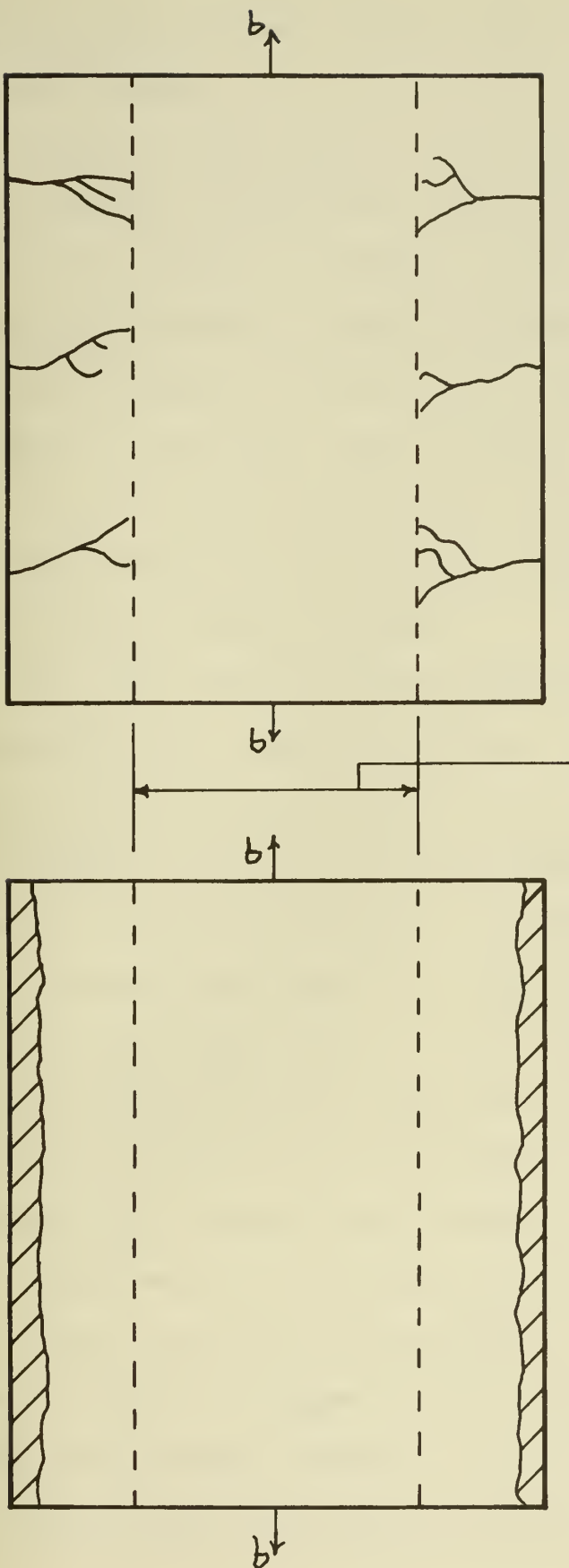


FIGURE 12.1. A COMPARISON OF THE AMOUNT OF METAL LOSS BEFORE FAILURE FOR: 52

- a. General Corrosion
- b. Localized Corrosion



less time with localized corrosion rather than with general or uniform corrosion.

Now that we have looked at a few types of corrosion, we will discuss methods of preventing or controlling corrosion. The two most obvious methods of combatting corrosive attack are to either change the environment or change the material. Since we are primarily interested in welded joints in ships, it would be impossible to change the environment (namely seawater). And, although there have been other materials used in ship construction, the majority of ships are fabricated out of steel. Thus, we need to look to other methods to control corrosion.

One method that has been used with some success is covering the material with a protective coating. This basically separates the material and the environment. There are many different types of coatings, and each has its own advantages and disadvantages. However, the biggest disadvantage of coatings in general is that, if the coating should break down by either chipping off or peeling, this sets up an ideal condition for localized attack. This is primarily because the anode-cathode area ratio is small due to the fact that the unprotected spot becomes the anode and is attacked faster than the area surrounding it.

Another method of controlling corrosion that should be obvious but is often overlooked is proper design and fabrication. Many times a structure is assumed to have a proper design if it is sound from a strength standpoint. And the corrosion engineer is not consulted until the structure is about to collapse due to



strength degradation resulting from corrosive action. At times this stems from complete disregard for the corrosion considerations of the design. A general example of different quality of designs for storage tank supports can be seen in Figure 12.2.

Now that we have discussed corrosion in general terms, we will examine corrosion considerations that directly pertain to welded joints. For general or uniform corrosion, the best method to ensure a proper design is the use of corrosion margin. The U.S. Navy specifications do not require a corrosion margin; however, A.B.S. requires a corrosion margin of 1.5 mm. A schematic diagram of the use of a corrosion margin for fillet welds can be seen in Figure 12.3. Using the uniform corrosion rate of 0.005 ipy for steel in sea water, this gives a service life of approximately 12 years. Since this rate is an average rate and as the time increases the rate decreases due to a build-up of oxides on the surface, normally a rate of 0.003 or 0.004 ipy is used for a period of ten years.<sup>53</sup> The slower rate would yield a service life of approximately 20 years. Since most surfaces on a ship that are exposed to sea water or bilge water are maintained so that some form of protective coating is kept intact most of the time, the corrosion margin required by A.B.S. is considered sufficient for steel weld joints in a sea water environment.

Another fact that makes the actual margin greater than the apparent margin is that weld sizes are based upon the minimum plate thickness. And, if there is a situation in which general corrosion may be a problem, the plate thickness will probably be



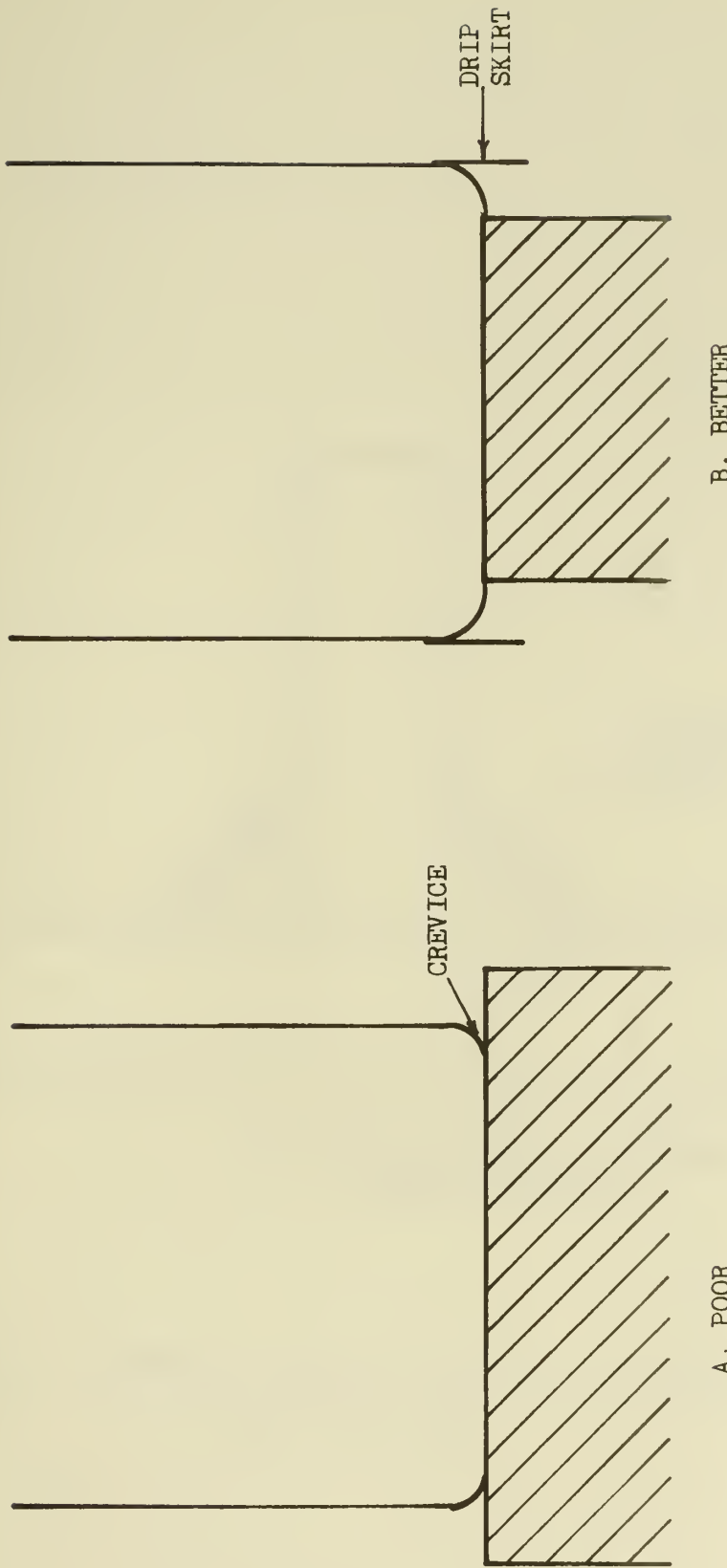


FIGURE 12.2. DESIGN OF TANK SUPPORTS<sup>52</sup>



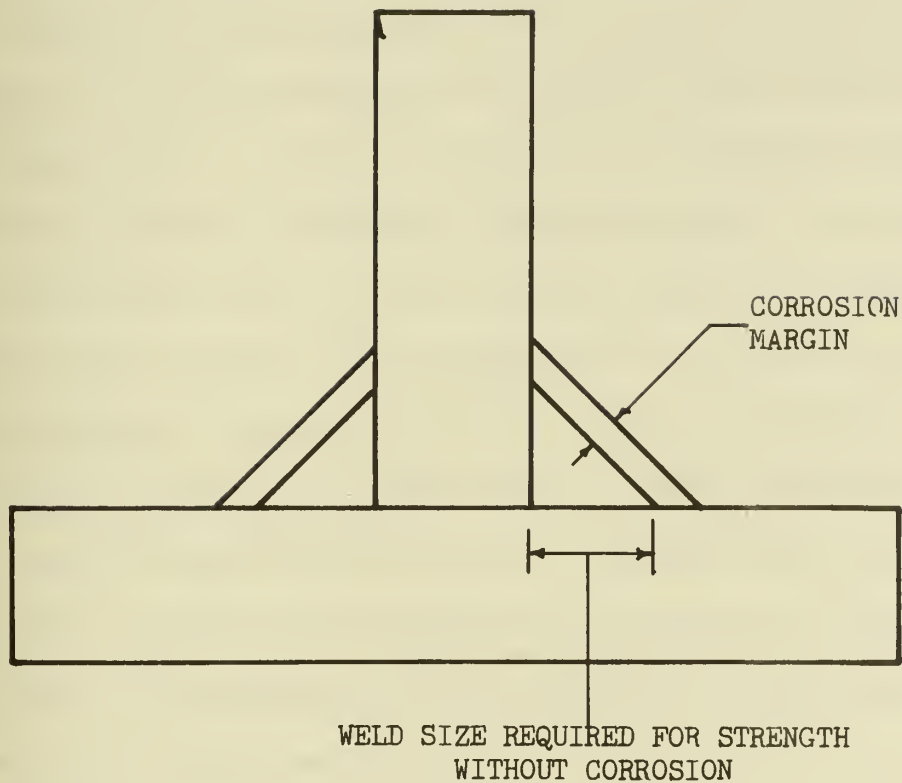


FIGURE 12.3. A SCHEMATIC DIAGRAM OF THE USE OF A CORROSION MARGIN FOR A FILLET WELD



increased which will result in an increased required weld size.

While the A.B.S. corrosion margin is considered appropriate for welded joints exposed to sea water or bilge water, no margin is considered necessary for joints exposed to air. Each joint environment must be considered separately. Then, if joints have the same environment, it may be advantageous to group these for the purpose of assigning the required corrosion margins.

Now that we have discussed uniform corrosive attack, we will proceed to localized corrosion considerations that directly pertain to welded joints. A corrosion margin is not generally the most efficient method of controlling localized corrosion. As can be seen from Figure 12.1, in order to provide sufficient margin against local corrosion, the designer would have to provide an extreme excess of material. A better method of controlling localized corrosion is to ensure that the design and fabrication are such that sites that would enhance localized attack are eliminated. Figure 12.2 demonstrates this approach in general, and Figure 12.4 provides a similar demonstration pertaining directly to a fillet welded joint.

Another consideration that has to be a part of the design of a structure is the polarity of the corrosive cell between the weld material and the parent metal. This is the same approach that has been used in riveted and bolted joints. We want the base metal to be more anodic than the weld material, the bolt, or the rivet. If this were not the case, the joint would fail because the "fastener" would corrode away. Normally the weld material used in the construc-



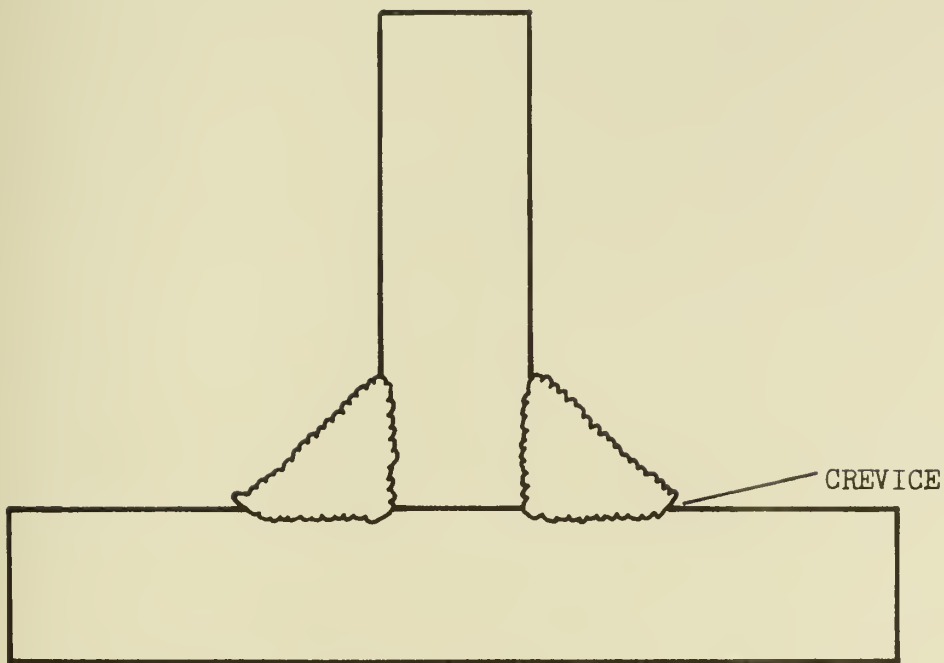


FIGURE 12.4. A FILLET WELD WITH A CREVICE AT THE TOE  
RESULTS IN A POOR QUALITY WELD



tion of ships sets up the right polarity, but this is something that should be checked in order to ensure adequate strength throughout the joint's useful life.

The details of the corrosion margin of a typical welded joint will be discussed further in section XV.



### XIII ECONOMIC ANALYSIS OF INTERMITTENT VERSUS CONTINUOUS WELDING

In this section, we will compare the relative cost of a given welding job employing manual continuous welding, manual intermittent welding, and automatic continuous welding.

We have already discovered that welding cost is a very important variable in the total construction cost of a ship's hull.

In a ship, fillet welds are used to join stiffeners to plating. For example, in deck stiffeners and bulkhead stiffeners, the fillet welds do not experience shear forces of great magnitudes; and, hence, welding specifications have allowed intermittent fillet welds to be used. The problem is now what welding procedure will yield the lowest welding cost. The welding procedure candidates that will be studied are manual continuous welding, manual intermittent welding, and automatic continuous welding.

Two approaches will be used to compare the costs of the various welding methods. The first approach will employ a laboratory experiment. The second approach will be based upon industrial data.

In order to compare these methods, both approaches will employ a computer program to calculate the welding cost of each method. The program was written based on equations given in reference 54, to be run on the programmable calculator, Texas Instruments TI-59. A copy of this program appears in Table 13-1.

Data for the manual continuous and manual intermittent welding was taken during experimental welding runs conducted in the welding laboratory at Massachusetts Institute of Technology. The welder



TABLE 13-1. Estimating Welding Cost\*

Loc.	Code	Key									
00	43	RCL	46	55	÷	92	14	14	138	09	09
01	01	01	47	43	RCL	93	54	)	139	55	÷
02	55	÷	48	07	07	94	95	=	140	06	6
03	53	(	49	55	÷	95	42	STO	141	00	0
04	43	RCL	50	43	RCL	96	23	23	142	95	=
05	01	01	51	08	08	97	93	•	143	42	STO
06	85	+	52	95	=	98	00	0	144	26	26
07	43	RCL	53	42	STO	99	03	3	145	43	RCL
08	02	02	54	23	23	100	65	X	146	04	04
09	54	)	55	03	3	101	43	RCL	147	65	X
10	95	=	56	65	X	102	11	11	148	43	RCL
11	42	STO	57	43	RCL	103	65	X	149	10	10
12	21	21	58	03	03	104	43	RCL	150	55	÷
13	43	RCL	59	55	÷	105	12	12	151	06	6
14	04	04	60	43	RCL	106	65	X	152	00	0
15	65	X	61	07	07	107	43	RCL	153	95	=
16	43	RCL	62	55	÷	108	03	03	154	42	STO
17	03	03	63	43	RCL	109	55	÷	155	27	27
18	55	÷	64	08	08	110	43	RCL	156	43	RCL
19	06	6	65	95	=	111	05	05	157	22	22
20	00	0	66	42	STO	112	95	=	158	85	+
21	55	÷	67	24	24	113	42	STO	159	43	RCL
22	43	RCL	68	91	R/S	114	24	24	160	23	23
23	05	05	69	61	GTO	115	43	RCL	161	85	+
24	55	÷	70	01	01	116	15	15	162	43	RCL
25	43	RCL	71	33	33	117	65	X	163	24	24
26	21	21	72	43	RCL	118	43	RCL	164	85	+
27	95	=	73	11	11	119	16	16	165	43	RCL
28	42	STO	74	65	X	120	65	X	166	25	25
29	22	22	75	43	RCL	121	43	RCL	167	85	+
30	01	1	76	12	12	122	03	03	168	43	RCL
31	32	X T	77	65	X	123	55	÷	169	26	26
32	43	RCL	78	43	RCL	124	06	6	170	85	+
33	00	00	79	03	03	125	00	0	171	43	RCL
34	77	GE	80	55	÷	126	55	÷	172	27	27
35	00	00	81	43	RCL	127	43	RCL	173	95	=
36	72	72	82	05	05	128	05	05	174	42	STO
37	01	1	83	65	X	129	95	=	175	28	28
38	00	0	84	53	(	130	42	STO	176	91	R/S
39	00	0	85	43	RCL	131	25	25			
40	65	X	86	06	06	132	68	NOP			
41	43	RCL	87	85	+	133	43	RCL			
42	03	03	88	43	RCL	134	04	04			
43	65	X	89	13	13	135	91	R/S			
44	43	RCL	90	65	X	136	65	X			
45	06	06	91	43	RCL	137	43	RCL			



TABLE 13-1. Continued

## Program Input

Data Registers	Description
00	0 Manual/1 Auto
01	$T_u$ Arc Time min
02	$T_d$ Downtime min
03	$l_x$ inches of weld
04	L Labor + OH Rate \$/hr.
05	S in/min Deposit Rate
06	E Electrode Cost \$/lb.
07	N No. Elect./100 lb.
08	$l_w$ inches weld/elect.
09	$H_u$ handling time, min.
10	$C_u$ Cleaning time, min.
11	M inch elect. melt/min.
12	$W_m$ lbs./in. electrode
13	Ratio flux to elect. wt.
14	Flux cost \$/lb.
15	Gas Cost \$/cu. ft.
16	Gas Flow $ft^3/hr.$

## Program Output

22	L + OH Cost \$
23	Electrode Cost \$
24	Power Cost \$
25	Gas Cost \$
26	Handling Cost \$
27	Cleaning Cost \$
28	Total Cost \$

\*This program estimates the cost welding per unit job for Manual (stick electrode), Submerged Arc Welding, and Gas Metal Arc (GMA or MIG). By inserting a 0 or 1 into Data Register 00, the operator selects either manual or automatic respectively. Enter remaining input in registers 01-16 as appropriate. Final display is total cost per job in dollars. To get other outputs RCL desired data register.



was Mr. Anthony Zona, and the author took the data.

Drawings of the test pieces used in this study can be found in Figures 13.1 and 13.2. Only one run was made for both types of manual welding. The data sheets can be found in Table 13-2 and Table 13-3 respectively.

For the automatic method, some of the data was obtained from welding data books while some of it was estimated based on the manual welding runs. An example of this is handling time. The data sheet for the automatic continuous welding can be found in Table 13-4.

All of the cost or price information was obtained from local vendors of welding supplies.

A local shipyard was contacted to obtain a realistic labor and overhead rate and an operating factor for each type of welding process; however, the author was informed that these numbers are confidential. The labor and overhead rate used was a value from reference 54 which was then adjusted for inflation. The operating factors were obtained from the experimental test runs.

The total cost of welding is the sum of the following costs:

1. The labor and overhead cost during actual welding.
2. The cost of handling and set up of the work piece.
3. The cost of post welding cleaning if necessary.
4. The cost of the electrode material consumed during welding.
5. The cost of the shielding gas consumed during welding.
6. The cost of the power to run the welding machine.



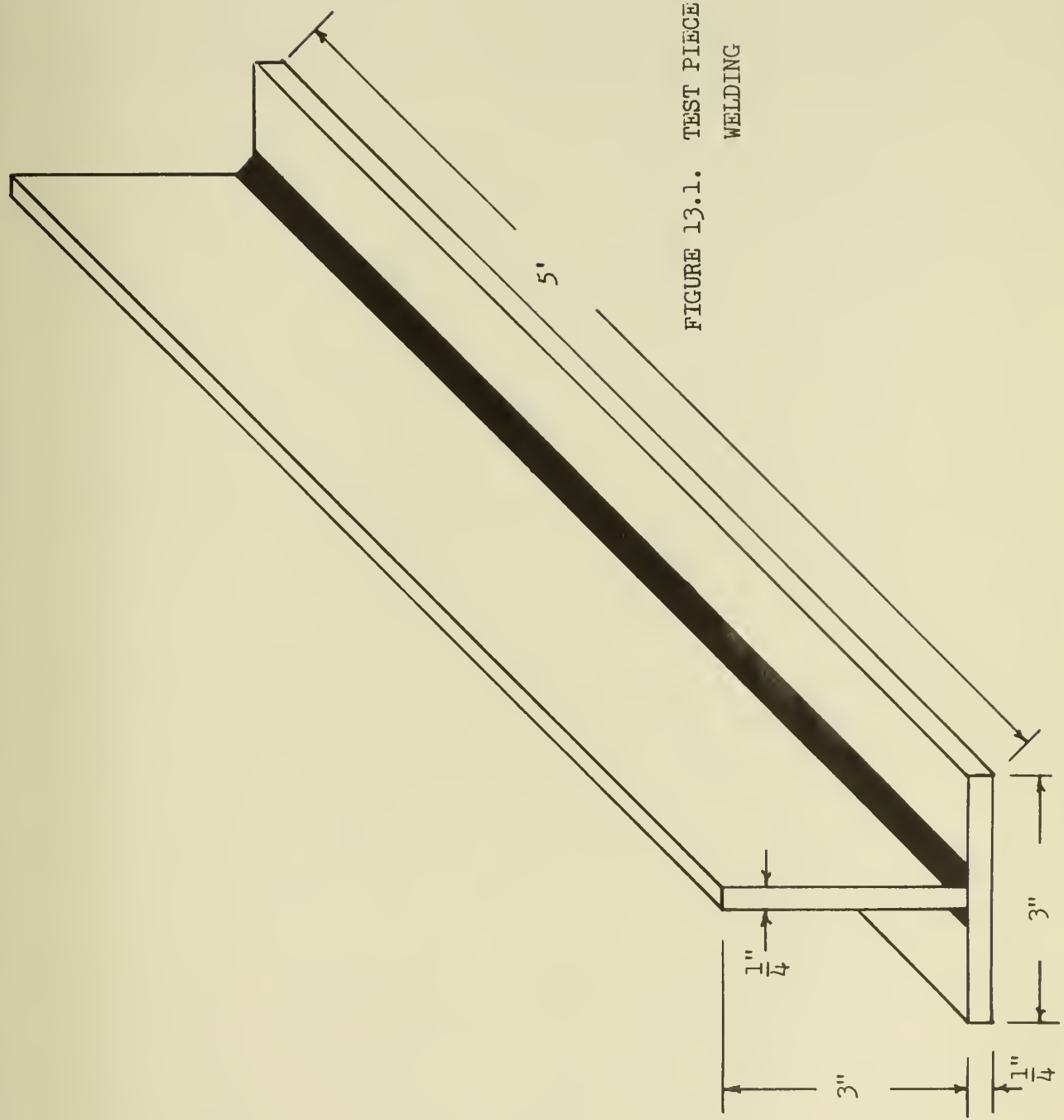


FIGURE 13.1. TEST PIECE FOR CONTINUOUS  
WELDING



FIGURE 13.2. TEST PIECE FOR INTERMITTENT WELDING

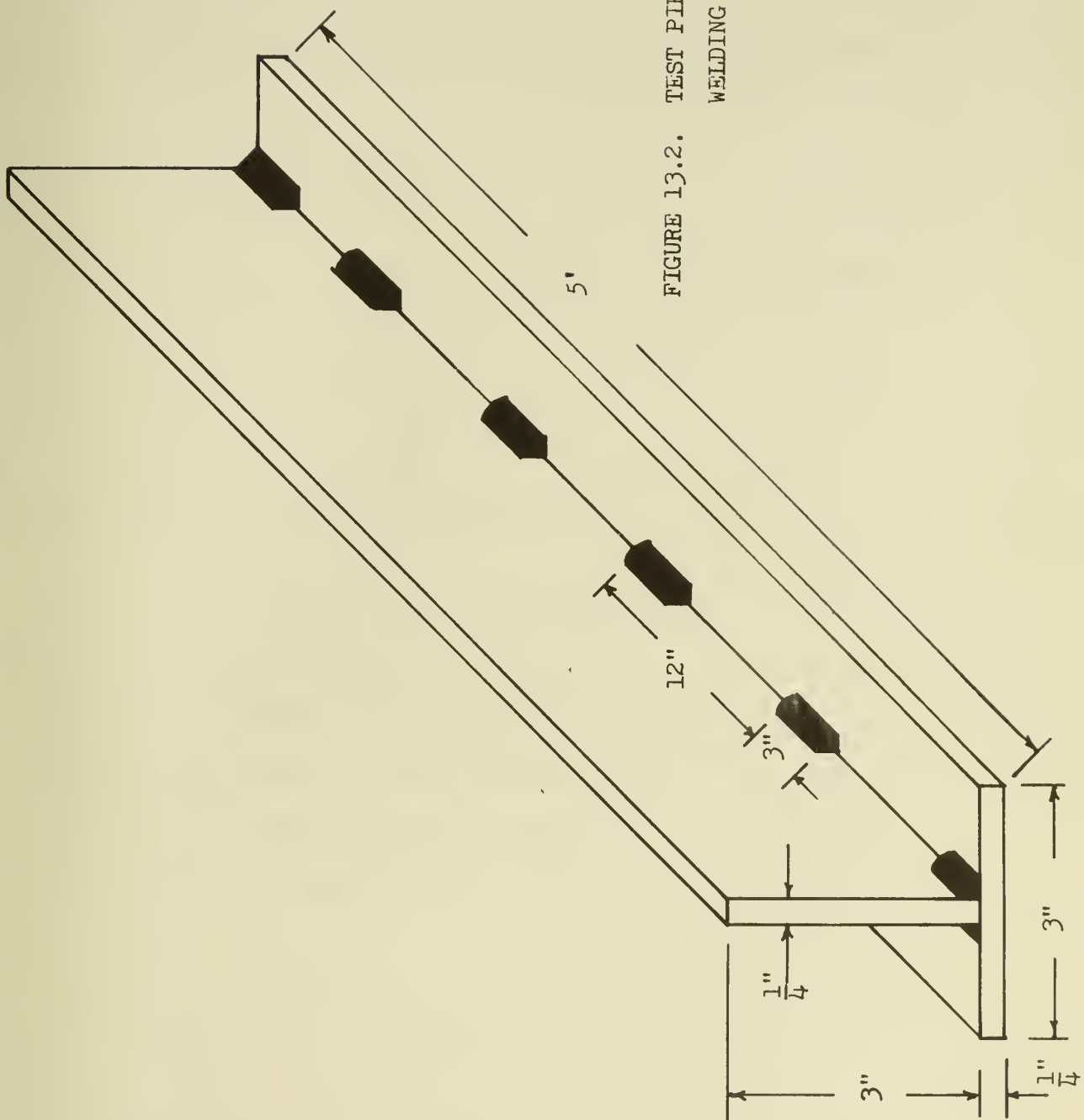




TABLE 13-2. Continuous Manual Welding  
(Experimental Approach)

Data Register	Parameter Title - Description	Value or Comment
--	Material	Mild Steel
--	Electrode	1/8" X 14" E7014
--	Weld Size (leg)	5/32"
--	Welding Conditions	150 Amp 18-22 Volt
00	Manual or Automatic Selection	0 (Manual)
01	$T_u$ = Arc Time min per unit	14.25
02	$T_d$ = Downtime min per unit	4.583
03	$l_x$ = Inches of Weld per unit (both sides)	120.
04	$L$ = Labor and Overhead rate \$ per hour	12.00
05	$S$ = Inches of Weld Deposited per min.	8.276
06	$E$ = Electrode Cost \$ per lb.	0.50
07	$N$ = Number of Electrodes per 100 lbs.	1280
08	$l_w$ = Inches of Weld per Electrode	7.5
09	$H_u$ = Handling Time per unit, min.	3.667
10	$C_u$ = Cleaning Time per unit, min.	6.00



TABLE 13-2. Continued

Data Register	Parameter Title - Description	Value or Comment
Program Output		
22	Labor and Overhead Cost per Job	\$ 3.83
23	Welding Consumables Cost per Job	.63
24	Power Cost per Job	.04
26	Handling Cost per Job	.73
27	Cleaning Cost per Job	1.20
28	Total Cost per Job	\$ 6.43



TABLE 13-3. Intermittent Manual Welding  
(Experimental Approach)

Data Register	Parameter Title - Description	Value or Comment
--	Material	Mild Steel
--	Electrode	1/8" X 14" E7014
--	Weld Size (leg)	3/16"
--	Welding Conditions	150 Amp 18-22 Volt
00	Manual or Automatic Selection	0 (Manual)
01	$T_u$ = Arc Time, min. per unit	4.633
02	$T_d$ = Downtime, min. per unit	2.750
03	$l_x$ = Inches of weld per unit	36.
04	$L$ = Labor and Overhead rate \$ per hour	12.00
05	$S$ = Inches of Weld deposited per min.	8.276
06	$E$ = Electrode Cost \$ per lb.	0.50
07	$N$ = Number of electrodes per 100 lb.	1280
08	$l_w$ = Inches of Weld per Electrode	7.5
09	$H_u$ = Handling time per unit, min.	4.167
10	$C_u$ = Cleaning time per unit, min.	1.917



TABLE 13-3. Continued

Data Register	Parameter Title - Description	Value or Comment
Program Output		
22	Labor and Overhead Cost per Job	\$ 1.39
23	Welding Consumables Cost per Job	.19
24	Power Cost per Job	.01
26	Handling Cost per Job	.83
27	Cleaning Cost per Job	.38
28	Total Cost per Job	\$ 2.80



TABLE 13-4. Continuous Automatic Welding  
(Experimental Approach)

Data Register	Parameter Title - Description	Value or Comment
--	Material	Mild Steel
--	Electrode	A 675 1/16"
--	Weld Size (leg)	5/32"
--	Welding Conditions	425 Amps 30 Volts
00	Manual or Automatic Selection	1 (Automatic)
01	$T_u$ = Arc Time min per unit	1.714
02	$T_d$ = Downtime min per unit	1.70
03	$l_x$ = Inches of Weld per unit (both sides)	120.
04	$L$ = Labor and Overhead rate \$ per hour	12.00
05	$S$ = Inches of Weld Deposited per min	70
06	$E$ = Electrode Cost \$ per lb.	0.61
09	$H_u$ = Handling Time per unit, min.	4.50
11	$M$ = Inches Electrode melted per min. (melting rate)	255.
12	$W_m$ = Weight of Electrode used per inch Electrode melted in lbs. per inch.	0.000868
15	$g$ = Gas Cost in \$ per cu. ft.	0.013
16	$r$ = Cu. Ft. of Gas Flow per hour during welding	35



TABLE 13-4. Continued

Data Register	Parameter Title - Description	Value or Comment
Program Output		
22	Labor and Overhead Cost per Job	\$ .68
23	Welding Electrode Cost per Job	.23
24	Power Cost per Job	.01
25	Gas Cost per Job	.01
26	Handling Cost per Job	.90
28	Total Cost per Job	\$ 1.83



While there is no capital cost or interest cost explicitly listed, these costs are taken into account in the labor and overhead rate that is used in all the formulas except for those used for calculating consumables cost.

Now we analyze the results of this experimental study. The total welding cost for the test piece was \$1.83 for continuous automatic welding (GMA), \$2.80 for intermittent manual welding, and \$6.43 for continuous manual welding.

In comparing the two manual methods, we find that the continuous method has an advantage for handling and setup cost but is bettered in every other category by the intermittent method. The reason the handling and setup cost is higher for the intermittent method is that the piece has to be marked so that the welder knows where to weld; whereas, the continuous method does not require marking. Since there is less welding in the intermittent method, all other costs are lower than the continuous method.

In proceeding to the automatic continuous method, we find that the handling and set up cost is the highest of any method, but the fact that the automatic method is so fast makes all the other costs the lowest. An additional advantage of the automatic method is that there is no post welding cleaning necessary because the shielding is done with a gas rather than with a slag as is the case for manual arc welding.

The operating factors, which are defined as the arc time divided by the total welding time, for manual continuous, manual intermittent, and automatic continuous were 75.7%, 62.8% and 50.2%



respectively. Although operating factors vary in industry from job to job and from company to company, it appears that the operating factors for the manual methods are relatively high. The operating factor of the automatic continuous method seems to be in keeping with current industrial values.

If the down time is adjusted so that the manual methods have an operating factor of 50%, the total cost changes to \$8.40 and \$3.16 for the continuous and intermittent methods respectively. These costs indicate that automatic continuous welding may be even a greater savings than we had at first thought.

We now look at the second estimating approach.

The industrial data approach will again estimate the cost of welding pieces identical to those shown in Figures 13.1 and 13.2 so that the results of both approaches can be compared. Instead of employing a laboratory experiment, this approach is based on data obtained from a welding data book.<sup>55</sup> This is very much like the method which was used for the automatic welding method as explained above. The same labor and material costs were used to keep both approaches on the same basis. The data sheets for the computer runs using the industrial data approach can be found in Tables 13-5, 13-6, and 13-7. The operating factors were taken to be the same as those of the experimental approach.

Again the costs were calculated for an operating factor of 50%. A comparison of the welding costs for each welding method estimated using both approaches can be found in Table 13-8.



TABLE 13-5. Continuous Manual Welding  
(Industrial Data Approach)

Data Register	Parameter Title - Description	Value or Comment
--	Material	Mild Steel
--	Electrode	Cellulose 4.00 mm Efficiency - 93%
--	Weld Size (leg)	5.0 mm
--	Welding Conditions	120 Amps
00	Manual or Automatic Selection	0 (Manual)
01	$T_u$ = Arc Time min per unit	20.42
02	$T_d$ = Downtime min per unit	6.55
03	$l_x$ = Inches of weld per unit (both sides)	120.
04	$L$ = Labor and Overhead rate \$ per hour	12.00
05	$S$ = Inches of Weld Deposited per min	5.876
06	$E$ = Electrode Cost \$ per lb.	0.50
07	$N$ = Number of Electrodes per 100 lbs.	1280.
08	$l_w$ = Inches of weld per electrode	9.37
09	$H_u$ = Handling time per unit, min.	3.667
10	$C_u$ = Cleaning time per unit, min.	4.90



TABLE 13-5. Continued

Data Register	Parameter Title - Description	Value or Comment
Program Output		
22	Labor and Overhead Cost per Job	\$ 5.39
23	Welding Consumables Cost per Job	.50
24	Power Cost per Job	.03
26	Handling Cost per Job	.73
27	Cleaning Cost per Job	.98
28	Total Cost per Job	\$ 7.64



TABLE 13-6. Intermittent Manual Welding  
(Industrial Data Approach)

Data Register	Parameter Title - Description	Value or Comment
--	Material	Mild Steel
--	Electrode	Cellulose 4.00 mm Efficiency - 93%
--	Weld Size (leg)	5.0 mm
--	Welding Conditions	120 Amps
00	Manual or Automatic Selection	0 (Manual)
01	$T_u$ = Arc Time, min. per unit	6.126
02	$T_d$ = Downtime, min. per unit	3.63
03	$l_x$ = Inches of Weld per unit	36
04	$L$ = Labor and Overhead rate \$ per hour	12.00
05	$S$ = Inches of Weld Deposited per min.	5.876
06	$E$ = Electrode Cost \$ per lb.	0.50
07	$N$ = Number of Electrodes per 100 lb.	1280
08	$l_w$ = Inches of Weld per Electrode	9.37
09	$H_u$ = Handling Time per unit, min.	4.167
10	$C_u$ = Cleaning Time per unit, min.	1.47



TABLE 13-6. Continued

Data Register	Parameter Title - Description	Value or Comment
Program Output		
22	Labor and Overhead Cost per Job	\$ 1.95
23	Welding Consumables Cost per Job	.15
24	Power Cost per Job	.01
26	Handling Cost per Job	.83
27	Cleaning Cost per Job	.29
28	Total Cost per Job	\$ 3.23



TABLE 13-7. Continuous Automatic Welding  
(Industrial Data Approach)

Data Register	Parameter Title - Description	Value or Comment
--	Material	Mild Steel
--	Electrode	0.8 mm
--	Weld Size (leg)	4.00 mm
--	Welding Conditions	CO <sub>2</sub> Solid Wire
00	Manual or Automatic Selection	1 (Automatic)
01	T <sub>u</sub> = Arc Time min. per unit	4.21
02	T <sub>d</sub> = Downtime min. per unit	4.11
03	l <sub>x</sub> = Inches of Weld per unit (both sides)	120
04	L = Labor and Overhead Rate \$ per hour	12.00
05	S = Inches of Weld Deposited per min.	28.40
06	E = Electrode Cost \$ per lb.	0.61
09	H <sub>u</sub> = Handling Time per unit, min.	4.50
11	M = Inches Electrode Melted per min. (melting rate)	735
12	W <sub>m</sub> = Weight of Electrode used per inch Electrode melted in lbs. per inch	.00021
15	g = Gas Cost in \$ per cu. ft.	.013
16	r = Cu. ft. of Gas Flow per hour during Welding	35



TABLE 13-7. Continued

Data Register	Parameter Title - Description	Value or Comment
Program Output		
22	Labor and Overhead Cost per Job	\$ 1.68
23	Welding Electrode Cost per Job	.40
24	Power Cost per Job	.02
25	Gas Cost per Job	.03
26	Handling Cost per Job	.90
28	Total Cost per Job	\$ 3.03



TABLE 13-8. A Comparison of Welding Costs

	Manual Continuous				Manual Intermittent				Automatic Continuous			
Approach	Exper.	Exper.	Indus.	Indus.	Exper.	Exper.	Indus.	Indus.	Exper.	Exper.	Indus.	Indus.
Operating Factor	0.757	0.500	0.757	0.500	0.628	0.500	0.628	0.500	0.502	0.500	0.502	0.500
Labor and Overhead	3.83	5.80	5.39	8.16	1.39	1.75	1.95	2.45	0.68	1.68	1.69	
Welding Electrodes	0.63	0.50	0.50	0.19	0.19	0.15	0.15	0.23	0.40	0.40	0.40	
Gas	--	--	--	--	--	--	--	0.01	0.03	0.03	0.03	
Power	0.04	0.04	0.03	0.03	0.01	0.01	0.01	0.01	0.02	0.02	0.02	
Handling	0.73	0.73	0.73	0.73	0.83	0.83	0.83	0.90	0.90	0.90	0.90	
Cleaning	1.20	1.20	0.98	0.98	0.38	0.38	0.29	0.29	--	--	--	
Total	6.43	8.40	7.64	10.41	2.80	3.16	3.23	3.73	1.83	3.03	3.04	



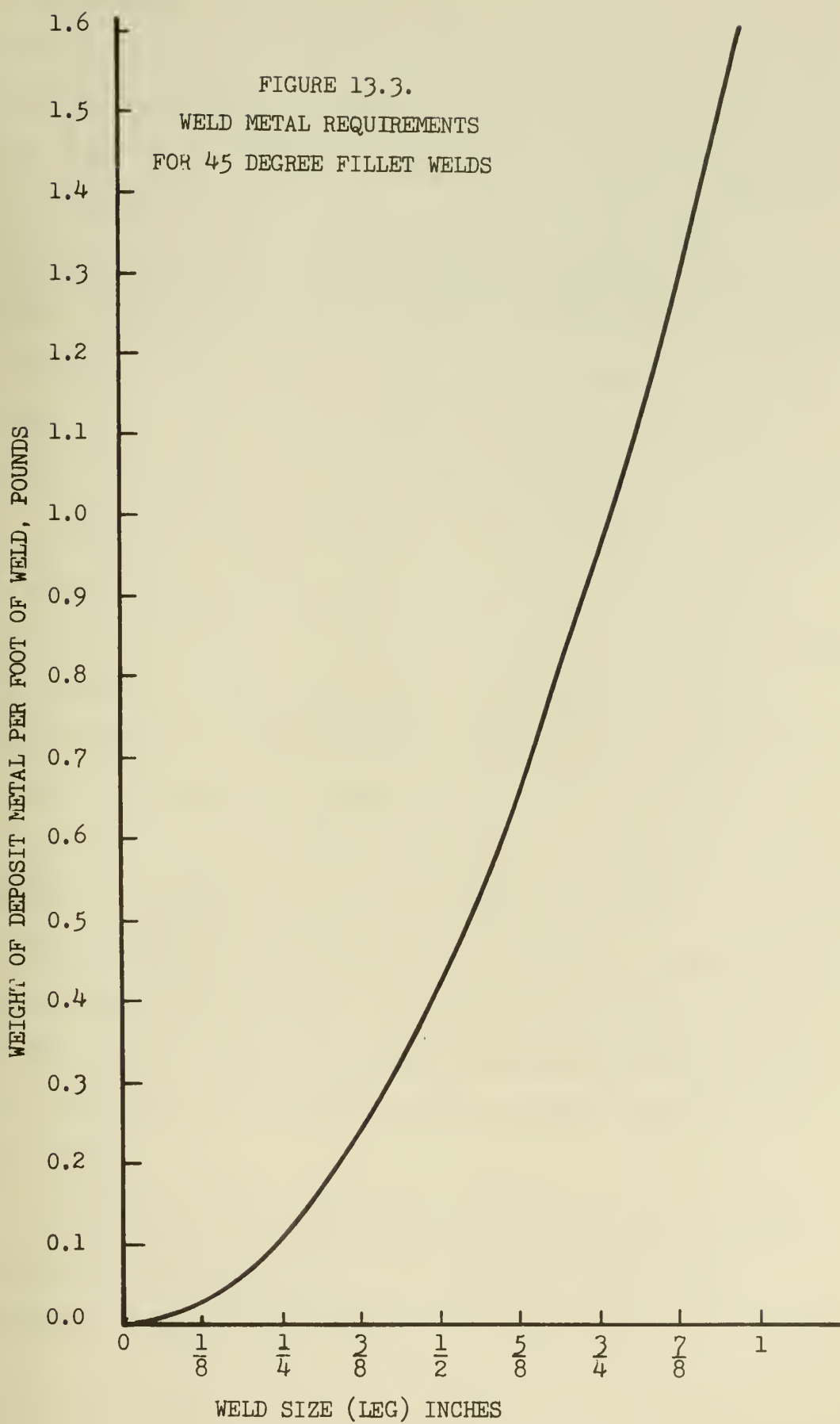
While the actual costs differ slightly, the welding methods remain in the same order of relative costs, with automatic continuous being the cheapest followed by manual intermittent, and the most expensive is the manual continuous.

The differences in cost obtained by the two approaches are reasonable because the weld sizes of the industrial data approach were given in millimeters and were larger than those of the experimental approach, which were given in inches. The important factor is that both approaches result in the same relative costs for the welding methods.

But before we jump to the conclusion that automatic continuous welding should be used in all cases, there are other factors to be considered. The most important factor is can automatic welding be done for the job under consideration. For example, when a ship hull is being assembled on the ways, it would be more difficult and, thus, costly to set up each welding job for automatic welding. In some cases, it would be physically impossible. On the other hand, it would be easier to employ an automatic method during the construction of subassemblies in a shop.

Another cost that can be associated with manual welding is the cost of overwelding. That is, if the specification calls for a weld size of  $3/16$  inch (minimum), you may end up with a  $1/4$  inch weld because the welder wants to make sure that his work passes inspection. Overwelding causes the electrode material cost to increase rapidly as can be seen in Figure 13.3 which is a plot of the weight of deposited weld metal per foot for welded steel versus







the weld size. In the above example, the overweld of 1/16 inch gives a 72% increase in weldment weight, thus cost. It also, in general, takes longer to deposit a larger weld which will increase the labor and overhead cost unnecessarily. Although overwelding can occur in automatic welding, it is less likely because the operator can obtain the machine setting required for a given weld size. Once set, the machine puts out a uniform weld of the size required. Another cost of overwelding that cannot be as easily quantified is that of the increase in distortion and residual stresses introduced into a work piece as a result of overwelding.

Based upon this limited study, it is recommended that ship builders employ automatic continuous welding methods whenever practical. However, if a job requires what is considered an excess of handling and setup time, further investigation is warranted before selecting a welding method. Where there is serious doubt, it is recommended that a program similar to the one employed in this study be used to estimate the cost of welding using different methods. For jobs where it is physically impossible to use automatic welding methods and where specifications permit, the next choice is intermittent manual welding. For the next case where the specifications call for continuous welding and automatic welding methods are impractical, the method of manual continuous welding is the best choice.

Now that we have examined the economics of various welding methods, the next area will be the economical impact that a reduction in weld size requirement might have on ship construction.



#### XIV THE ECONOMIC IMPACT OF THE REDUCTION OF WELD SIZE REQUIREMENTS IN SHIP CONSTRUCTION

In this section, we will take a brief look at the economic impact that would result from a reduction in weld size requirement. Since at this point in time we do not know each and every weld in a ship which may be reduced, the following analysis will be based upon only transverse welds and a simplified model of a ship's structure. The model is based upon the midship section of the destroyer tender (AD-37 class). And we will assume that the cross section at any point of the ship is the same as the midship section.

While this is a very crude assumption and one that will overestimate the savings resulting from a reduction in the required weld size, we are only taking into account the fillet welds between the transverse bulkheads and the ship's shell plating.

Thus while overestimating the savings for these joints, we will be drastically underestimating the savings for the construction of the entire ship hull.

A diagram of our ship model can be seen in Figure 14.1. In this model there are 154 transverse frames and 15 transverse bulkheads. For each transverse frame or bulkhead, there are 101 linear feet of weld from the keel to the main deck along the ship's hull plating on each side of the frame or bulkhead. Since double fillet welds are used, this means that each frame or bulkhead has 404 linear feet of fillet weld. Presently the weld size used for the transverse bulkhead is 3/16 inch from the base line to the



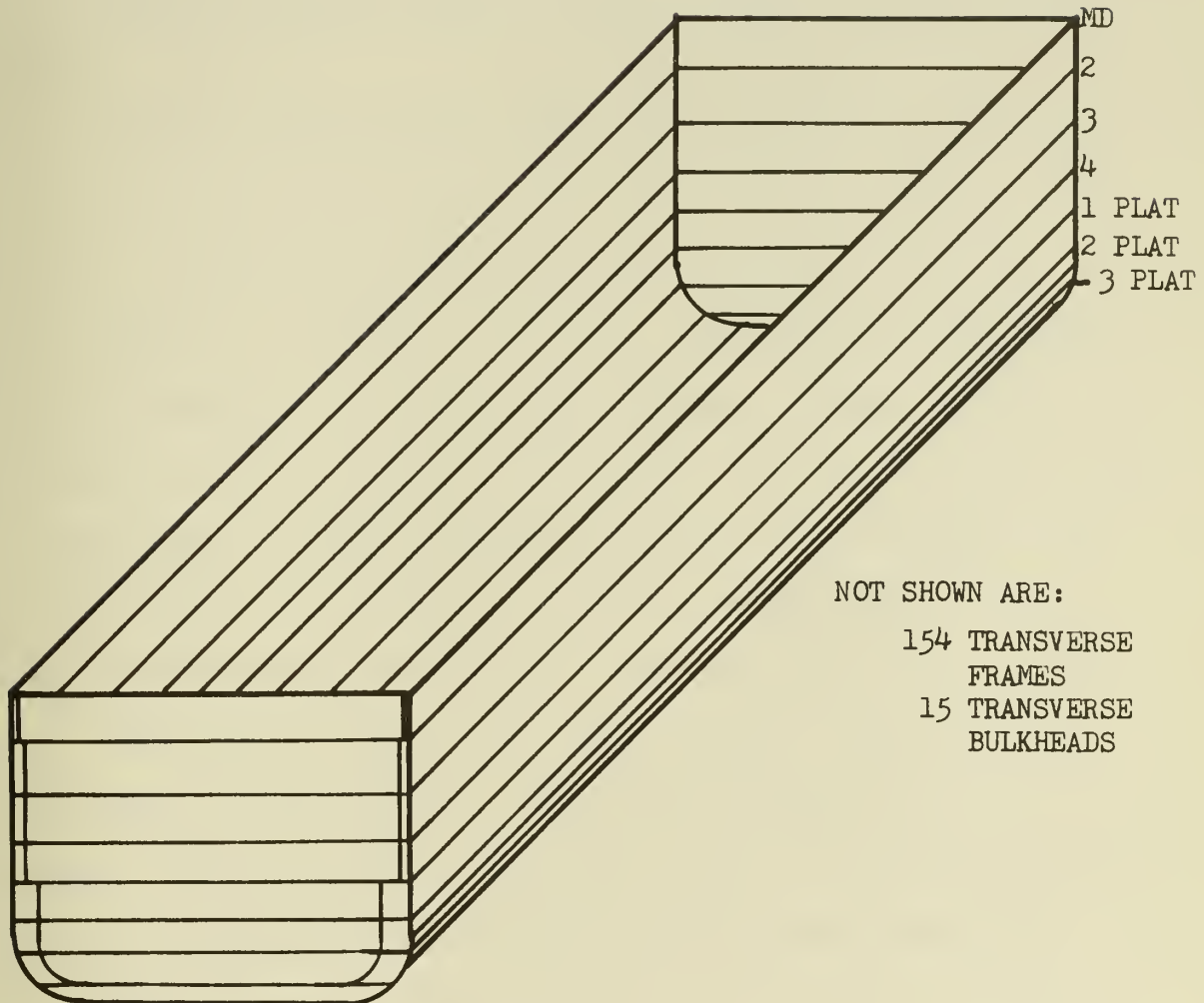


FIGURE 14.1. A DIAGRAM OF THE SHIP MODEL USED FOR THE ECONOMIC IMPACT STUDY



first platform and 1/8 inch from the first platform to the main deck. These same sizes are used for typical transverse frames.

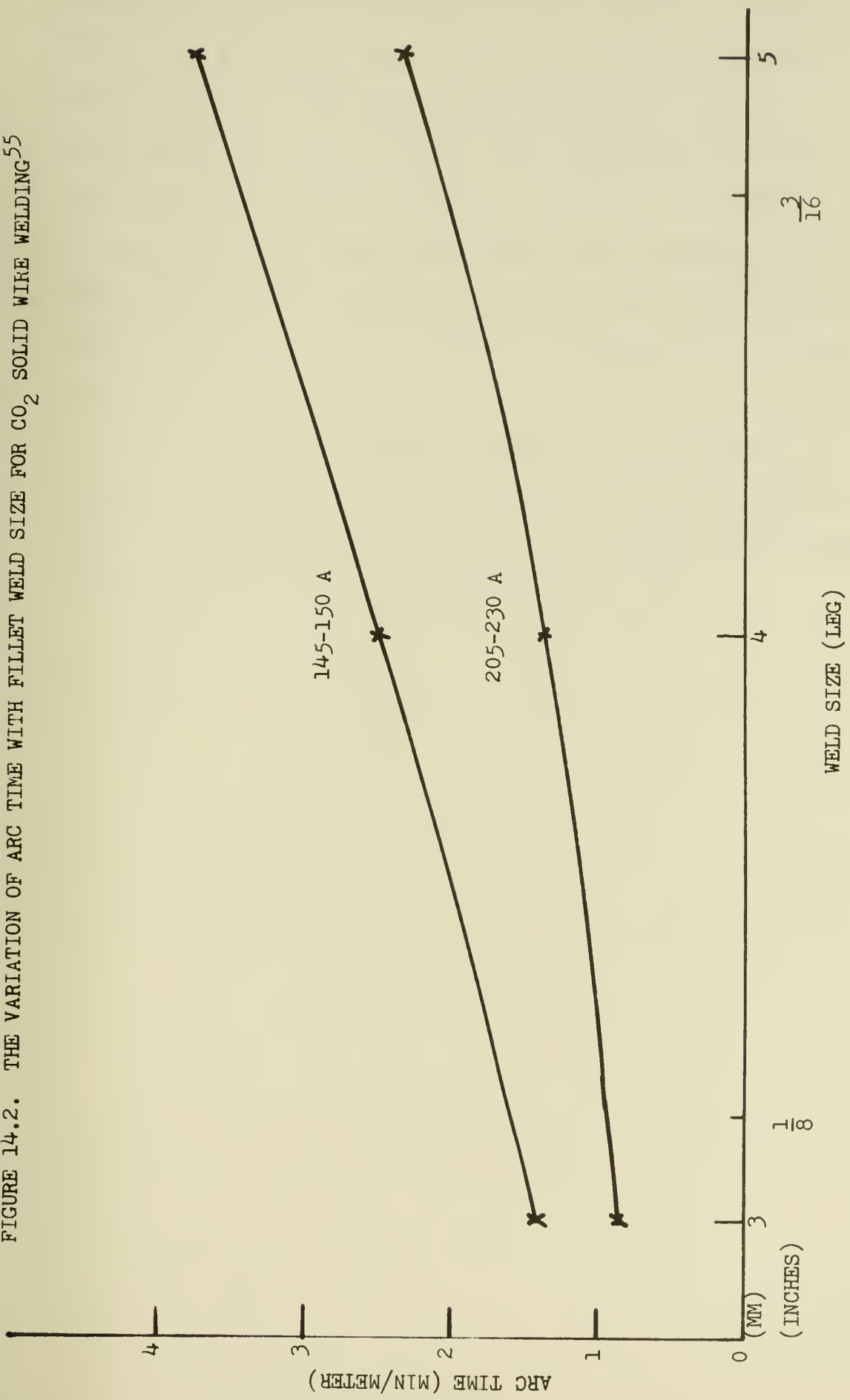
From the computer analysis as discussed in section XI, we have seen that it might be possible to reduce the weld size for the transverse bulkhead joint as shown in Figure 9.1 by at least 30%.

For the economic impact study, we will assume that the welds that are presently 3/16 of an inch can be reduced by 33.3% to 1/8 inch. This means that 256 linear feet of fillet weld per frame are assumed to be reduced to 1/8 inch. Since there are 154 frames and 15 bulkheads, the total length of fillet weld that would be involved in the reduction is 43,264 feet. Since a 1/8 inch weld is rather small for manual welding, we will use some industrial data for CO<sub>2</sub> solid wire welding as was done in section XIII. A plot of arc time versus weld size can be seen in Figure 14.2.

Since there is data for two current ranges using the 0.8 mm electrode, we will calculate the arc time difference for both ranges. As can be seen in Figure 14.2, the arc times for the 3/16 inch fillet weld are 3.48 and 2.07 minutes per meter for the lower and higher currents respectively, while the arc times for the 1/8 inch fillet weld are 1.60 and 0.93 respectively.

This results in arc time differences of 1.88 and 1.14 minutes per meter respectively. For our ship model having 43,264 feet of weld that possibly could be reduced, this gives us an arc time savings of between 250 and 413 hours. If we use a 50% operating factor, this gives us a man hour savings of between 500 and 826.



FIGURE 14.2. THE VARIATION OF ARC TIME WITH FILLET WELD SIZE FOR  $\text{CO}_2$  SOLID WIRE WELDING<sup>55</sup>



Using the same labor and overhead rate that was used in section XIII, namely \$12.00 per hour, leads us to a savings of between \$6,000 and \$9,912. While this seems like a small amount, we must remember that this only takes into account the transverse welds that join bulkheads and frames to the skin of the ship. It should be obvious at this point that there are many other welds that might possibly be reduced and, thus, increase this estimated savings tremendously. Just a glance at the model shown in Figure 14.1 demonstrates this fact.

As more results are known as to what welds are presently conservative and by how much, future researchers will be better able to predict the man-hour savings that a reduction in the welding requirements would have in the construction of a ship.



## XV RECOMMENDATIONS AND CONCLUSIONS

We have reviewed some of the work that has been done in the field of strength of fillet welds. This included static strength, fatigue strength, and shear strength. We have seen, for example, that a transverse weld is approximately 44% stronger than a longitudinal weld and that the fatigue strength of welded connections is independent of the tensile strength of the members employed in the connection. Since fatigue strength is one of the major factors in a fillet weld, studies have investigated various treatments to improve the fatigue strength. It has been found that both local machining and peening improve the fatigue strength of fillet welds if it is properly done.

The fatigue strength of a joint is not normally increased by increasing the weld size.

We have found that most of the relationships that are used by designers to determine the allowable design stress for joints are modifications of the Von Mises equation. Also when the designer specifies the required weld size, he should be aware of the fact that the fillet weld that is found connecting two structural members on a ship may not look at all like the ideal model weld that is used to analyze the strength of fillet welds.

We have discussed a proposed system for analyzing the strength of fillet welds. This is an algorithm approach which can be easily computerized. A brief explanation of this system can be found in section VII.

We will now recommend values for some of the incremental



increases in weld size,  $d_i$ . These recommendations are based upon the joint between a transverse bulkhead and the ship's hull plating as shown in Figure 9.1. The results found from the computer analysis, as discussed in section XI indicate that a reduction of at least 30% is possible in the weld size of this joint. This gives us a  $d_1$  of 0.125 inches. The  $d_2$  value will be zero because in most cases increasing the weld size does not improve the fatigue strength of a joint. We will also set  $d_3$ ,  $d_4$  and  $d_5$  equal to zero because we will assume that the welding is carried out under good conditions by a qualified welder. This brings us to the environmental  $d_i$ 's.

For  $d_6$ , we will assume 0.0125 inches (10% of  $d_1$ ) for a general corrosion margin since we will assume that this joint is not in a location where bilge water sloshes around, and, thus, we do not need a full 1.5 mm. This assumes that the weld metal and the base metal have the correct polarity. If the joint were in a location where there was dry air, we would set  $d_6$  equal to zero. Since a corrosion margin is not the best way of combating local corrosion, we will set  $d_7$  equal to zero and encourage designers to use proper design methods to avoid local corrosion where possible. Based on the assumption that proper welding techniques are followed and quality assurance procedures are followed and that the structure in which the weld will be used is not a completely new design with many unanswered questions, we will set  $d_8$ ,  $d_9$ , and  $d_{10}$  equal to zero.

By summing the  $d_i$ 's, we obtain a recommended weld size of



0.1375 inches; whereas, the current specifications call for 0.1875 inches of weld. This is 36.4% more than what we obtained based upon the purposed system for determining fillet weld strength.

In reviewing the current welding specifications, we have seen the similarity between these specifications and those used for joints employing rivets as the joining medium. This may indicate that there is room for improvement in some areas of the current specifications.

We have just discussed only one of the many typical joints that are involved in the construction of ships. Much more work needs to be done in this area. Now that the computer model has been developed, the next step is to select a ship which has been recently designed with the aid of a computer. The reason for this is to be able to readily obtain not only the detailed joint geometry of many typical joints that are in various locations in the ship, but also the local loading of the structural members that make up the joint. This loading information is more precise than the loads that were obtained by the method of structural analysis that was used in this study.

With this information, future researchers can easily employ the computer model to study a large sample of joints at various locations in the ship to obtain a better general picture as to whether current fillet weld specifications are too conservative and the areas where concentrated effort is warranted in the attempt to minimize excess conservatism in weld size requirements.

After obtaining a better general picture, a much more



precise economic analysis as to the overall manhour and cost savings that could result from the reduction, where possible, of the weld size requirements regarding the construction of ships can be made. We have seen that there is a potential savings there waiting to be discovered. A good source of data for a computer-aided designed ship is the American Bureau of Shipping, which has a computer program for oil tankers.

Another area that should be developed is that of the fatigue strength of fillet welds. A computer program can be developed for fatigue analysis.

Getting back to the question at hand, namely, "Are current fillet weld specifications too conservative?" the answer is definitely "Yes, some are." Future work will make it possible to eliminate or minimize the excess conservatism.



## APPENDIX

A SAMPLE COMPUTER OUTPUT FOR THE CASE OF  
A 30 PERCENT REDUCTION IN THE SPECIFIED WELD SIZE  
FOR THE TRANSVERSE BULKHEAD JOINT (FIGURE 9.1)



NODE	DISPLACEMENTS	Z-ROTATION		
		X-DISPLACEMENT	Y-DISPLACEMENT	Z-DISPLACEMENT
1	0.0	0.0	0.0	0.0
2	0.0	-0.217395D+J1	-0.181396D-02	0.0
3	0.0	-0.217433D+01	0.0	0.0
4	0.0	-0.199805D+J1	-0.141843D-01	0.0
5	0.0	-0.199856D+01	-0.105654D-01	0.0
6	0.0	-0.182230D+01	-0.251961D-01	0.0
7	0.0	-0.182261D+01	-0.233863D-01	0.0
8	0.0	-0.182284D+01	-0.215767D-01	0.0
9	0.0	-0.166253D+01	-0.359799D-01	0.0
10	0.0	-0.166313D+01	-0.323547D-01	0.0
11	0.0	-0.150280D+01	-0.478211D-01	0.0
12	0.0	-0.150311D+01	-0.460159D-01	0.0
13	0.0	-0.150346D+01	-0.442111D-01	0.0
14	0.0	-0.139625D+01	-0.564380D-01	0.0
15	0.0	-0.139697D+01	-0.528575D-J1	0.0
16	0.0	-0.128975D+01	-0.658783D-01	0.0
17	0.0	-0.129014D+01	-0.643800D-01	0.0
18	0.0	-0.129053D+01	-0.622824D-01	0.0
19	0.0	-0.123647D+01	-0.739197D-01	0.0
20	0.0	-0.123728D+01	-0.672763D-01	0.0
21	0.0	-0.116323D+01	-0.760882D-01	0.0
22	0.0	-0.118365D+01	-0.743050D-01	0.0
23	0.0	-0.118407D+01	-0.725213D-01	0.0
24	0.0	-0.115658D+01	-0.788126D-01	0.0
25	0.0	-0.115744D+01	-0.751484D-01	0.0
26	0.0	-0.112996D+01	-0.815135D-01	0.0
27	0.0	-0.113040D+01	-0.797580D-01	0.0
28	0.0	-0.113087D+01	-0.780977D-01	0.0
29	0.0	-0.111024D+01	-0.837337D-01	0.0
30	0.0	-0.111115D+J1	-0.800367D-01	0.0
31	0.0	-0.109606D+01	-0.856360D-01	0.0
32	0.0	-0.109109D+01	-0.839516D-01	0.0
33	0.0	-0.109144D+01	-0.822386D-01	0.0
34	0.0	-0.109008D+01	-0.856521D-01	0.0
35	0.0	-0.109085D+01	-0.858950D-01	0.0
36	0.0	-0.108959D+01	-0.857535D-01	0.0
37	0.0	-0.109042D+01	-0.841411D-01	0.0
38	0.0	-0.109023D+01	-0.820859D-01	0.0
39	0.0	-0.108957D+J1	-0.858950D-01	0.0
40	0.0	-0.109015D+01	-0.821305D-01	0.0
41	0.0	-0.108954D+01	-0.860227D-01	0.0
42	0.0	-0.108936D+01	-0.841296D-01	0.0
43	0.0	-0.109008D+01	-0.821901D-01	0.0
44	0.0	-0.108949D+01	-0.861482D-01	0.0
45	0.0	-0.108999D+01	-0.822296D-01	0.0
46	0.0	-0.108943D+01	-0.862501D-01	0.0











152 -0. 108479D+01 -0. 853102D-01 0. 0  
 153 -0. 108443D+01 -0. 847254D-01 0. 0  
 154 -0. 108814D+01 -0. 860235D-01 0. 0  
 155 -0. 106812D+01 -0. 362132D-01 0. 0  
 156 -0. 108798D+01 -0. 960209D-01 0. 0  
 157 -0. 108797D+01 -0. 867152D-01 0. 0  
 158 -0. 108654D+01 -0. 863737D-01 0. 0  
 159 -0. 108555D+01 -0. 863160D-01 0. 0  
 160 -0. 1085045E+01 -0. 858234D-01 0. 0  
 161 -0. 108643D+01 -0. 855376D-01 0. 0  
 162 -0. 105664D+01 -0. 852556D-01 0. 0  
 163 -0. 108665D+01 -0. 860679D-01 0. 0  
 164 -0. 105667D+01 -0. 862389D-01 0. 0  
 165 -0. 109568L+01 -0. 963015D-01 0. 0  
 166 -0. 108723D+01 -0. 867343D-01 0. 0  
 167 -0. 108789D+01 -0. 866448D-01 0. 0  
 168 -0. 104789D+01 -0. 866136D-01 0. 0  
 169 -0. 108790D+01 -0. 864455D-01 0. 0  
 170 -0. 105769D+01 -0. 962218D-01 0. 0  
 171 -0. 106775D+01 -0. 864539D-01 0. 0  
 172 -0. 105776D+01 -0. 865930D-01 0. 0  
 173 -0. 108777L+01 -0. 866695D-01 0. 0  
 174 -0. 108680D+01 -0. 863212D-01 0. 0  
 175 -0. 108680D+01 -0. 862839D-01 0. 0  
 176 -0. 108681D+01 -0. 869756D-01 0. 0  
 177 -0. 108690D+01 -0. 862872D-01 0. 0  
 178 -0. 108692D+01 -0. 863392D-01 0. 0  
 179 -0. 108728D+01 -0. 867619D-01 0. 0  
 180 -0. 108764D+01 -0. 866883D-01 0. 0  
 181 -0. 108766D+01 -0. 866375D-01 0. 0  
 182 -0. 103759D+01 -0. 867922D-01 0. 0  
 183 -0. 108729D+01 -0. 867175D-01 0. 0  
 184 -0. 108698L+01 -0. 864455D-01 0. 0  
 185 -0. 108607D+01 -0. 865397D-01 0. 0  
 186 -0. 108784D+01 -0. 866638D-01 0. 0  
 187 -0. 108880D+01 -0. 866878D-01 0. 0  
 188 -0. 108386D+01 -0. 866840D-01 0. 0  
 189 -0. 108843D+01 -0. 865340D-01 0. 0  
 190 -0. 108960D+01 -0. 865588D-01 0. 0  
 191 -0. 108945D+01 -0. 869042D-01 0. 0  
 192 -0. 109057D+01 -0. 866840D-01 0. 0  
 193 -0. 109343D+01 -0. 867050D-01 0. 0  
 194 -0. 109029D+01 -0. 865272D-01 0. 0  
 195 -0. 109176D+01 -0. 865496D-01 0. 0  
 196 -0. 109164D+01 -0. 893949D-01 0. 0  
 197 -0. 109339D+01 -0. 868812D-01 0. 0  
 198 -0. 109297D+01 -0. 867073D-01 0. 0  
 199 -0. 109286D+01 -0. 865359D-01 0. 0  
 200 -0. 109465D+01 -0. 865489D-01 0. 0  
 201 -0. 109455D+01 -0. 868942D-01 0. 0  
 202 -0. 109343D+01 -0. 869437D-01 0. 0



2.2.3	$0.0 - 0.10962324u^1$	$-0.967114D-01$
2.2.4	$0.0 - 0.109514D+u^1$	$-0.965333D-01$
2.2.5	$0.0 - 0.109346D+u^1$	$-0.865473D-01$
2.2.6	$0.0 - 0.1093365+u^1$	$-0.868926D-01$
2.2.7	$0.0 - 0.110395u^1$	$-0.863666D-01$
2.2.8	$0.0 - 0.1103592+u^1$	$-0.967134D-01$
2.2.9	$0.0 - 0.1103495+u^1$	$-0.865412D-01$
2.2.10	$0.0 - 0.110281D+u^1$	$-0.865458D-01$
2.2.11	$0.0 - 0.110272D+u^1$	$-0.9638911D-01$
2.2.12	$0.0 - 0.110503D+u^1$	$-0.8688875D-01$
2.2.13	$0.0 - 0.110494D+u^1$	$-0.965166D-01$
2.2.14	$0.0 - 0.110485D+u^1$	$-0.865422D-01$
2.2.15	$0.0 - 0.110716D+u^1$	$-0.865463D-01$
2.2.16	$0.0 - 0.1107075+u^1$	$-0.968916D-01$
2.2.17	$0.0 - 0.1109382+u^1$	$-0.868943D-01$
2.2.18	$0.0 - 0.1109295+u^1$	$-0.867153D-01$
2.2.19	$0.0 - 0.1109290+u^1$	$-0.865490D-01$



NUM/IFT STATE	STRESS-ZZ	STRESS-YZ	MAX STRESS	MIN STRESS	ANGLE
1 ELASTIC	0.126355E+02	0.472569D+00	0.627297D-02	0.472565D+00	0.03
2 ELASTIC	0.116375E+02	-0.746290D+00	0.439899D+00	0.111799D+02	2.12
3 ELASTIC	0.126647E+02	0.191160D+00	-0.750523D-02	0.126647D+02	-0.03
4 ELASTIC	0.113850E+02	-0.435806D-01	0.497732D+00	0.112076D+02	2.53

NUM/IFT STATE	STRESS-ZZ	STRESS-YZ	MAX STRESS	MIN STRESS	ANGLE
1 ELASTIC	0.126646E+02	0.4044312D+00	-0.276065D-01	0.126627D+02	0.204251D+00
2 ELASTIC	0.114525E+02	0.371975D+00	0.541326D+00	0.111724D+02	0.344843D+00
3 ELASTIC	0.126711D+02	0.514092D+00	-0.541725D-01	0.126713D+02	0.513852D+00
4 ELASTIC	0.110473E+02	0.8434932D+00	0.509550D+00	0.110731D+02	0.809572D+00

NUM/IFT STATE	STRESS-ZZ	STRESS-YZ	MAX STRESS	MIN STRESS	ANGLE
1 ELASTIC	0.127595D+02	0.906709D+00	-0.101254D+00	0.127599D+02	0.908844D+00
2 ELASTIC	0.1166572D+02	0.121981D+01	0.457984D+00	0.166908D+02	0.119767D+01
3 ELASTIC	0.125893E+02	0.146304D+01	-0.482149D+00	0.126303D+02	0.144993D+01
4 ELASTIC	0.112302D+02	0.239601D+01	0.356416D+01	0.112836D+02	0.232117D+01

NUM/IFT STATE	STRESS-ZZ	STRESS-YZ	MAX STRESS	MIN STRESS	ANGLE
1 ELASTIC	-0.791332D+00	-0.535137D+01	-0.134612D+01	-0.424077D+00	-0.571912D+01
2 ELASTIC	0.662222D+01	-0.217393D+01	-0.255320D+01	0.730958D+01	0.286131D+01
3 ELASTIC	-0.112301D+01	-0.525439D+01	-0.356416D+01	0.930802D+01	0.730821D+01
4 ELASTIC	0.631044D+01	-0.206864D+01	-0.146009D+01	0.655774D+01	0.231598D+01

NUM/IFT STATE	STRESS-ZZ	STRESS-YZ	MAX STRESS	MIN STRESS	ANGLE
1 ELASTIC	-0.434405D+01	-6.19287D+02	-0.388387D+01	-0.341036D+01	-0.205587D+02
2 ELASTIC	-0.863191D+01	-0.214678D+02	0.133552D+01	-0.844948D+01	-0.216049D+02
3 ELASTIC	-0.369723D+01	-0.295939E+01	-0.217676D+01	-0.112050D+01	-0.533613D+01
4 ELASTIC	-0.249852L+01	-0.244566D+01	-0.165640D+01	-0.815473D+00	-0.412870D+01

NUM/IFT STATE	STRESS-ZZ	STRESS-YZ	MAX STRESS	MIN STRESS	ANGLE
1 ELASTIC	-0.126255E+02	-0.247721D+02	-0.785912D+01	-0.847297D+01	-0.285616D+02
2 ELASTIC	-0.122625D+02	-0.247721D+02	-0.785912D+01	-0.847297D+01	-0.285616D+02
3 ELASTIC	-0.122625D+02	-0.247721D+02	-0.785912D+01	-0.847297D+01	-0.285616D+02
4 ELASTIC	-0.122625D+02	-0.247721D+02	-0.785912D+01	-0.847297D+01	-0.285616D+02

NUM/IFT STATE	STRESS-ZZ	STRESS-YZ	MAX STRESS	MIN STRESS	ANGLE
1 ELASTIC	-0.177869D+01	-0.153707D+02	-0.388208D+01	-0.748060D+00	-0.164013D+02
2 ELASTIC	-0.177369D+01	-0.153707D+02	-0.388208D+01	-0.748060D+00	-0.164013D+02
3 ELASTIC	-0.177869D+01	-0.153707D+02	-0.388208D+01	-0.748060D+00	-0.164013D+02
4 ELASTIC	-0.177869D+01	-0.153707D+02	-0.388208D+01	-0.748060D+00	-0.164013D+02

NUM/IFT STATE	STRESS-ZZ	STRESS-YZ	MAX STRESS	MIN STRESS	ANGLE
1 ELASTIC	-0.811333U+01	-0.149889D+02	-0.424622D+01	-0.608771D+01	-0.170145D+02
2 ELASTIC	-0.860854E+01	-0.152011D+02	-0.128516D+01	-0.836687D+01	-0.154428D+02
3 ELASTIC	-0.367173D+01	-0.462515D+01	-0.438771D+01	-0.265094D+00	-0.856197D+01
4 ELASTIC	-0.416593U+01	-0.483733U+01	-0.142664U+01	-0.303666D+00	-0.596765D+01

NUM/IFT STATE	STRESS-ZZ	STRESS-YZ	MAX STRESS	MIN STRESS	ANGLE
1 ELASTIC	-0.742253U+01	-0.381330U+01	-0.329120U+01	-0.135343D+01	-0.590969U+01
2 ELASTIC	0.520035U+01	-0.124303D+01	-0.206809D+01	0.586285D+01	-0.194253D+01
3 ELASTIC	0.120355U+01	-0.174754U+01	-0.240355U+01	0.289632D+01	-0.344056U+01
4 ELASTIC	0.400202U+01	-0.511380U+01	-0.230139U+01	0.509340D+01	-0.152518U+01

NUM/IFT STATE	STRESS-ZZ	STRESS-YZ	MAX STRESS	MIN STRESS	ANGLE
1 ELASTIC	-0.6355710U+01	-0.105397D+02	-0.105397D+02	0.63555710U+01	-32.50
2 ELASTIC	0.672132U+01	-0.776064D+01	-0.776064D+01	0.672132U+01	-16.24
3 ELASTIC	0.548898U+01	-0.782249D+01	-0.782249D+01	0.548898U+01	-11.12
4 ELASTIC	0.311226D+01	-0.577611D+01	-0.577611D+01	0.311226D+01	-38.39



1	ELASTIC	0.302572e+01	-0.139010D+00	-0.297979D+01	0-459946D+01	-0.106968D+01	-2.3-9.2
2	-ELASTIC	0.535565D+01	0-160778D+C1	-0.304495D+01	0-707650D+01	-0-520665D-01	-2.9-4.2
3	ELASTIC	0.283592e+01	0.507467D+03	-0.242099D+01	0.438016D+01	-0.956776D+00	-32.54
4	ELASTIC	0.506911D+01					
35							
1	ELASTIC	0.. 13e-372e+01	-0.. 709047D-01	0.. 173260D+00	0.. 136429D+01	-0.. 918210D-01	6..-3.8
2	ELASTIC	0.. 214603e+01	0.. 273349D+00	0.. 381352D+00	0.. 222129D+01	0.. 198692D+00	11..0.8
3	ELASTIC	0.. 177-1+2e+01	0.. 53e1616D-01	0.. 248080D+01	0.. 347139D+01	-0.. 164418D+01	35..-1.7
4	ELASTIC	0.. 5304152e+01	0.. 145342D+01	0.. 210715D+01	0.. 607640D+01	0.. 418673D+00	25..3.2
36							
1	ELASTIC	0.. 75232e+01	0.. 298217D+01	-0.. 334415D+01	0.. 929483D+01	0.. 121060D+01	-27..9.1
2	-ELASTIC	0.. 75222e+01	0.. 298217D+01	-0.. 334415D+01	0.. 929483D+01	0.. 121060D+01	-27..9.1
3	ELASTIC	0.. 75232e+01	0.. 298217D+01	-0.. 334415D+01	0.. 929483D+01	0.. 121060D+01	-27..9.1
4	ELASTIC	0.. 75232e+01	0.. 298217L+01	-0.. 334415D+01	0.. 929483D+01	0.. 121060D+01	-27..9.1
37							
1	ELASTIC	0.. 137374e+02	0.. 451823D+01	0.. 645777D+00	0.. 138279D+02	0.. 347778D+01	3..-5.8
2	ELASTIC	0.. 3375972e+01	0.. 119907D+01	0.. 503070D+00	0.. 841106D+01	0.. 116398D+01	3..-9.9
3	ELASTIC	0.. 124302e+02	-0.. 640698D-01	-0.. 760409D+01	0.. 160036D+02	-0.. 366662D+01	-25..-3.2
4	ELASTIC	0.. 1243072e+01	-0.. 2448232e+01	-0.. 785226D+01	0.. 113300D+02	-0.. 692359D+01	-29..-0.8
38							
1	*PLASTIC	0.. 559499D+02	0.. 4477926D+02	-0.. 784153D+01	0.. 584806D+02	0.. 313019D+02	-17..-6.2
2	*PLASTIC	0.. 559499D+02	0.. 337926D+02	-0.. 784153D+01	0.. 584806D+02	0.. 313019D+02	-17..-6.2
3	*PLASTIC	0.. 559499D+02	0.. 337926D+02	-0.. 784153D+01	0.. 584806D+02	0.. 313019D+02	-17..-6.2
4	*PLASTIC	0.. 559499D+02	0.. 337926D+02	-0.. 784153D+01	0.. 584806D+02	0.. 313019D+02	-17..-6.2
39							
1	ELASTIC	0.. 366686D+01	-0.. 325230D-01	-0.. 214867L+01	0.. 482008D+01	-0.. 983924D+00	-23..-8.8
2	ELASTIC	0.. 308941L+01	-0.. 483253D+00	-0.. 183118D+01	0.. 386349D+01	-0.. 124244D+01	-22..-9.2
3	ELASTIC	0.. 260733D+01	0.. 223399D+01	-0.. 274444D+01	0.. 520986D+01	-0.. 298543D+00	-42..-5.9
4	ELASTIC	0.. 240602D+01	0.. 290218D+01	-0.. 222163D+01	0.. 488954D+01	0.. 18662D+00	-48..-1.9
40							
1	ELASTIC	0.. 60278e+01	-0.. 104582D+01	-0.. 215254D+00	0.. 663387D+01	-0.. 105185D+01	-1..-6.1
2	ELASTIC	0.. 574411D+01	0.. 153740L+00	-0.. 544642D+00	0.. 579668D+01	0.. 101173D+00	-5..-5.1
3	ELASTIC	0.. 490512D+01	-0.. 195534D+01	-0.. 199270D+01	0.. 488557D+01	-0.. 253580U+01	-16..-2.4
4	ELASTIC	0.. 445587D+01	-0.. 146783D+01	-0.. 17198D+01	0.. 494547D+01	-0.. 195742D+01	-15..-4.5
41							
1	ELASTIC	0.. 607358D+01	0.. 221527D+01	0.. 221952D+01	0.. 708516D+01	0.. 120369D+01	24..-5.0
2	ELASTIC	0.. 306614D+01	0.. 925945D+00	0.. 258395D+01	0.. 479212D+01	-0.. 801037D+00	33..-7.6
3	ELASTIC	0.. 506883D+01	0.. 205142D+01	0.. 160797D+01	0.. 576506D+01	0.. 135518D+01	23..-4.1
4	ELASTIC	0.. 289844D+01	0.. 112125D+01	0.. 133690D+01	0.. 361512D+01	0.. 404572D+00	28..-1.9
42							
1	ELASTIC	0.. 112070D+02	0.. 340982L+01	0.. 303301L+01	0.. 122479D+02	0.. 236896D+01	18..-9.4
2	ELASTIC	0.. 112070D+02	0.. 340982D+01	0.. 303301D+01	0.. 122479D+02	0.. 236896D+01	18..-9.4
3	ELASTIC	0.. 112070L+02	0.. 340982L+01	0.. 303301D+01	0.. 122479D+02	0.. 236896D+01	18..-9.4
4	ELASTIC	0.. 112070D+02	0.. 340982D+01	0.. 303301D+01	0.. 122479L+02	0.. 236896D+01	18..-9.4
43							
1	ELASTIC	0.. 674066D+01	0.. 185955D+01	0.. 182969D+01	0.. 735036D+01	0.. 124985D+01	18..-4.3
2	ELASTIC	0.. 674066D+01	0.. 185955D+01	0.. 182969D+01	0.. 735036D+01	0.. 124985D+01	18..-4.3
3	ELASTIC	0.. 674066L+01	0.. 185955L+01	0.. 182969D+01	0.. 735036D+01	0.. 124985D+01	18..-4.3
4	ELASTIC	0.. 674066D+01	0.. 185955D+01	0.. 182969U+01	0.. 735036D+01	0.. 124985D+01	18..-4.3



2	ELASTIC	$0.22624524 \cdot 10^1$	$0.1503652 \cdot 10^1$	$-0.194583 D-01$	$0.-2263400 D+01$	$0.-156308 D+01$	$-1.63$	$0.-976199 D+00$
3	ELASTIC	$0.35594704 \cdot 10^1$	$-0.12226020 \cdot 10^1$	$-0.793356 D+00$	$0.-368759 D+01$	$-0.135076 D+01$	$-9.18$	$0.-4388312 D+01$
4	ELASTIC	$0.91652464 \cdot 10^1$	$-0.13946420 \cdot 10^1$	$0.317357 D-01$	$0.917060 D+00$	$-0.139448 D+01$	$0.79$	$0.-200412 D+01$
<i>b</i>								
1	ELASTIC	$-0.270124 D+01$	$-0.110913 D+02$	$0.-115743 D+01$	$-0.-260341 D+01$	$-0.112491 D+02$	$7.77$	$0.-798352 D+01$
2	ELASTIC	$-0.270124 D+01$	$-0.-110913 D+02$	$0.-115743 D+01$	$-0.-260341 D+01$	$-0.-112491 D+02$	$7.77$	$0.-798352 D+01$
3	ELASTIC	$-0.270124 D+01$	$-0.-110913 D+02$	$0.-115743 D+01$	$-0.-260341 D+01$	$-0.-112491 D+02$	$7.77$	$0.-798352 D+01$
4	ELASTIC	$-0.270124 D+01$	$-0.-110913 D+02$	$0.-115743 D+01$	$-0.-260341 D+01$	$-0.-112491 D+02$	$7.77$	$0.-798352 D+01$
<i>b</i>								
1	ELASTIC	$0.8162203 D+00$	$0.-1994416 L+01$	$-0.-228894 D+01$	$0.-379665 D+01$	$-0.-914289 D+00$	$-51.79$	$0.-412032 D+01$
2	ELASTIC	$0.-2339627 D+01$	$0.-191943 D+00$	$-0.-146341 D+01$	$0.-310620 D+01$	$-0.-607985 D+00$	$-25.93$	$0.-325515 D+01$
3	ELASTIC	$0.-789115 D+00$	$0.-282130 D+01$	$-0.-110849 D+01$	$0.-330893 D+01$	$-0.-301484 D+00$	$-66.26$	$0.-270277 D+01$
4	ELASTIC	$0.-919547 D+00$	$0.-295818 E+00$	$-0.-445386 D+00$	$0.-108167 D+01$	$0.-336894 D-01$	$-30.01$	$0.-934593 D+00$
<i>b</i>								
1	ELASTIC	$0.8162203 D+00$	$0.-1994416 L+01$	$-0.-228894 D+01$	$0.-379665 D+01$	$-0.-914289 D+00$	$-51.79$	$0.-412032 D+01$
2	ELASTIC	$0.-2339627 D+01$	$0.-191943 D+00$	$-0.-146341 D+01$	$0.-310620 D+01$	$-0.-607985 D+00$	$-25.93$	$0.-325515 D+01$
3	ELASTIC	$0.-789115 D+00$	$0.-282130 D+01$	$-0.-110849 D+01$	$0.-330893 D+01$	$-0.-301484 D+00$	$-66.26$	$0.-270277 D+01$
4	ELASTIC	$0.-919547 D+00$	$0.-295818 E+00$	$-0.-445386 D+00$	$0.-108167 D+01$	$0.-336894 D-01$	$-30.01$	$0.-934593 D+00$



	X-DISPLACEMENT	Y-DISPLACEMENT	Z-DISPLACEMENT	X-ROTATION	Y-ROTATION	Z-ROTATION
1	0.0	-0.490829D+1	-0.502818D-02	0.0	0.0	0.0
2	0.0	-0.300844D+01	-0.251409D-02	0.0	0.0	0.0
3	0.0	-0.300895D+1	0.0	0.0	0.0	0.0
4	0.0	-0.276504D+01	-0.183996D-01	0.0	0.0	0.0
5	0.0	-0.276571D+01	-0.133953D-01	0.0	0.0	0.0
6	0.0	-0.252182D+01	-0.333819D-01	0.0	0.0	0.0
7	0.0	-0.252223D+01	-0.308736D-01	0.0	0.0	0.0
8	0.0	-0.252254D+01	-0.283656D-01	0.0	0.0	0.0
9	0.0	-0.230073D+01	-0.475539D-01	0.0	0.0	0.0
10	0.0	-0.230152D+01	-0.425410D-01	0.0	0.0	0.0
11	0.0	-0.297969D+01	-0.631270D-01	0.0	0.0	0.0
12	0.0	-0.208011D+01	-0.606250D-01	0.0	0.0	0.0
13	0.0	-0.208056D+01	-0.581236D-01	0.0	0.0	0.0
14	0.0	-0.193225D+01	-0.745166D-01	0.0	0.0	0.0
15	0.0	-0.193319D+01	-0.694965D-01	0.0	0.0	0.0
16	0.0	-0.178486D+01	-0.868684D-01	0.0	0.0	0.0
17	0.0	-0.178536D+01	-0.843760D-01	0.0	0.0	0.0
18	0.0	-0.178549D+01	-0.818845D-01	0.0	0.0	0.0
19	0.0	-0.171113D+01	-0.234937D-01	0.0	0.0	0.0
20	0.0	-0.171220D+01	-0.884585D-01	0.0	0.0	0.0
21	0.0	-0.163746D+01	-0.100292D+00	0.0	0.0	0.0
22	0.0	-0.163802D+01	-0.978206D-01	0.0	0.0	0.0
23	0.0	-0.163857D+01	-0.953482D-01	0.0	0.0	0.0
24	0.0	-0.160058D+01	-0.103871D+00	0.0	0.0	0.0
25	0.0	-0.160172D+01	-0.988043D-01	0.0	0.0	0.0
26	0.0	-0.156375D+01	-0.107425D+00	0.0	0.0	0.0
27	0.0	-0.156433D+01	-0.104991D+00	0.0	0.0	0.0
28	0.0	-0.156494D+01	-0.102567D+00	0.0	0.0	0.0
29	0.0	-0.153645D+01	-0.110346D+00	0.0	0.0	0.0
30	0.0	-0.153765D+01	-0.105235D+00	0.0	0.0	0.0
31	0.0	-0.150928D+01	-0.112843D+00	0.0	0.0	0.0
32	0.0	-0.150992D+01	-0.110505D+00	0.0	0.0	0.0
33	0.0	-0.151039D+01	-0.108129D+00	0.0	0.0	0.0
34	0.0	-0.1509857D+01	-0.112865D+00	0.0	0.0	0.0
35	0.0	-0.1509957D+01	-0.108073D+00	0.0	0.0	0.0
36	0.0	-0.150792D+01	-0.113001D+00	0.0	0.0	0.0
37	0.0	-0.150899D+01	-0.110757D+00	0.0	0.0	0.0
38	0.0	-0.150872D+01	-0.107920D+00	0.0	0.0	0.0
39	0.0	-0.150786D+01	-0.113191D+00	0.0	0.0	0.0
40	0.0	-0.150861D+01	-0.107979D+00	0.0	0.0	0.0
41	0.0	-0.150792D+01	-0.113362D+00	0.0	0.0	0.0
42	0.0	-0.150821D+01	-0.110739D+00	0.0	0.0	0.0
43	0.0	-0.150650D+01	-0.108669D+00	0.0	0.0	0.0
44	0.0	-0.150774D+01	-0.113529D+00	0.0	0.0	0.0
45	0.0	-0.150838D+01	-0.108202D+00	0.0	0.0	0.0
46	0.0	-0.150766D+01	-0.113664D+00	0.0	0.0	0.0



48 -0. 120/155D+J1 -0. 110869D+J1  
 49 -0. 150 827D+01 -0. 108367D+00  
 50 -0. 150 730D+01 -0. 113334D+00  
 51 -0. 150 746D+J1 -0. 110844D+00  
 52 -0. 150 786D+01 -0. 108067D+00  
 53 -0. 150 426D+01 -0. 113230D+00  
 54 -0. 150 402D+01 -0. 108325D+00  
 55 -0. 150 120D+01 -0. 11199D+00  
 56 -0. 150 907D+01 -0. 110665D+00  
 57 -0. 150 020D+01 -0. 108036D+00  
 58 -0. 150 124D+01 -0. 113253D+00  
 59 -0. 150 128D+01 -0. 113300D+00  
 60 -0. 150 037D+J1 -0. 110567D+00  
 61 -0. 150 260D+01 -0. 108181D+00  
 62 -0. 150 131D+01 -0. 113080D+00  
 63 -0. 150 925D+01 -0. 103103D+00  
 64 -0. 150 135D+01 -0. 112820D+00  
 65 -0. 149 959D+01 -0. 110693D+00  
 66 -0. 150 025D+01 -0. 108066D+00  
 67 -0. 150 134D+01 -0. 112610D+00  
 68 -0. 150 017D+01 -0. 108177D+00  
 69 -0. 150 133D+01 -0. 112368D+00  
 70 -0. 149 888D+01 -0. 110512D+00  
 71 -0. 150 011D+01 -0. 108329D+00  
 72 -0. 150 098D+01 -0. 111832D+00  
 73 -0. 149 943D+01 -0. 108452D+00  
 74 -0. 150 027D+01 -0. 111229D+00  
 75 -0. 149 805D+01 -0. 110492D+00  
 76 -0. 149 877D+J1 -0. 109605D+00  
 77 -0. 149 841D+01 -0. 111508D+00  
 78 -0. 149 753D+01 -0. 10936D+00  
 79 -0. 147 181D+01 -0. 109841D+00  
 80 -0. 147 026D+01 -0. 103494D+00  
 81 -0. 144 478D+01 -0. 104070D+00  
 82 -0. 144 399D+01 -0. 103080D+00  
 83 -0. 144 324D+01 -0. 102992D+00  
 84 -0. 140 770D+01 -0. 101647D+00  
 85 -0. 140 620D+01 -0. 949804D-01  
 86 -0. 137 112D+01 -0. 942697D-01  
 87 -0. 137 040D+01 -0. 936502D-01  
 88 -0. 136 966D+01 -0. 930317D-01  
 89 -0. 129 709D+01 -0. 981995D-01  
 90 -0. 129 568D+01 -0. 810958D-01  
 91 -0. 122 375D+01 -0. 762640D-01  
 92 -0. 122 240D+J1 -0. 755496D-01  
 93 -0. 197 594D+J1 -0. 631454D-01  
 94 -0. 197 470D+01 -0. 559188D-01  
 95 -0. 928921D+00 -0. 449612D-01  
 96 -0. 928370D+J0 -0. 447482D-01  
 97 -0. 927819D+J0 -0. 445396D-01  
 98 -0. 707325D+J0 -0. 297892D-01







187



223	0.0	-0. 151577 D+01
224	0.0	-0. 151663 D+01
225	0.0	-0. 151974 D+01
226	0.0	-0. 151996 D+01
227	0.0	-0. 152272 D+01
228	0.0	-0. 152259 D+01
229	0.0	-0. 152246 D+01
230	0.0	-0. 152557 D+01
231	0.0	-0. 152544 D+01
232	0.0	-0. 152854 D+01
233	0.0	-0. 152842 D+01
234	0.0	-0. 152830 D+01
235	0.0	-0. 153140 D+01
236	0.0	-0. 153127 D+01
237	0.0	-0. 153437 D+01
238	0.0	-0. 153425 D+01
239	0.0	-0. 153412 D+01
		-0. 114297 D+00
		-0. 114065 D+00
		-0. 114077 D+00
		-0. 114539 D+00
		-0. 114531 D+00
		-0. 114299 D+00
		-0. 114069 D+00
		-0. 114075 D+00
		-0. 114537 D+00
		-0. 114532 D+00
		-0. 114304 D+00
		-0. 114070 D+00
		-0. 114076 D+00
		-0. 114538 D+00
		-0. 114542 D+00
		-0. 114302 D+00
		-0. 114079 D+00



13

1 ELASTIC  $0.17504400 \times 0.2$   $0.47587600 \times 0.0$   $0.93384400 \times 0.1$   $0.17504500 \times 0.2$   $0.47536300 \times 0.0$   $0.31$   
 2 ELASTIC  $0.15611500 \times 0.2$   $0.10225100 \times 0.1$   $0.55403300 \times 0.0$   $0.15629900 \times 0.2$   $0.10409500 \times 0.1$   $1.91$   
 3 ELASTIC  $0.17403500 \times 0.2$   $0.16671800 \times 0.0$   $0.85607100 \times 0.1$   $0.17464000 \times 0.2$   $0.10629400 \times 0.0$   $0.28$   
 4 ELASTIC  $0.15689900 \times 0.2$   $0.39339900 \times 0.1$   $0.61127100 \times 0.0$   $0.15704600 \times 0.2$   $0.63072900 \times 0.1$   $2.22$

14

1 ELASTIC  $0.17457900 \times 0.2$   $0.20150700 \times 0.0$   $0.58093200 \times 0.1$   $0.17459100 \times 0.2$   $0.20131100 \times 0.0$   $0.19$   
 2 ELASTIC  $0.15632900 \times 0.2$   $0.51559000 \times 0.1$   $0.68166700 \times 0.0$   $0.15663600 \times 0.2$   $0.48491500 \times 0.0$   $2.58$   
 3 ELASTIC  $0.17402500 \times 0.2$   $0.80775600 \times 0.1$   $0.37791900 \times 0.1$   $0.17462600 \times 0.2$   $0.80767000 \times 0.0$   $0.13$   
 4 ELASTIC  $0.15523600 \times 0.2$   $0.10744200 \times 0.1$   $0.58068200 \times 0.0$   $0.15546900 \times 0.2$   $0.10511200 \times 0.1$   $2.30$

15

1 ELASTIC  $0.17524300 \times 0.2$   $0.12093900 \times 0.1$   $0.31597000 \times 0.1$   $0.17584400 \times 0.2$   $0.12093300 \times 0.1$   $0.11$   
 2 ELASTIC  $0.15515900 \times 0.2$   $0.17919900 \times 0.1$   $0.28628700 \times 0.0$   $0.15024200 \times 0.2$   $0.17857700 \times 0.1$   $1.24$   
 3 ELASTIC  $0.17416200 \times 0.2$   $0.14850000 \times 0.1$   $0.47021900 \times 0.0$   $0.17330200 \times 0.2$   $0.14710400 \times 0.1$   $-1.70$   
 4 ELASTIC  $0.15592000 \times 0.2$   $0.41576400 \times 0.1$   $0.16265500 \times 0.0$   $0.40438500 \times 0.2$   $0.16016000 \times 0.1$   $5.60$

27

1 ELASTIC  $-0.11244700 \times 0.1$   $0.70310300 \times 0.1$   $-0.17262500 \times 0.1$   $-0.65696100 \times 0.0$   $-0.74985400 \times 0.1$   $-15.15$   
 2 ELASTIC  $-0.92391900 \times 0.1$   $-0.25894600 \times 0.1$   $-0.37981600 \times 0.1$   $0.10353600 \times 0.2$   $-0.37040200 \times 0.1$   $-16.35$   
 3 ELASTIC  $-0.17560400 \times 0.1$   $-0.71405200 \times 0.1$   $-0.49488700 \times 0.1$   $0.11781100 \times 0.1$   $-0.10084700 \times 0.2$   $0.99151800 \times 0.1$   
 4 ELASTIC  $-0.87152300 \times 0.1$   $-0.26480900 \times 0.1$   $-0.22561100 \times 0.1$   $0.91477900 \times 0.1$   $-0.30796000 \times 0.1$   $-10.83$

28

1 ELASTIC  $-0.73002100 \times 0.1$   $-0.27418200 \times 0.2$   $-0.61914900 \times 0.1$   $-0.56214800 \times 0.1$   $-0.29177000 \times 0.2$   $-15.86$   
 2 ELASTIC  $-0.12522600 \times 0.2$   $-0.29562100 \times 0.2$   $0.89585900 \times 0.0$   $-0.12336000 \times 0.2$   $-0.29608700 \times 0.2$   $0.17150300 \times 0.2$   
 3 ELASTIC  $-0.90696500 \times 0.1$   $-0.45536300 \times 0.1$   $-0.38579100 \times 0.1$   $-0.13880200 \times 0.1$   $-0.92552500 \times 0.1$   $-50.63$   
 4 ELASTIC  $-0.40269200 \times 0.1$   $-0.36096000 \times 0.1$   $-0.31362400 \times 0.1$   $-0.70693800 \times 0.0$   $-0.69895800 \times 0.1$   $0.56544800 \times 0.1$

29

1 \* PLASTIC  $-0.23626800 \times 0.2$   $-0.34817000 \times 0.2$   $-0.11732000 \times 0.2$   $-0.16224000 \times 0.2$   $-0.42219800 \times 0.2$   $-32.25$   
 2 \* PLASTIC  $-0.23626800 \times 0.2$   $-0.34817000 \times 0.2$   $-0.11732000 \times 0.2$   $-0.16224000 \times 0.2$   $-0.42219800 \times 0.2$   $0.24624200 \times 0.2$   
 3 \* PLASTIC  $-0.23626800 \times 0.2$   $-0.34817000 \times 0.2$   $-0.11732000 \times 0.2$   $-0.16224000 \times 0.2$   $-0.42219800 \times 0.2$   $0.24624200 \times 0.2$   
 4 \* PLASTIC  $-0.23626800 \times 0.2$   $-0.34817000 \times 0.2$   $-0.11732000 \times 0.2$   $-0.16224000 \times 0.2$   $-0.42219800 \times 0.2$   $0.24624200 \times 0.2$

30

1 ELASTIC  $-0.37972800 \times 0.1$   $-0.20865800 \times 0.2$   $-0.69922100 \times 0.1$   $-0.13009100 \times 0.1$   $-0.23382200 \times 0.2$   $-19.65$   
 2 ELASTIC  $-0.37972800 \times 0.1$   $-0.20855800 \times 0.2$   $-0.69922100 \times 0.1$   $-0.13009100 \times 0.1$   $-0.23382200 \times 0.2$   $0.19749800 \times 0.2$   
 3 ELASTIC  $-0.37972800 \times 0.1$   $-0.20845800 \times 0.2$   $-0.69922100 \times 0.1$   $-0.13009100 \times 0.1$   $-0.23382200 \times 0.2$   $0.19749800 \times 0.2$   
 4 ELASTIC  $-0.37972800 \times 0.1$   $-0.20885800 \times 0.2$   $-0.69922100 \times 0.1$   $-0.13009100 \times 0.1$   $-0.23382200 \times 0.2$   $0.19749800 \times 0.2$

31

1 ELASTIC  $-0.15904200 \times 0.2$   $-0.21881900 \times 0.2$   $-0.74696100 \times 0.1$   $-0.19847600 \times 0.2$   $-0.26938400 \times 0.2$   $-34.10$   
 2 ELASTIC  $-0.13677300 \times 0.2$   $-0.20927500 \times 0.2$   $-0.34605900 \times 0.1$   $-0.12290800 \times 0.2$   $-0.22314100 \times 0.2$   $-21.84$   
 3 ELASTIC  $-0.98906200 \times 0.1$   $-0.78502900 \times 0.1$   $-0.68333800 \times 0.1$   $-0.19613400 \times 0.1$   $-0.15779600 \times 0.2$   $-49.25$   
 4 ELASTIC  $-0.76638200 \times 0.1$   $-0.68959400 \times 0.1$   $-0.28243600 \times 0.1$   $-0.44295400 \times 0.1$   $-0.10130200 \times 0.2$   $-48.87$

32

1 ELASTIC  $-0.15930700 \times 0.1$   $-0.53520100 \times 0.1$   $-0.46979700 \times 0.1$   $0.15159400 \times 0.1$   $-0.85186100 \times 0.1$   $-33.98$   
 2 ELASTIC  $0.72246800 \times 0.1$   $-0.15920000 \times 0.1$   $-0.30550700 \times 0.1$   $0.81801000 \times 0.1$   $-0.25474800 \times 0.1$   $-17.36$   
 3 ELASTIC  $0.24664000 \times 0.1$   $-0.25849600 \times 0.1$   $-0.40750500 \times 0.1$   $0.36117300 \times 0.1$   $-0.52700500 \times 0.1$   $-33.36$   
 4 ELASTIC  $0.54592600 \times 0.1$   $-0.64284100 \times 0.1$   $-0.34406000 \times 0.1$   $0.70059700 \times 0.1$   $-0.21905500 \times 0.1$   $-24.22$



2	ELASTIC	0.472657D+01	0.384933D-01	-0.2220701D+00	0-103492D+01	-0.217754D+00	-10.32	0.109709D+01
3	ELASTIC	0.615192D+01	0.233416D+01	-0.407770D+01	0-874543D+01	-0.259342D+00	-32.46	0.798091D+01
4	ELASTIC	0.350840D+01	0.120122D+01	-0.326830D+01	0-578350D+01	-0.107368D+01	-35.17	0.601290D+01
35								
1	ELASTIC	0.994745D+00	-0.177501D+01	-0.2220701D+00	0-103492D+01	-0.217754D+00	-10.32	0.109709D+01
2	ELASTIC	0.200227D+01	0.454214D+01	0-965359D-01	0-200758D+01	0-248894D+00	3.15	0.158852D+01
3	ELASTIC	0.245718D+01	0.161196D+01	0-263562D+01	0-472251D+01	0-573366D+00	42.15	0.466083D+01
4	ELASTIC	0.626573D+01	0.349563D+01	0-263092D+01	0-785391D+01	0-190744D+01	31.12	0.550743D+01
36								
1	ELASTIC	0.858798D+01	0-366731D+01	-0-3939396D+01	0-108583D+02	0-159698D+01	-29.68	0.839849D+01
2	ELASTIC	0.858798D+01	0-386731D+01	-0-398396D+01	0-108583D+02	0-159698D+01	-29.68	0.839849D+01
3	ELASTIC	0.858798D+01	0-386731D+01	-0-398396D+01	0-108583D+02	0-159698D+01	-29.68	0.839849D+01
4	ELASTIC	0.858798D+01	0-386731D+01	-0-398396D+01	0-108583D+02	0-159698D+01	-29.68	0.839849D+01
37								
1	ELASTIC	0.1P7969L+02	0-663527D+01	0-816750D+00	0-188515D+02	0-658066D+01	3.82	0.117814D+02
2	ELASTIC	0.107057D+02	0-316763D+01	0-357277D+00	0-107226D+02	0-315073D+01	2.71	0.712032D+01
3	*PLASTIC	0-125004D+02	-0-667866D+01	-0-103956D+02	0-170547D+02	-0-112330D+02	-23.66	0-245233D+02
4	ELASTIC	0.483898D+01	-0-105036D+02	-0-118172D+02	0-112565D+02	-0-1699212D+02	-28.51	0-244289D+02
38								
1	*PLASTIC	0-833037D+02	0-595105D+02	-0-821751D+01	0-8588659D+02	0-569483D+02	-17.32	0-261462D+02
2	*PLASTIC	0-833037D+02	0-595105D+02	-0-821751D+01	0-858659D+02	0-569483D+02	-17.32	0-261462D+02
3	*PLASTIC	0-833037D+02	0-595105D+02	-0-821751D+01	0-858659D+02	0-569483D+02	-17.32	0-261462D+02
4	*PLASTIC	0-833037D+02	0-595105D+02	-0-821751D+01	0-858659D+02	0-569483D+02	-17.32	0-261462D+02
39								
1	ELASTIC	0-502424D+01	-0-206794D+00	-0-277017D+01	0-621858D+01	-0-140109D+01	-23.32	0-666888D+01
2	ELASTIC	0-407064D+01	-0-751491D+00	-0-234930D+01	0-502594D+01	-0-170679D+01	-22.13	0-586838D+01
3	ELASTIC	0-327882D+01	0-275677D+01	-0-351508D+01	0-654255D+01	-0-506925D+00	-42.88	0-622325D+01
4	ELASTIC	0-307084D+01	0-373835D+01	-0-279216D+01	0-621671D+01	-0-592624D+00	-48.41	0-505741D+01
40								
1	ELASTIC	0-916471D+01	-0-146411D+01	-0-181808D+00	0-916782D+01	-0-146722D+01	-0.98	0-933809D+01
2	ELASTIC	0-783626D+01	0-174963D+00	-0-632726D+00	0-788817D+01	0-123060D+00	-4.69	0-691302D+01
3	ELASTIC	0-580342D+01	-0-276377D+01	-0-267736D+01	0-663139D+01	-0-352674D+01	-15.91	0-881909D+01
4	ELASTIC	0-603978D+01	-0-209859D+01	-0-235401D+01	0-6671162D+01	-0-2730443D+01	-15.02	0-618048D+01
41								
1	ELASTIC	0-931235D+01	0-314826L+01	0-312757D+01	0-978596D+01	0-167460D+01	25.23	0-738914D+01
2	ELASTIC	1-411990D+01	0-135112D+01	0-3633859D+01	0-662795D+01	-0-115784D+01	34.59	0-683087D+01
3	ELASTIC	0-6847905D+01	0-495161D+01	0-429338D+01	0-793968D+01	0-185253D+01	24.45	0-562366D+01
4	ELASTIC	0-387562D+01	0-170266D+01	0-196055D+01	0-495770D+01	0-518171D+01	29.58	0-399768D+01
42								
1	ELASTIC	0-154703D+02	0-481049D+01	0-424501D+01	0-169595D+02	0-332723D+01	19.26	0-124836D+02
2	ELASTIC	0-154703D+02	0-481049D+01	0-424501D+01	0-169595D+02	0-332723D+01	19.26	0-124836D+02
3	ELASTIC	0-154703D+02	0-481049D+01	0-424501D+01	0-169595D+02	0-332723D+01	19.26	0-124836D+02
4	ELASTIC	0-154703D+02	0-481049D+01	0-424501D+01	0-169595D+02	0-332723D+01	19.26	0-124836L+02
43								
1	ELASTIC	0-925771D+01	0-268904D+01	0-257713D+01	0-101482D+02	0-179918D+01	19.06	0-761505D+01
2	ELASTIC	0-925771D+01	0-268904D+01	0-257713D+01	0-101482D+02	0-179918D+01	19.06	0-761505D+01
3	ELASTIC	0-925771D+01	0-268904D+01	0-257713D+01	0-101482D+02	0-179918D+01	19.06	0-761505D+01
4	ELASTIC	0-925771D+01	0-268904D+01	0-257713D+01	0-101482D+02	0-179918D+01	19.06	0-761505D+01



2	ELASTIC	0. 293632E+01	0. 211351E+01	0. 744400D-01	0. 294499D+01	0. 210685D+01	5.12
3	ELASTIC	0. +75000E+01	-0. 178156E+01	-0. 925729D+00	0. 487951D+01	-0. 191021D+01	-7.91
4	ELASTIC	0. 102911D+01	-0. 206853D+01	0. 221103D+00	0. 104482D+01	-0. 208424D+01	4.36
64							
1	ELASTIC	-0. 350930D+01	-0. 152868D+02	0. 182137D+01	-0. 360537D+01	-0. 155703D+02	8.86
2	ELASTIC	-0. 350936D+01	-0. 152868D+02	0. 182137D+01	-0. 360537D+01	-0. 155708D+02	8.86
3	ELASTIC	-0. 350930D+01	-0. 152868D+02	0. 182137D+01	-0. 360537D+01	-0. 155703D+02	8.86
4	ELASTIC	-0. 350930D+01	-0. 152868D+02	0. 182137D+01	-0. 360537D+01	-0. 155708D+02	8.86
65							
1	ELASTIC	0. 111660D+01	0. 245177D+01	-0. 302223D+01	0. 487927D+01	-0. 131090D+01	-51.23
2	ELASTIC	0. 310572D+01	-0. 474536D-01	-0. 181111D+01	0. 393034D+01	-0. 872066E+00	-24.48
3	ELASTIC	0. 103530D+01	0. 394725D+01	-0. 138779D+01	0. 424693D+01	0. 435618D+00	-66.63
4	ELASTIC	0. 937127D+01	0. 2534640+00	-0. 428738D+01	0. 114362D+01	0. 469665D-01	-25.72



NODE	DISPLACEMENTS		
	X-DISPLACEMENT	Y-DISPLACEMENT	Z-DISPLACEMENT
1	0.0	-0.718166D+02	0.0
2	0.0	-0.359384D+02	0.0
3	0.0	0.0	0.0
4	0.0	0.0	0.0
5	0.0	0.0	0.0
6	0.0	0.0	0.0
7	0.0	0.0	0.0
8	0.0	0.0	0.0
9	0.0	0.0	0.0
10	0.0	0.0	0.0
11	0.0	0.0	0.0
12	0.0	0.0	0.0
13	0.0	0.0	0.0
14	0.0	0.0	0.0
15	0.0	0.0	0.0
16	0.0	0.0	0.0
17	0.0	0.0	0.0
18	0.0	0.0	0.0
19	0.0	0.0	0.0
20	0.0	0.0	0.0
21	0.0	0.0	0.0
22	0.0	0.0	0.0
23	0.0	0.0	0.0
24	0.0	0.0	0.0
25	0.0	0.0	0.0
26	0.0	0.0	0.0
27	0.0	0.0	0.0
28	0.0	0.0	0.0
29	0.0	0.0	0.0
30	0.0	0.0	0.0
31	0.0	0.0	0.0
32	0.0	0.0	0.0
33	0.0	0.0	0.0
34	0.0	0.0	0.0
35	0.0	0.0	0.0
36	0.0	0.0	0.0
37	0.0	0.0	0.0
38	0.0	0.0	0.0
39	0.0	0.0	0.0
40	0.0	0.0	0.0
41	0.0	0.0	0.0
42	0.0	0.0	0.0
43	0.0	0.0	0.0
44	0.0	0.0	0.0
45	0.0	0.0	0.0
46	0.0	0.0	0.0



$-0.2152675+01$   
 $-0.2154666+01$   
 $-0.2153333+01$   
 $-0.2153550+01$   
 $-0.2154110+01$   
 $-0.2148970+01$   
 $-0.2148619+01$   
 $-0.2144570+01$   
 $-0.2143830+01$   
 $-0.2143160+01$   
 $-0.2144670+01$   
 $-0.2144770+01$   
 $-0.214350+01$   
 $-0.2143320+01$   
 $-0.2144850+01$   
 $-0.2143360+01$   
 $-0.2144940+01$   
 $-0.2142210+01$   
 $-0.2143390+01$   
 $-0.2144970+01$   
 $-0.2143340+01$   
 $-0.2145000+01$   
 $-0.2141020+01$   
 $-0.2143300+01$   
 $-0.2144990+01$   
 $-0.2142200+01$   
 $-0.2143170+01$   
 $-0.2140080+01$   
 $-0.2141120+01$   
 $-0.2141470+01$   
 $-0.2143600+01$   
 $-0.2139360+01$   
 $-0.2102540+01$   
 $-0.2100420+01$   
 $-0.2063920+01$   
 $-0.1958700+01$   
 $-0.1957710+01$   
 $-0.1956700+01$   
 $-0.2010960+01$   
 $-0.2008920+01$   
 $-0.1951020+01$   
 $-0.1748180+01$   
 $-0.1746330+01$   
 $-0.1537020+01$   
 $-0.1535330+01$   
 $-0.1327000+01$   
 $-0.1326240+01$   
 $-0.1325490+01$   
 $-0.1910440+01$   
 $-0.1474330+00$   
 $-0.1479320+00$   
 $-0.1559520+00$   
 $-0.1514900+00$   
 $-0.1475150+00$   
 $-0.1474140+00$   
 $-0.1549730+00$   
 $-0.1550550+00$   
 $-0.1510720+00$   
 $-0.1476390+00$   
 $-0.1547160+00$   
 $-0.1475180+00$   
 $-0.1543230+00$   
 $-0.1511400+00$   
 $-0.147530+00$   
 $-0.1540310+00$   
 $-0.1476630+00$   
 $-0.1536890+00$   
 $-0.1509170+00$   
 $-0.1479270+00$   
 $-0.1528800+00$   
 $-0.1481410+00$   
 $-0.1520310+00$   
 $-0.1509710+00$   
 $-0.1483610+00$   
 $-0.1524050+00$   
 $-0.1506790+00$   
 $-0.1489420+00$   
 $-0.1502930+00$   
 $-0.1412020+00$   
 $-0.1422430+00$   
 $-0.1408470+00$   
 $-0.1394540+00$   
 $-0.1391030+00$   
 $-0.1295660+00$   
 $-0.1268390+00$   
 $-0.1279630+00$   
 $-0.1270880+00$   
 $-0.1206140+00$   
 $-0.1105880+00$   
 $-0.1042250+00$   
 $-0.1032010+00$   
 $-0.8650840-01$   
 $-0.7618110-01$   
 $-0.6144560-01$   
 $-0.6114410-01$   
 $-0.6084430-01$   
 $-0.4093370-01$



32	$0.0$	$-0.100926D+01$	$-0.304214D-01$
33	$0.0$	$-0.695104D+00$	$-0.168857D-01$
34	$0.0$	$-0.6947012D+00$	$-0.167366D-01$
35	$0.0$	$-0.6944293D+00$	$-0.165902D-01$
36	$0.0$	$-0.340892D+00$	$-0.945965D-02$
37	$0.0$	$-0.346492D+00$	$0.120327D-02$
38	$0.0$	$0.0$	$0.0$
39	$0.0$	$0.0$	$0.0$
40	$0.0$	$0.0$	$0.0$
41	$0.0$	$0.0$	$0.0$
42	$0.0$	$0.0$	$0.0$
43	$0.0$	$0.0$	$0.0$
44	$0.0$	$0.0$	$0.0$
45	$0.0$	$0.0$	$0.0$
46	$0.0$	$0.0$	$0.0$
47	$0.0$	$0.0$	$0.0$
48	$0.0$	$0.0$	$0.0$
49	$0.0$	$0.0$	$0.0$
50	$0.0$	$0.0$	$0.0$
51	$0.0$	$-0.215394D+01$	$-0.154482D+00$
52	$0.0$	$-0.215362D+01$	$-0.154737D+00$
53	$0.0$	$-0.215336D+01$	$-0.155179D+00$
54	$0.0$	$-0.215331D+01$	$-0.155760D+00$
55	$0.0$	$-0.215344D+01$	$-0.156135D+00$
56	$0.0$	$-0.215134D+01$	$-0.156484D+00$
57	$0.0$	$-0.215189D+01$	$-0.156683D+00$
58	$0.0$	$-0.215204D+01$	$-0.155659D+00$
59	$0.0$	$-0.215227D+01$	$-0.155353D+00$
60	$0.0$	$-0.215234D+01$	$-0.154945D+00$
61	$0.0$	$-0.215240D+01$	$-0.154568D+00$
62	$0.0$	$-0.215193D+01$	$-0.154767D+00$
63	$0.0$	$-0.215169D+01$	$-0.155084D+00$
64	$0.0$	$-0.215180D+01$	$-0.155396D+00$
65	$0.0$	$-0.215164D+01$	$-0.155772D+00$
66	$0.0$	$-0.215138D+01$	$-0.156187D+00$
67	$0.0$	$-0.215157D+01$	$-0.156144D+00$
68	$0.0$	$-0.215123D+01$	$-0.156527D+00$
69	$0.0$	$-0.215130D+01$	$-0.156506D+00$
70	$0.0$	$-0.214801D+01$	$-0.155728D+00$
71	$0.0$	$-0.214813D+01$	$-0.155335D+00$
72	$0.0$	$-0.214808D+01$	$-0.155899D+00$
73	$0.0$	$-0.214800D+01$	$-0.155866D+00$
74	$0.0$	$-0.214790D+01$	$-0.155719D+00$
75	$0.0$	$-0.214801D+01$	$-0.155501D+00$
76	$0.0$	$-0.214813D+01$	$-0.155535D+00$
77	$0.0$	$-0.214796D+01$	$-0.155527D+00$
78	$0.0$	$-0.214790D+01$	$-0.155551D+00$
79	$0.0$	$-0.214790D+01$	$-0.155450D+00$
80	$0.0$	$-0.214510D+01$	$-0.155207D+00$
81	$0.0$	$-0.214511D+01$	$-0.155062D+00$
82	$0.0$	$-0.214497D+01$	$-0.155112D+00$
83	$0.0$	$-0.214489D+01$	$-0.154700D+00$
84	$0.0$	$-0.214491D+01$	$-0.155142D+00$
85	$0.0$	$-0.214798D+01$	$-0.155039D+00$
86	$0.0$	$-0.214516D+01$	$-0.155075D+00$
87	$0.0$	$-0.214475D+01$	$-0.154991D+00$
88	$0.0$	$-0.214516D+01$	$-0.154700D+00$
89	$0.0$	$-0.214783D+01$	$-0.154629D+00$
90	$0.0$	$-0.214742D+01$	$-0.154571D+00$
91	$0.0$	$-0.214516D+01$	$-0.154349D+00$
92	$0.0$	$-0.214516D+01$	$-0.154991D+00$
93	$0.0$	$-0.214772D+01$	$-0.154102D+00$
94	$0.0$	$-0.214729D+01$	$-0.154092D+00$
95	$0.0$	$-0.214513D+01$	$-0.154010D+00$
96	$0.0$	$-0.214771D+01$	$-0.153892D+00$



151  
 152  
 153  
 154  
 155  
 156  
 157  
 158  
 159  
 160  
 161  
 162  
 163  
 164  
 165  
 166  
 167  
 168  
 169  
 170  
 171  
 172  
 173  
 174  
 175  
 176  
 177  
 178  
 179  
 180  
 181  
 182  
 183  
 184  
 185  
 186  
 187  
 188  
 189  
 190  
 191  
 192  
 193  
 194  
 195  
 196  
 197  
 198  
 199  
 200  
 201  
 202

-U. 2147229\*U  
 -U. 2145010D+U  
 -U. 2144469D+U  
 -U. 215142D+U  
 -U. 215138D+U  
 -U. 215112D+U  
 -U. 215110D+U  
 -U. 214841L+U  
 -U. 214842D+U  
 -U. 214824D+U  
 -U. 214821D+U  
 -U. 214863D+U  
 -U. 214863U+U  
 -U. 214866D+U  
 -U. 214970D+U  
 -U. 215095D+U  
 -U. 215095D+U  
 -U. 215097D+U  
 -U. 215097D+U  
 -U. 2150969D+U  
 -U. 215070D+U  
 -U. 215070D+U  
 -U. 214892D+U  
 -U. 214892D+U  
 -U. 2148959+U  
 -U. 214911D+U  
 -U. 214913D+U  
 -U. 21498D+U  
 -U. 215046D+U  
 -U. 215052D+U  
 -U. 215037D+U  
 -U. 214981D+U  
 -U. 214924D+U  
 -U. 215125D+U  
 -U. 215080D+U  
 -U. 215259D+U  
 -U. 215224D+U  
 -U. 215190D+U  
 -U. 215404D+U  
 -U. 215800D+U  
 -U. 215778D+U  
 -U. 216042D+U  
 -U. 215531D+U  
 -U. 215800D+U  
 -U. 215376D+U  
 -U. 215562D+U  
 -U. 21556D+U  
 -U. 215531D+U  
 -U. 215800D+U  
 -U. 215376D+U  
 -U. 215562D+U  
 -U. 21556D+U  
 -U. 215531D+U  
 -U. 215800D+U  
 -U. 215376D+U  
 -U. 215562D+U  
 -U. 21556D+U  
 -U. 215531D+U  
 -U. 215800D+U  
 -U. 216330D+U  
 -U. 216310D+U  
 -U. 216638D+U

-0. 153665D+U  
 -0. 1524122\*U  
 -0. 155489D+U  
 -0. 155447D+U  
 -0. 152200D+U  
 -0. 156394D+U  
 -0. 155783D+U  
 -0. 155669D+U  
 -0. 154673D+U  
 -0. 154088D+U  
 -0. 154699D+U  
 -0. 155170D+U  
 -0. 155614D+U  
 -0. 155640D+U  
 -0. 156465D+U  
 -0. 156261D+U  
 -0. 156255D+U  
 -0. 155886D+U  
 -0. 155462D+U  
 -0. 155896D+U  
 -0. 156165D+U  
 -0. 155311D+U  
 -0. 155777D+U  
 -0. 155003D+U  
 -0. 155186D+U  
 -0. 155610D+U  
 -0. 155709D+U  
 -0. 156551D+U  
 -0. 156420D+U  
 -0. 155917D+U  
 -0. 155909D+U  
 -0. 156722D+U  
 -0. 156714D+U  
 -0. 156702D+U  
 -0. 156356D+U  
 -0. 156083D+U  
 -0. 156129D+U  
 -0. 156761D+U  
 -0. 156744D+U  
 -0. 156718D+U  
 -0. 156400D+U  
 -0. 156021D+U  
 -0. 156000D+U  
 -0. 156330D+U  
 -0. 156310D+U  
 -0. 156742D+U  
 -0. 156723D+U



203	0.0
204	0.0
205	0.0
206	0.0
207	0.0
208	0.0
209	0.0
210	0.0
211	0.0
212	0.0
213	0.0
214	0.0
215	0.0
216	0.0
217	0.0
218	0.0
219	0.0
-0.216615D+01	-0.156407D+00
-0.216600D+01	-0.156090D+00
-0.217027D+01	-0.156197D+00
-0.217059D+01	-0.156739D+00
-0.217434D+01	-0.156728D+00
-0.217416D+01	-0.156411D+00
-0.217398D+01	-0.156096D+00
-0.217824D+01	-0.156104D+00
-0.217806D+01	-0.156736D+00
-0.218231D+01	-0.156730D+00
-0.218213D+01	-0.156417D+00
-0.218196D+01	-0.156098D+00
-0.218620D+01	-0.156105D+00
-0.218603D+01	-0.156738D+00
-0.219028D+01	-0.156743D+00
-0.219010D+01	-0.156415D+00
-0.213993D+01	-0.156110D+00



13

1 \*ELASTIC U. 249628D+02 0.575399D+00 0.219882D+00  
 2 \*ELASTIC J. 243792+02 -0.159107D+01 0.682319D+00  
 3 \*ELASTIC U. 24890UD+02 -0.194819D+01 0.225650D+00  
 4 \*ELASTIC U. 225779+02 -0.502698D+01 0.726383D+00

15 \*ELASTIC U. 246744D+02 0.161461D+00 0.188553D+00  
 2 \*ELASTIC U. 225606D+02 0.763044D+00 0.830300D+00  
 3 \*ELASTIC U. 24888UD+02 0.123203D+01 0.171440D+00  
 4 \*ELASTIC U. 223653D+02 0.148820D+01 0.645935D+00

15 \*ELASTIC U. 250665D+02 0.194147D+01 0.131866D+00  
 2 \*ELASTIC U. 216495D+02 0.25W778D+01 0.323953D+00  
 3 \*ELASTIC U. 24367D+02 0.2364c3D+01 -0.596387D+00  
 4 \*ELASTIC U. 230907L+02 0.00932D+01 0.155114D+01

27 \*ELASTIC -U. 153018D+01 -0.905464D+01 -0.224964D+01  
 2 \*ELASTIC U. 131173D+02 -0.272294D+C1 -0.553742D+01  
 3 \*ELASTIC -U. 244402L+01 -U.443841D+01 -0.647015D+01  
 4 \*ELASTIC U. 123115D+02 -0.311466D+01 -0.330549D+01

28 \*PLASTIC -U. 807120D+01 -0.323758D+02 -0.666859D+01  
 2 \*PLASTIC -U. 173551D+02 -0.422651D+02 -0.150417D+01  
 3 \*PLASTIC -U. 674749D+01 -0.519290D+01 -0.610356D+01  
 4 \*ELASTIC -U. 521038D+01 -0.453414D+01 -0.520788D+01

29 \*PLASTIC -U. 458159D+02 -0.208180D+02 -0.136039D+02  
 2 \*PLASTIC -U. 458159D+02 -0.508180D+02 -0.136039D+02  
 3 \*PLASTIC -U. 458159D+02 -0.508180D+02 -0.136039D+02  
 4 \*PLASTIC -U. 458159D+02 -U.508180D+02 -0.136039D+02

30 \*PLASTIC -U. 426425D+01 -0.238019D+02 -0.103245D+02  
 2 \*PLASTIC -U. 426425D+01 -0.238019D+02 -0.103245D+02  
 3 \*PLASTIC -U. 426425D+01 -0.238019D+02 -0.103245D+02  
 4 \*PLASTIC -U. 196276D+02 -U.976706D+01 -0.615098D+01

31 \*PLASTIC -U. 308157D+02 -0.58303D+02 -0.125281D+02  
 2 \*ELASTIC -U. 206579D+02 -0.331711D+02 -0.905547D+01  
 3 \*ELASTIC -U. 209433D+02 -U.141238D+02 -U.128378D+02  
 4 \*ELASTIC -U. 196276D+02 -U.976706D+01 -0.615098D+01

32 \*ELASTIC -U. 249675D+01 -U.737951D+01 -0.634453D+01  
 2 \*ELASTIC U. 102467D+02 -U.191720D+01 -0.430922D+01  
 3 \*ELASTIC U. 311079D+00 -U.3494834L+01 -0.558621D+01  
 4 \*ELASTIC U. 73394L+01 -U.623349D+00 -0.475851D+01



2	ELASTIC	0.679077D+01	0.170310D+00	-0.402449D+01	0.868784D+01	-0.172746D+01	-25.27	0.912671D+01
3	ELASTIC	0.744294D+01	0.291613D+01	-0.553883D+01	0.11630D+02	-0.803910D+00	-33.89	0.105687D+02
4	ELASTIC	0.520073D+01	0.195517D+01	-0.430186D+01	0.81757D+01	-0.101982D+01	-34.67	0.809113D+01
35								
1	ELASTIC	-0.122544D+01	-0.605168D+00	-0.665590D+00	-0.180088D+00	-0.165048D+01	-57.47	0.132498D+01
2	ELASTIC	0.123655D+01	0.449956D+00	-0.699257D-01	0.124272D+01	0.443788D+00	-5.04	0.769737D+00
3	ELASTIC	0.102439D+01	0.305535D+01	0.430747D+01	0.646560D+01	-0.238539D+01	51.63	0.770850D+01
4	ELASTIC	0.743466D+01	0.580241D+01	0.430805D+01	0.110032D+02	0.223387D+01	39.64	0.804268D+01
36								
1	ELASTIC	0.112455D+02	0.325721D+01	-0.572064D+01	0.147135D+02	0.178921D+01	-31.20	0.116693D+02
2	ELASTIC	0.112455D+02	0.525721D+01	-0.572664D+01	0.147135D+02	0.178921D+01	-31.20	0.116693D+02
3	ELASTIC	0.112455D+02	0.525721D+01	-0.572664D+01	0.147135D+02	0.178921D+01	-31.20	0.116693D+02
4	ELASTIC	0.112455D+02	0.525721D+01	-0.572664D+01	0.147135D+02	0.178921D+01	-31.20	0.116693D+02
37								
1	ELASTIC	0.307311D+02	0.924937D+01	-0.163047D+00	0.307325D+02	0.924814D+01	-0.43	0.202515D+02
2	ELASTIC	0.147915D+02	0.241801D+01	-0.134802D+01	0.149366D+02	0.227286D+01	-6.15	0.114946D+02
3	*PLASTIC	0.946645D+01	-0.747185D+01	-0.117719D+02	0.154992D+02	-0.135046D+02	-27.13	0.251181D+02
4	*PLASTIC	-0.315039D+01	-0.161809D+02	-0.128619D+02	0.475226D+01	-0.240836D+02	-31.57	0.250761D+02
38								
1	*PLASTIC	0.104500D+03	0.427684D+02	-0.110732D+02	0.109146D+03	0.781224D+02	-22.77	0.274073D+02
2	*PLASTIC	0.104500D+03	0.827684D+02	-0.110702D+02	0.109146D+03	0.781224D+02	-22.77	0.274073D+02
3	*PLASTIC	0.104500D+03	0.827684D+02	-0.110732D+02	0.109146D+03	0.781224D+02	-22.77	0.274073D+02
4	*PLASTIC	0.104500D+03	0.827684D+02	-0.110702D+02	0.109146D+03	0.781224D+02	-22.77	0.274073D+02
39								
1	ELASTIC	0.737183D+01	-0.560297D+00	-0.378260D+01	0.888644D+01	-0.297490D+01	-21.82	0.959005D+01
2	ELASTIC	0.589643D+01	-0.137478D+01	-0.321193D+01	0.711203D+01	-0.259037D+01	-20.73	0.845105D+01
3	ELASTIC	0.515509D+01	0.386415D+01	-0.509939D+01	0.964970D+01	-0.630457D+00	-41.39	0.908378D+01
4	ELASTIC	0.461303D+01	0.527197D+01	-0.402125D+01	0.897725D+01	0.907802D+00	-47.34	0.726262D+01
40								
1	ELASTIC	0.129663D+02	-0.197438D+01	0.470219D-02	0.129663D+02	-0.197438D+01	0.02	0.131244D+02
2	ELASTIC	0.110218D+02	0.273504D+00	-0.728303D+00	0.110709D+02	0.224379D+00	-3.86	0.966120D+01
3	ELASTIC	0.850310D+01	-0.396444D+01	-0.353773D+01	0.949310D+01	-0.489445D+01	-14.73	0.124939D+02
4	ELASTIC	0.604876D+01	-C 310211D+01	-0.311001D+01	0.942110D+01	-0.387445D+01	-13.95	0.115676D+02
41								
1	ELASTIC	0.115780D+02	0.446270D+01	0.446613D+01	0.137303D+02	0.231043D+01	25.73	0.103972D+02
2	ELASTIC	0.565735D+01	0.192529D+01	0.519449D+01	0.931081D+01	-0.172817D+01	35.12	0.967958D+01
3	ELASTIC	0.959544D+01	0.418199D+01	0.327795D+01	0.111397D+02	0.263768D+01	25.23	0.786172D+01
4	ELASTIC	0.534479D+01	0.236029D+01	0.274872D+01	0.698020D+01	0.724876D+00	30.75	0.563219D+01
42								
1	ELASTIC	0.216318D+02	0.681288D+01	0.605023D+01	0.237882D+02	0.465649D+01	19.62	0.175180D+02
2	ELASTIC	0.216318D+02	0.691288D+01	0.605023D+01	0.237882D+02	0.465649D+01	19.62	0.175180D+02
3	ELASTIC	0.216318D+02	0.681288D+01	0.605023D+01	0.237882D+02	0.465649D+01	19.62	0.175180D+02
4	ELASTIC	0.216318D+02	0.681288D+01	0.605023D+01	0.237882D+02	0.465649D+01	19.62	0.175180D+02
43								
1	ELASTIC	0.129421L+02	0.385421D+01	0.371775D+01	0.142568D+02	0.252553D+01	19.67	0.106996D+02
2	ELASTIC	0.129281D+02	0.385421D+01	0.371775D+01	0.142568D+02	0.252553D+01	19.67	0.106996D+02
3	ELASTIC	0.129421L+02	0.385421D+01	0.371775D+01	0.142568D+02	0.252553L+01	19.67	0.106996D+02
4	ELASTIC	0.129281D+02	0.385421D+01	0.371775D+01	0.142568D+02	0.252553D+01	19.67	0.106996D+02



1	ELASTIC	0.779963D+01	0.792681D+00	0.922444D+00	0.791903D+01	0.673279D+00	7.38	0.650606D+01
2	ELASTIC	0.400067D+01	0.296526D+01	0.190945D+00	0.404057D+01	0.293136D+01	10.07	0.169325D+01
3	ELASTIC	0.671081D+01	-0.262981D+01	-0.113471D+01	0.684668D+01	-0.276568D+01	-6.83	0.836446D+01
4	ELASTIC	0.129478D+01	-0.304947D+01	0.457008D+00	0.134250D+01	-0.309719L+01	5.95	0.386087D+01
64								
1	ELASTIC	-0.557329D+01	-0.416473D+02	0.271661D+01	-0.512658D+01	-0.220944D+02	9.34	0.156703D+02
2	ELASTIC	-0.557329D+01	-0.216473D+02	0.271661D+01	-0.512658D+01	-0.220944D+02	9.34	0.156703D+02
3	ELASTIC	-0.557329D+01	-0.216473D+02	0.271661D+01	-0.512658D+01	-0.220944D+02	9.34	0.156703D+02
4	ELASTIC	-0.557329D+01	-0.216473D+02	0.271661D+01	-0.512658D+01	-0.220944D+02	9.34	0.156703D+02
65								
1	ELASTIC	0.146313D+01	0.331798D+01	-0.427062D+01	0.676072D+01	-0.197961D+01	-51.13	0.762951D+01
2	ELASTIC	0.446664D+01	-0.223523D+00	-0.248422D+01	0.553781D+01	-0.129469D+01	-23.33	0.597766D+01
3	ELASTIC	0.12777D+01	0.510719D+01	-0.165825D+01	0.585996D+01	0.519997D+00	-67.95	0.479735D+01
4	ELASTIC	0.119816D+01	0.242202D+00	-0.460737D+00	0.137548D+01	0.548877D-01	-22.12	0.117890D+01



## REFERENCES

1. Burner, W. K., "Accurately Specified and Controlled Fillet Weld Size in Ship Hull Construction," Coast Guard Engineers Digest, Jan., Feb., Mar., 1975.
2. Automatic Welding Journal of the Japan Welding Society. 32 (7). pp. 562-580. 1963.
3. Butler, L. J. and Kulak, G. L., "Strength of Fillet Welds as a Function of Direction of Load," Welding Journal, Vol. 50, No. 5, May, 1971. 231<sub>s</sub> - 5.
4. Kato, B. and Morita, K., "Strength of Transverse Fillet Welded Joints," Welding Journal, Vol. 53. No. 2. Feb., 1974. pp. 59<sub>s</sub> - 64.
5. Nishida, Yoshihiro; Tanaka, Tohachiro; and Tanaka, Shigeyoshi, "Strength of Fillet Weld in V-Shapes - Part I Strength of General Fillet Weld - Part II Strength of Deformed Fillet Weld," Sumitomo Search, May, 1971, -5- pp. 114-132.
6. Macfarland, D. S. and Harrison, J. D., "Some Fatigue Tests of Load Carrying Transverse Fillet Welds," British Welding Journal, Vol. 12, No. 12, December, 1965. pp. 613-623.
7. Solumsmoen, O. H., "Fatigue Tests on Specimens with Holes, Butt and Fillet Welds in Mild and High Tensile Structural Steels," Metal Construction. Vol. 1, No. 3, March, 1969. pp. 138-142.
8. "Effect of Peening and Grinding on the Fatigue Strength of Fillet Welded Joints," British Welding Journal, Vol. 15, No. 12, December, 1968. pp. 601-609.
9. Maddox, S. J., "An Analysis of Fatigue Cracks in Fillet Welded Joints," International Journal of Fracture, Vol. 11, No. 2, April, 1975.
10. Irwin, G. R., "Crack Extension Force for a Part-through Crack in a Plate," Paper No. 62-WA-13, Journal of Applied Mechanics. Trans. ASME, December, 1962.
11. Swannell, P., "Deformation of Longitudinal Fillet Welds Subjected to a Uniform Shearing Intensity," British Welding Journal, Vol. 15, No. 3, March, 1968. pp. 120-126.
12. Kassov, D. S., "Selecting Safe Limiting Stresses in the Calculation of Fillet Welds," Weld Prod., Feb., 1970. 17 --2--. pp. 17-18.



## REFERENCES CONTINUED

13. Boniszewski, T. and Eldridge, G. H., "Association Between Service Failures and Fillet Profiles of Tube Stub-Header Weldments," Metal Construction and British Welding Journal, Vol. III. 1971. pp. 433-437.
14. Clark, P. J., "Basis of Design for Fillet-Welded Joints Under Static Loading," Improving Welded Product Design Conference, The Welding Institute. 1971. pp. 85-96.
15. Van Douwen, A. A. and Witteveen, J., "Proposed Modification of the ISO Formula for the Calculation of Welded Joints," Lastechniek, 32, (6), 1966.
16. American Bureau of Shipping, Letter of 14 November 1977, to Dr. K. Masubuchi from Robert Curry, Principle Surveyor.
17. "Fillet Weld Size, Strength, and Efficiency Determination," Department of the Navy, Naval Ship Engineering Center. MIL-STD-1628 (Ships).
18. Hovgaard, W. Structural Design of Warships, 2nd Ed., 1940. The United States Naval Institute. Annapolis, Maryland. pp. 226-234.
19. Pilkey, Walter D. and Pilkey, Orrin H., Mechanics of Solids. New York, New York. 1974.
20. "American Welding Society Structural Welding Code," Part III. 2.6-2.7. (1972).
21. Germanischer Lloyd, Rules. 1969.
22. American Bureau of Shipping, "Rules for Building and Classing Steel Vessels," 1976.
23. "Fabrication, Welding and Inspection of Non-Combatant Ship Hulls," Department of the Navy. Naval Ships Engineering Center. December, 1966. NAVSHIPS 0900-014-5010.
24. Bureau Veritas, "Classification Society Rules," 1971.
25. Lloyds, "Register of Shipping Rules," 1976.
26. Det Norske Veritas, "Classification Society Rules," 1971.
27. "Military Standard Welded Joint Design," Department of Defense. FSC-THJM. 8 May 1969. MIL-STD-0022B (SHIPS).



## REFERENCES CONTINUED

28. "Fabrication Welding and Inspection; and Casting Inspection and Repair for Machinery, Piping and Pressure Vessels in Ships of the United States Navy," Department of Defense. MIL-STD-278 E (SH). 29 March 1976.
29. "Fabrication, Welding and Inspection of Ship Hulls," Department of the Navy, Naval Ship Systems Command. NAVSHIPS 0900-000-1000. October, 1968.
30. "Military Specification: Steel Plate, Alloy, Structural, High Yield Strength (HY 80 and HY 100)," Department of Defense. MIL-S-16216 H (SHIPS). 15 March 1972.
31. "Military Specification: Electrodes, Welding Covered, Coated, Aluminum and Aluminum Alloy." Department of Defense. MIL-E-15597 C. 10 June 1959.
32. "Military Specification: Steel Plate High Tensile (HT), Hull and Structural," Department of Defense. MIL-S-16113 C. (SHIPS). 25 March 66.
33. "Welding and Brazing Procedure and Performance Qualification," Department of Defense. MIL-STD-248 C. 12 October 1973. FSC THJM.
34. "Mechanical Tests for Welded Joints," Department of Defense. MIL-STD-418 C. 15 June 1972.
35. Moore, John, Capt. RN, Janes' Fighting Ships. 1973-74.
36. Cochran, C. S., and Jordan, C. R., "In Service Performance of Structural Details," Newport News Shipbuilding. Hull Technical Department E-12. Newport News, Virginia, 23607. March, 1977.
37. U. S. Navy, Bureau of Ships Drawing # AD-37, 100, 1926037. Rev. G. Shell Expansion. FR 66<sup>+</sup> - 89<sup>+</sup>. 4 June 1963.
38. U. S. Navy, Bureau of Ships Drawing # AD-37, 101, 1926061. Rev. E. Floors. FR 67<sup>+</sup> - 88<sup>+</sup>. 12 June 1964.
39. U. S. Navy, Bureau of Ships Drawing # AD-37, 114, 1926135. Rev. E. Transverse Bulkhead. FR 69 $\frac{1}{2}$ . Below Main Deck. 12 August 1964.
40. U. S. Navy, Bureau of Ships Drawing # AD-37, 102, 1926086. Rev. D. Inner Bottom. Plating and Beams. FR 58<sup>+</sup> - 75<sup>+</sup>. 14 July 1964.



## REFERENCES CONTINUED

41. U. S. Navy, Bureau of Ships Drawing # AD-37, 101, 1926169. Rev. C. Shell Long #7. Fwd. Fr. 90 and Aft. Fr. 100. 4 June 1964.
42. U. S. Navy, Bureau of Ships Drawing # AD-37, 101, 1926054. Rev. B. Shell Stringers #19 - 32. Fr. 66<sup>+</sup> - 89<sup>+</sup>. 29 June 1964.
43. U. S. Navy, Bureau of Ships Drawing # AD-37, 103, 1926092. Rev. F. 3rd Platf Plating and Beams. Fr. 66<sup>+</sup> to 89<sup>+</sup>. 30 June 1963.
44. U. S. Navy, Bureau of Ships Drawing # AO-143, S 1103 H, 1232 198. Rev. F. Fleet Oiler AO-143 Class, Shell Side Girders and Main Deck Side Girders. Fr. 42-92. 6 February 1952.
45. U. S. Navy, Bureau of Ships Drawing # AO-144, S 1101 H, 1384 708. Rev. E. Fleet Oiler AO-143 Class, Outside Plating. Fr. 63-92. 2 October 1953.
46. U. S. Navy, Bureau of Ships Drawing # AO-143, S 1105 H, 1232001. Rev. G. Fleet Oiler AO-143 Class. Transverse OT Bulkhead. 80. 15 May 1952.
47. Evans, J. Harvey, Ship Structural Design Concepts. Cambridge, Maryland. 1975.
48. "Specifications for Building Destroyer Tender AD-39," Department of the Navy, N. S. 0902-005-5000. Section 9110. 27 August 1965.
49. Malliris, A., "Static Strength of Fillet Welds Using the Finite Element Method," Masters Thesis, Massachusetts Institute of Technology. Department of Ocean Engineering. Cambridge, Massachusetts. 1978.
50. Bathe, K. J., "ADINA, Finite Element Program for Automatic Dynamic Incremental Non-linear Analysis," Report 82448-1, Mechanical Engineering Department, Massachusetts Institute of Technology, Cambridge, Massachusetts. May, 1976.
51. Uhlig, Herbert H., Corrosion and Corrosion Control, New York, New York. 1971.
52. Gellings, P. J., Introduction to Corrosion Prevention and Control for Engineers. Netherlands. 1976.
53. Uhlig, H. H., Professor of Metallurgy. Massachusetts Institute of Technology, Cambridge, Massachusetts. Personal Contact, 9 December 1977.



## REFERENCES CONTINUED

54. Blodgett, O. W., "How to Determine the Cost of Welding," The Lincoln Electric Company. (G 610). March, 1977.
55. Itoga, Kouyu, Research Associate. Massachusetts Institute of Technology. Cambridge, Massachusetts. Personal Contact with Kawasaki Heavy Industries. Japan. February, 1978.



Thesis  
M1633  
c.1

McCabe

187437

A comparison of fil-  
let weld strength and  
U.S. Navy design speci-  
fications for non-com-  
batant ships and the  
economic implications.

Thesis

M1633

c.1

McCabe

187437

A comparison of fil-  
let weld strength and  
U.S. Navy design speci-  
fications for non-com-  
batant ships and the  
economic implications.

thesM1633

A comparison of fillet weld strength and



3 2768 001 88695 5

DUDLEY KNOX LIBRARY